The Relationship between Heuweltjies and Saline Groundwater along the West Coast of South Africa

Report to the
Water Research Commission

by

ML Francis, CE Clarke, J van Gend, M Vermooten, MG Maponya, E Mashimbye,
L Palcsu, AP Watson, JD van Rooyen and JA Miller
Department of Earth Sciences
Stellenbosch University

WRC Report No. 2825/1/22
ISBN 978-0-6392-0466-6

July 2022

WATER
RESEARCH
COMMISSION

Obtainable from
Water Research Commission
Private Bag X03
Gezina
PRETORIA, 0031

orders@wrc.org.za or download from www.wrc.org.za

Acknowledgements

We would like to thank Dr Freddie Ellis for sharing his insights and knowledge on heuweltjies with us. We would also like to thank the land-owners for access to their land.

We thank Prof Matthys Dippenaar, Prof Shayne Jacobs and Dr Freddie Ellis for their participation on the reference team for this project.

We thank the WRC for their support and patience with the delay in submission of this final report owing to the pandemic.

Finally, we dedicate this report to Prof Shayne Jacobs who inspired new avenues of heuweltjie research within this team

– Lost to the pandemic, taken far too soon –

Publications derived from this project

Clarke, C.E., Vermooten, M., Watson, A.P., Hattingh, M., Miller, J.A., Francis, M.L., Submitted, Downward migration of salts in termite-affected soils: Implications for groundwater salinization. Geoderma, accepted pending revisions.

Vermooten, M., Miller, J.A., Clarke, C.E. and Francis, M. Investigation of heuweltjie structure and soil chemistry in the Buffels River valley and implications for transfer of salts to groundwater. Goldschmidt Geochemical Conference, Barcelona, 18-23 August 2019, Abstract 3469.

Van Gend-Muller, J., Miller, J.A., Palcsu, L., Clarke, C.E. and Francis, M. Saline groundwater generation from paleo-termite mounds in the Buffels River valley, South Africa. Goldschmidt Geochemical Conference, Barcelona, 18-23 August 2019, Abstract 3498.

Van Gend, J., Miller, J.A., Clarke, C.E., Palcsu, L. and de Clercq, W.P. (2018). Saline groundwater generation from palaeo-termite mounds in the Buffels River valley, South Africa. 45th International Association of Hydrogeologists Congress, Daejeon, Korea, 9-14 September, Conference Abstract.

Van Gend, J., Francis, M.L., Watson, A.P., Palcsu, L., Horváth, A., Macey, P.H., le Roux, P., Clarke, C.E. and Miller, J.A. (2021). Saline groundwater in the Buffels River catchment, Namaqualand, South Africa: A new look at an old problem. Science of The Total Environment, 762, p.143140.

Watson, A., Kralisch, S., Van Rooyen, J. and Miller, J. (2021). Quantifying and understanding the source of recharge for alluvial systems in arid environments through the development of a seepage model. Journal of Hydrology, 601, p.126650.

TABLE OF CONTENTS

List of Figures

List of Tables

1 INTRODUCTION

By J.A. Miller, C.E. Clarke and M.L. Francis

1.1 Overview

Large parts of the coastal zone of the Western and Northern Cape of South Africa are affected by variably saline groundwater, traditionally attributed to the effects of evaporation and evapotranspiration that exceed the mean annual precipitation (MAP). However, the larger coastal zone of southern Africa (including Namibia) has similar MAP profiles and associated high evaporation rates and yet does not suffer from the same level of salinization. Moreover, the saline groundwater is not uniformly distributed and together these features suggests that other factors are at play in the development of saline groundwater.

Heuweltjies are palaeo-termite mounds (5 to 20 m in diameter with 0.5 m elevation) that form a distinct landscape across much of the west coast region of South Africa. They are not uniformly distributed and the soil compositions and vegetation cover in and on these domal structures vary in comparison to that of the surrounding material. In line with previous studies, recent research confirmed that heuweltjies in the area around Buffelsrivier, west of Springbok, have elevated salinity levels compared to the surrounding inter-heuweltjie material. This study will examine the relationship between heuweltjies and saline groundwater on the west coast of South Africa in both the Western Cape and the Northern Cape to see if there is a potential causal relationship.

1.2 Project Rationale

In recent times, increasing population densities coupled with variable improvements in the average standard of living has led to growing pressure on global water resources. As a result, more and more emphasis is being placed on shallow, recently recharged, groundwater resources to supply the demands of the world's population. Recent estimates of recently recharge groundwater (i.e. <50 year old), have suggested that it makes up less than ~ 20% of extractable groundwater worldwide (Gleeson et al., 2016). This is significant in that this groundwater is the most vulnerable to climate change and to pollution but is also the main source of water for large-scale agricultural production. Through the intersection of increasing population, agricultural production and demands on groundwater resources, numerous large-scale aquifers involved in significant crop production (e.g. High Plains Aquifer, USA; Central Valley, California; North China Plain; Upper Ganges) are showing substantial groundwater depletions (Konikov and Kendy, 2005; Scalon et al., 2012; Döll et al., 2014). Management of these aquifer systems is therefore critical to their long-term sustainability.

Africa, with its rapidly developing economies, is currently at the apex of this intersection and this has magnified the need for potable water resources both for domestic water consumption and for sustainable crop production. Although large parts of sub-Saharan Africa record relatively high rainfall, climate variability coupled to erratic periods of drought (Rouault and Richard, 2005) along with contamination of groundwater resources (Nyenje et al., 2010; Sorensen et al., 2015) means that access to safe drinking water in this region remains a challenge. In southern Africa, particularly on the western seaboard, low rainfall (typically > 300 mm/yr) coincides with semi-arid to arid environments and high evaporation rates (<2000 mm/yr) and is thought to be the leading cause of moderate to severe groundwater salinization (Naicker and Demlie, 2014). Into this mix is the ongoing impact of climate change. In South Africa, the increasing incidence of extreme rainfall events in response to climate change has already been documented (Mason et al., 1999). In addition, the western seaboard of southern Africa is predicted to become drier with different climate models indicating rainfall decreases in excess of up to 50% in the arid south west (Faramarzi et al., 2013). Perhaps more importantly, evapotranspiration is likely to increase as daily average temperatures increase (Davis et al., 2016). Such scenarios are likely to exacerbate the lack of fresh potable drinking water in southern Africa and have focussed attention on identifying secure, sustainable potable water supplies particularly in rural communities which lack access to large municipal water supply networks.

Heuweltjies (Afrikaans for little hills) are distinctive geomorphological features that occur along the southern Cape coast as the western seaboard of South Africa. They usually form low elevation (<0.5 m) domes up to 50 m in diameter. Because the composition of the soil on the domes is different to that of the surrounding inter-domal area, the domes typically show up as paler spots on the landscape (Figure 1.1) but also have distinctly different vegetation patterns. They are not uniformly distributed and there is ongoing debate about the mode of formation although it is generally agreed that they represent palaeo-features. Recent research confirmed that heuweltjies in the area around Buffelsrivier, west of Springbok, have elevated salinity levels compared to the surrounding inter-heuweltjie material. This is similar to previous studies on heuweltjies in other regions. Given the high density of heuweltjies in some parts of the landscape and the apparent close correlation between higher salinity groundwater on the west and southern cape coasts and the distribution of heuweltjies, the possibility arises that heuweltjies and saline groundwater are linked. The core aim of this study is to determine whether there may be a causal link between heuweltjies and saline groundwater. The study will use a multi-disciplinary approach including hydrochemistry, isotope hydrology, soil mapping and characterisation as well as GIS based methods of determining heuweltjie distribution, to establish if this link does exist. The results will have implications for management of groundwater in areas dominated by heuweltjies and in particular the management of agricultural land in areas where heuweltjies are particularly common.

Figure 1.1: pale spots on the landscape in the Buffels River catchment indicative of heuweltjies

1.3 Aims and Key Objectives

In the set up of this project, a number of key objectives were setup to examine the causal link between heuweltjies and saline groundwater. Not all of these objectives could be achieved because of the impact of the Covid-19 pandemic that severely curtailed field work and analytical work during 2020. We also had difficulty with the set up of the GIS analysis of heuweltjie distribution which impacted on the large scale transferability of the project results. However, the hydrochemical and isotope hydrology work was very successful and the project objectives have been reshaped towards this focus.

1.3.1 Original Aims and Objectives

The following objectives were developed for this project:

- To establish the spatial relationship between the distribution of heuweltjies, the type of heuweltjie and the distribution of saline groundwater through the use of integrated spatial datasets.

- To fully characterise the salt profile within the heuweltjies including the type of salts, their distribution throughout the heuweltjie structure, where the salts are hosted including mineral hosts or salt coatings and what is the leachable salt fraction.
- To establish the residence time of the groundwater, the age of the salts in both the groundwater and heuweltjies, and the age of the heuweltjies themselves to establish whether there is a temporal relationship between saline groundwater, heuweltjie salts and the heuweltjies.
- To constrain the origin of the heuweltjie salts through the use of Li and Sr isotopes and Li/Ti ratios to establish the weathering history of the granitic basement rocks and their contribution to the formation of the heuweltjies.
- To establish the mechanism(s), pathway and scale of salt transfer from the heuweltjies to the groundwater system and the impact of changing precipitation patterns, particularly the impact of heavy rain events, on this transfer process.

1.3.2 Revised Aims and Objectives

The revised project objectives are as follows:

- To fully characterise the salt profile within the heuweltjies including the salt composition, their distribution throughout the heuweltjie structure, and what is the leachable salt fraction.
- To relate salt profiles in heuweltjies to salt profiles in groundwater to evaluate whether there is any correlation.
- To establish the residence time of the groundwater, the age of carbonates in the heuweltjies as a proxy for salt age groundwater and heuweltjies, and the age of the heuweltjies themselves to establish whether there is a temporal relationship between saline groundwater, heuweltjie salts and the heuweltjies.
- To evaluate whether the spatial distribution of heuweltjies in the Buffels river catchment can be established through remote sensing techniques.
- To examine the mechanism(s), pathway and scale of salt transfer from the heuweltjies to the groundwater system and the impact of changing precipitation patterns, particularly the impact of heavy rain events, on this transfer process.

1.4 Project Hypothesis

Saline groundwater is prevalent along the northern west coast of South Africa. Although the salinity is proposed to be a result of evaporation exceeding precipitation, the distribution of saline groundwater is uneven. Heuweltjies are known to contain elevated concentrations of nutrients and salts but also

represent sites of preferential water movement owing to the tunnelling and burrowing of various animals both large and small. During high rainfall events, these preferential pathways could channel precipitation down through the heuweltjies, dissolving salts along the way and transferring them to the groundwater system. This would result in downward salt percolation profiles and correlations between regions of saline groundwater and high heuweltjie distribution.

Recently, it has been observed that heuweltjie soils in the Buffels River valley have salinity levels an order of a magnitude higher than the surrounding interheuweltjie soil (Van Gend et al., 2021). Studies from other areas have also noted that heuweltjies were saline, but no further details were mentioned (Francis et al., 2007; Kunz et al., 2012; McAuliffe et al., 2019a; McAuliffe et al., 2019b). As previously mentioned, heuweltjies are commonly associated with the termite *Microhodotermes viator,* however the exact role of *M. viator* in mound formation is not agreed upon (McAuliffe et al., 2019a; McAuliffe et al., 2019b). Regardless of their formation, the occurrence of *M. viator* in heuweltjies results in a dynamic ecosystem on and within the mound which includes a wide variety of burrowing meso and macro fauna (*Figure 1.*). The net result is a high density of burrows and interconnected channels that might harvest and rapidly translocate rainfall to greater depths compared to normal infiltration through the surrounding soil surface. This could result in the salinity of these mounds being gradually translocated with percolating rainwater to the groundwater. It is therefore hypothesised that heuweltjies contribute to the irregular distribution of saline groundwater in the Buffels River Region.

Figure 1.2: Macrofaunal excavations and burrows on heuweltjie mounds

1.5 Outline of Report

The project was completed through a series of postgraduate student projects including two PhD students and two MSc students and one BSc Hons student. The results of each project have contributed to different parts of the project and the report thus is divided into chapters that represent different postgraduate project foci. These can be broken down as follows:

1. Characterisation of salt profiles in the heuweltjies including the reporting on the heuweltjie excavations – MSc Vermooten and Walker.
2. Characterisation of radiocarbon data to understand groundwater residence time, formation of heuweltjies and salt distribution – PhD Van Gend.
3. Remote sensing work to evaluate the distribution of heuweltjies – PhD Maponya, BSc Hons Husselmann.

1.6 Capacity Development

The following student projects were produced through or involved with this project.

1. Ms Deone Husselmann, BSc Honours, 2019: TITLE: The spatial distribution of heuweltjies (palaeo-termite mounds) in relation to groundwater salinity between Springbok and Garies, South Africa.
2. Ms Marli Vermooten, MSc 2019: TITLE: Investigation of heuweltjie structure and soil chemistry in the Buffels River valley and implications for transfer of salts to groundwater.
3. Mr Ruairi Walker, MSc, 2020: TITLE: Assessing acid mine drainage potential in reworked base metal sulphide ore deposits: An example from the Spektakel Copper Mine, Northern Cape, South Africa
4. Ms Jani van Gend, PhD 2021: TITLE: Investigating the relationship between saline groundwater, heuweltjies and climate change in the Buffels River Catchment, South Africa
5. Ms Grace Maponya, PhD, First registered 2020 (ongoing): TITLE: The value of machine learning based on satellite imagery and environmental variables to map the spatial distribution of earth mounds at catchment level.

1.7 References

Davis, C.L., Timm Hoffman, M. and Roberts, W., 2016. Recent trends in the climate of Namaqualand, a megadiverse arid region of South Africa. South African Journal of Science, 112(3-4), pp.1-9.

Faramarzi, M., Abbaspour, K.C., Vaghefi, S.A., Farzaneh, M.R., Zehnder, A.J., Srinivasan, R. and Yang, H., 2013. Modeling impacts of climate change on freshwater availability in Africa. Journal of Hydrology, 480, pp.85-101.

Francis, M.L. et al., 2007. Soils of Namaqualand: Compensations for aridity. J. Arid Environ., 70, 588-603.

Konikov, LF, and Kendy, E. 2005. Groundwater depletion: a global problem. Hydrogeology Journal 13, 317-320. doi: 10.1007/s10040-004-0411-8

Kunz, N.S., Hoffman, M.T., Weber, B., 2012. Effects of heuweltjies and utilization on vegetation patterns in the Succulent Karoo, South Africa. J. Arid Environ., 87, 198-205.

Mason, S.J., Waylen, P.R., Mimmack, G.M., Rajaratnam, B. and Harrison, J.M., 1999. Changes in extreme rainfall events in South Africa. Climatic Change, 41(2), pp.249-257.

McAuliffe, J.R. et al., 2019a. Landscape patterning created by the southern harvester termite, Microhodotermes viator: Spatial dispersion of colonies and alteration of soils. J. Arid Environ., 162, 26-34.

McAuliffe, J.R. et al., 2019b. Whether or not heuweltjies: Context-dependent ecosystem engineering by the southern harvester termite, Microhodotermes viator. Journal of Arid Environments, 163, 26-33.

Naicker, S. and Demlie, M., 2014. Environmental isotopic and hydrochemical characteristics of groundwater from the Sandspruit Catchment, Berg River Basin, South Africa. Water science and technology, 69(3), pp.601-611.

Nyenje, P.M., Foppen, J.W., Uhlenbrook, S., Kulabako, R. and Muwanga, A., 2010. Eutrophication and nutrient release in urban areas of sub-Saharan Africa—a review. Science of the total environment, 408(3), pp.447-455.

Scanlon, B.R., Faunt, C.C., Longuevergne, L., Reedy, R.C., Alley, W.M., McGuire, V.L. and McMahon, P.B., 2012. Groundwater depletion and sustainability of irrigation in the US High Plains and Central Valley. Proceedings of the national academy of sciences, 109(24), pp.9320-9325.

Rouault, M. and Richard, Y., 2005. Intensity and spatial extent of droughts in southern Africa. Geophysical research letters, 32(15).

Sorensen, J.P.R., Lapworth, D.J., Read, D.S., Nkhuwa, D.C.W., Bell, R.A., Chibesa, M., Chirwa, M., Kabika, J., Liemisa, M. and Pedley, S., 2015. Tracing enteric pathogen contamination in sub-Saharan African groundwater. Science of the Total Environment, 538, pp.888-895.

Van Gend, J. et al., 2021. Saline groundwater in the Buffels River catchment, Namaqualand, South Africa: A new look at an old problem. Science of The Total Environment, 143140.

2 REVIEW OF HEUWELTJIES

By M.L. Francis

2.1 General Description

Heuweltjies (Afrikaans: small hills) are 20-50 m diameter earth mounds with a slightly raised (1-2.5 m) surface compared to the surrounding soil. The main characteristic of the heuweltjie landscape is the distinct vegetation pattern which is visible from the field to the satellite image, presenting a typical "ostrich leather" (Laurie, 2002) texture in aerial view. Termites (*Microhodotermes viator*) presently inhabit some but not all of the mounds. *Microhodotermes viator* is a non-mound building termite species, and its nests can be observed over much of the Western Cape (Picker et al., 2007). Unlike the spire-building *Macrotermes* species that occupy the humid eastern parts of South Africa, *Microhodotermes* occupy the western part, lack a fungus culture and differ from most termites worldwide by being a detritivore as well as a herbivore, consuming fresh faeces of herbivores and harvesting fresh foliage (Fey, 2010). *Microhodotermes viator* is a Fynbos and Succulent Karoo specialist (Vernon, 1999) that consumes woody plants (Coaton and Sheasby, 1974; Rohland, 2010) and has a stable isotope signature consistent with this predominantly C_3-diet (Midgley et al., 2002; Potts et al., 2009).

2.2 Understanding of Geographical Spread

Heuweltjies occur throughout the western and southern Cape coasts in the Fynbos and Succulent Karoo biomes (Cramer et al., 2017; Cramer and Midgley, 2015; Picker et al., 2007). They occupy 14-25% of the land surface in these regions (Lovegrove and Siegfried, 1989; Moore and Picker, 1991). The oldest ones have been present in the landscape since at least the Last Glacial ca. 20 000-35 000 years BP (Coaton, 1981; Midgley et al., 2002; Potts et al., 2009). Ellis (2002) described the relationship between hardpan occurrence and rainfall in heuweltjies: where the rainfall is at its lowest, termite activity is relict, with only tunnels present but not active termites. The mounds are characterized by a central petrocalcic (calcrete) to petroduric (dorbank) hardpan, with a petroduric (dorbank) horizon over petrocalcic (calcrete) horizon towards the outer edge of the mound and the surrounding inter-mound areas. In the higher rainfall zone (250-450 mm), the general tendency is that limited termite activity is present almost exclusively in the centre of the mounds, where the areas of activity have non-cemented, calcic horizons with petroduric (dorbank) or petrocalcic (calcrete) horizons on the perimeter of the mound, even when no hardpans occur in surrounding soils. With increasing rainfall and age of mounds and with relict termite activity, a broken hardpan and/or more base-rich soil material is found on the

mounds. In these latter cases the soils of the inter-mound areas have moderate to low base status without any hardpans.

Microhodotermes viator distribution generally overlaps that of the heuweltjies along the west Coast except in the south and eastern part of their ranges (Cramer et al., 2017; Lovegrove and Siegfried, 1986). However, satellite images show that landscape spots are indeed present in the eastern areas where Cramer et al. (2017), Cramer and Midgley (2015) and Lovegrove and Siegfried (1986) marked them as absent, extending to the easternmost limit *of M. viator*. In the Ruensveld in the southern Cape it is possible that the heuweltjies have been eroded leaving only the basal layers (Lovegrove and Siegfried, 1986). There are also omissions in the heuweltjie distribution pattern published by Cramer et al. (2017) and Cramer and Midgley (2015) in the areas around Helderburg-Stellenbosch-Kraaifontein, Paarl, Durbanville, and Malmesbury where heuweltjies persist through agricultural disturbance . Heuweltjies have been recorded by other authors from these areas (Bekker et al., 2016; Lovegrove and Siegfried, 1986).

Most of these regions where heuweltjies have been indicated as absent but *M. viator* is present are either under intensive agriculture (wheat, orchards and vineyards) or have been used as grazing. In the very arid or overgrazed areas, the vegetation is so sparse that only the lighter coloured centre of the mounds are still visible. Many of these arid areas are in fact marginal for grazing, and the heuweltjies themselves may not remain visible in the landscape where they have been preferentially grazed as a result of their high grazing quality (Esler et al., 2006; Kunz et al., 2012; Schmiedel et al., 2016; Wilcox et al., 2017).

Areas under intensive orchards do not retain any evidence of previous heuweltjies, whereas areas under wheat retain seasonal greener vegetation associated with the nutrient-enrichment of the soils associated with the previous heuweltjies, and in some cases only the historical satellite images show the typical greener vegetation. Pine plantations mask the present of heuweltjies, and the clearing of the pines reveals the distinctive green patches (for example in Paradyskloof). The area around Grabouw has been planted with pines which are now being cleared as part of the alien vegetation clearing scheme in the Western Cape. Google Earth historical images show that the circular features appear soon after clearing, and eventually disappear after a few years with ploughing.

Urbanisation and intensification of agriculture are masking or removing the presence of mounds, and in the future it may only be possible to map the heuweltjie extent using historical records, since the few remnants of the ecosystem in its natural state do not give an accurate picture of the extent of the mounds.

2.3 Method of Formation

Heuweltjie origins are still being debated (Cramer et al., 2016; Cramer and Midgley, 2015; McAuliffe et al., 2014; Moore and Picker, 1991). There is often evidence of fossil termite activity preserved in the calcrete horizons (Francis et al., 2012; Francis and Poch, 2019; Moore and Picker, 1991) and active termites with frass (Francis et al., 2012; McAuliffe et al., 2014; Potts et al., 2009) associated with the mounds, but there is no consensus on termite's exact role in the formation of the mound (Cox et al., 1987; Cramer et al., 2017, 2016, 2012; Cramer and Barger, 2014; Cramer and Midgley, 2015; Laurie, 2002; Lovegrove and Siegfried, 1989, 1986; McAuliffe et al., 2014; Midgley and Hoffman, 1991; Midgley et al., 2002; Moore and Picker, 1991; Picker et al., 2007). Contrasting conclusions are often drawn: Lovegrove and Siegfried (1986), Laurie (2002) and Picker et al. (2007) attributed the mound distribution pattern to termites, whereas Cramer and Midgley (2015) found no evidence that the pattern of the mounds was set up by termites.

Cause-effect relationships are complicated by the age of the heuweltjies with the oldest so far being dated to ca. 20 000-35 000 years BP (Coaton, 1981; Midgley et al., 2002; Potts et al., 2009). The mounds have been eroded in some regions (Lovegrove and Siegfried, 1986), burrowed by mole rats and other mammals (Cox et al., 1987), affected by accretion of aeolian sediments (McAuliffe et al., 2014) and subjected to soil forming factors such as neoformation of clay and calcite (Francis et al., 2012).

The "pro-termite" view of heuweltjie formation is that the termites modified the soil locally around their nests via the foraging of plant material (Francis et al., 2012; Francis and Poch, 2019; McAuliffe et al., 2018, 2014, 2019). These chemical and physical soil modifications associated with the nests resulted in a heterogeneous soil pattern of nutrient-rich islands over the landscape, and resulted in the characteristic vegetation pattern observed over the heuweltjie landscape.

In the "non-termite camp" are the publications proposing that the mound distribution is instead consistent with a pre-existing vegetation pattern and not termite activity (Cramer et al., 2012; Cramer and Barger, 2014; Cramer and Midgley, 2015). Cramer and Midgley (2015) suggested that this sets up a positive feedback in which larger plants continue to trap aeolian sediment (McAuliffe et al., 2014) and aerosols resulting in large nutrient-rich mounds with distinctive flora and secondary fauna that are self-sustaining. These patches became the favoured locations for the termite communities associated with the heuweltjies.

2.4 Composition

Heuweltjie calcretes are an important sink of atmospheric CO_2, marine aerosols and soluble elements (Midgley et al., 2012), preserving a stable isotope signature of the vegetation from before the Last Glacial Maximum (Potts et al., 2009). Potts et al. (2009) noted that the $\delta^{13}C$ and $\delta^{18}O$ signatures found in calcrete from a heuweltjie near Worcester were not consistent with the signature of the nearest geological source of Ca. The origin of the Ca content of rainwater for the area is seawater-derived Ca (Midgley et al., 2012; Soderberg and Compton, 2007).

Compared to off-mound soils, heuweltjie soils tend to have more water soluble salts (Van Gend et al., 2021), higher nutrient (C, N, P) levels (Bekker et al., 2016; Kunz et al., 2012; Midgley and Hoffman, 1991; Midgley and Musil, 1990) and higher base status (Ca, Mg, K, Na) (Bekker, 2011; Ellis, 2004, 2002; Francis et al., 2012). This has been attributed to the cycling of organic matter (Francis et al., 2012; Francis and Poch, 2019; Mcauliffe et al., 2019; Midgley and Hoffman, 1991) and aerosols (Midgley et al., 2012; Van Gend et al., 2021) into the mounds.

In arid areas the lack of leaching allows the nutrients, secondary minerals and salts (calcite, gypsum, halite) that have been built up in the center of the heuweltjie to remain in the soil (Booi, 2011; Francis and Poch, 2019). Higher rainfall will result in more leaching, and soluble cations (Ca^{2+}, Mg^{2+}, Na^{+}, K^{+}) as well as nutrients (C, N, P) will be moved lower in the profile or removed completely. The lack of leaching in the arid regions allows the nutrients that have been built up in the center of the heuweltjie to remain in the soil. Thus, the on-off mound nutrient discrepancy is preserved in the soil compared to regions with higher rainfall, where the leaching intensity is higher and the on-off mound discrepancy is more quickly homogenized.

2.5 References

Bekker, S.J., 2011. Exploiting soil and terrain heterogeneity : an investigation into vigour and physiology of grapevines on and off “heuweltjies” in the Western cape, South Africa. MSc thesis, University of Stellenbosch.

Bekker, S.J., Hoffman, J.E., Jacobs, S.M., Strever, A.E., Van Zyl, J.L. 2016. Ecophysiology, vigour, berry and wine characteristics of grapevines growing on and off heuweltjies. South African J. Enol. Vitic. 37, 176-192. doi:10.21548/37-2-690

Booi, N., 2011. Structure and function of heuweltjies across a rainfall gradient in the South-Western Cape. University of Stellenbosch.

Coaton, W.G.H., 1981. Fossilised nests of Hodotermitidae (Isoptera) from the Clanwilliam district, Cape Province. J. Entomol. Soc. South Africa 44 (2), 79-81.

Coaton, W.G.H., Sheasby, J.L., 1974. National survey of the Isoptera of southern Africa. 6. The genus Microhodotermes Sjöstedt (Hodotermitidae). Cimbebasia (Series A) 3, 47-59.

Cox, G.W., Lovegrove, B.G., Siegfried, W.R., 1987. The small stone content of mima-like mounds in the South African Cape region: Implications for mound origin. Catena 14, 165-176. doi:10.1016/S0341-8162(87)80015-2

Cramer, M.D., Barger, N.N., 2014. Are mima-like mounds the consequence of long-term stability of vegetation spatial patterning? Palaeogeogr. Palaeoclimatol. Palaeoecol. 409, 72-83. doi:10.1016/j.palaeo.2014.04.026

Cramer, M.D., Innes, S.N., Midgley, J.J., 2012. Hard evidence that heuweltjie earth mounds are relictual features produced by differential erosion. Palaeogeogr. Palaeoclimatol. Palaeoecol. 350-352, 189-197. doi:10.1016/j.palaeo.2012.06.030

Cramer, M.D., Midgley, J.J., 2015. The distribution and spatial patterning of mima-like mounds in South Africa suggests genesis through vegetation induced aeolian sediment deposition. J. Arid Environ. 119, 16-26. doi:10.1016/j.jaridenv.2015.03.011

Cramer, M.D., von Holdt, J.R.C., Khomo, L., Midgley, J.J., 2016. Evidence for aeolian origins of heuweltjies from buried gravel layers. S. Afr. J. Sci. 112, 1-10. doi:http://dx.doi.org/10.17159/sajs.2016/20150025

Cramer, M.D., von Holdt, J.R.C., Uys, V.M., Midgley, J.J., 2017. The present and likely past climatic distribution of the termite Microhodotermes viator in relation to the distribution of heuweltjies. J. Arid Environ. 146, 35-43. doi:10.1016/j.jaridenv.2017.07.010

Ellis, F., 2004. Soil variation on and between heuweltjies in arid and semi-arid regions of South Africa.

Ellis, F., 2002. Contribution of termites to the formation of hardpans in soils of arid and semi-arid regions of South Africa, in: Proceedings of the 17th World Congress of Soil Science, Bangkok, Thailand, August 2002, Volume 2, Symposium 20. p. 791.

Esler, K.J., Milton, S.J., Dean, W.R.J., 2006. Karoo Veld – Ecology and Management. Briza Press, Pretoria.

Fey, M. V, 2010. Soils of South Africa. Cambridge University Press. doi:https://doi.org/10.1017/CBO9780511782183

Francis, M.L., Ellis, F., Lambrechts, J.J.N., Poch, R.M., 2012. A micromorphological view through a Namaqualand termitaria (Heuweltjie, a Mima-like mound). Catena 100, 57-73. doi:10.1016/j.catena.2012.08.004

Francis, M.L., Poch, R.M., 2019. Calcite accumulation in a South African heuweltjie: Role of the termite Microhodotermes viator and oribatid mites. J. Arid Environ. 170, 103981. doi:10.1016/j.jaridenv.2019.05.009

Kunz, N.S., Hoffman, M.T., Weber, B., 2012. Effects of heuweltjies and utilization on vegetation patterns in the Succulent Karoo, South Africa. J. Arid Environ. 87, 198-205. doi:10.1016/j.jaridenv.2012.05.007

Laurie, H., 2002. Optimal transport in central place foraging, with an application to the overdispersion of heuweltjies. S. Afr. J. Sci. 98, 141-146.

Lovegrove, B.G., Siegfried, W.R., 1989. Spacing and origin(s) of Mima-like earth mounds in the Cape Province of South Africa. S. Afr. J. Sci. 85, 108-112.

Lovegrove, B.G., Siegfried, W.R., 1986. Distribution and formation of Mima-like earth mounds in the western Cape Province of South Africa. S. Afr. J. Sci. 82, 432-436.

McAuliffe, J., Hoffman, M., McFadden, L., King, M., 2014. Role of aeolian sediment accretion in the formation of heuweltjie earth mounds, western South Africa. Earth Surf. Process. Landforms 39, 1900-1912. doi:10.1002/esp.3583

McAuliffe, J., McFadden, L., Hoffman, M., 2018. Role of Aeolian Dust in Shaping Landscapes and Soils of Arid and Semi-Arid South Africa. Geosciences 8, 171. doi:10.3390/geosciences8050171

Mcauliffe, J.R., Hoffman, M.T., Mcfadden, L.D., Bell, W., Jack, S., King, M.P., Nixon, V., 2019. Landscape patterning created by the southern harvester termite, Microhodotermes viator: Spatial dispersion of colonies and alteration of soils. J. Arid Environ. 3, 1-9. doi:10.1016/J.JARIDENV.2018.11.010

McAuliffe, J.R., Hoffman, M.T., McFadden, L.D., Jack, S., Bell, W., King, M.P., 2019. Whether or not heuweltjies: Context-dependent ecosystem engineering by the southern harvester termite, Microhodotermes viator. J. Arid Environ. 163, 26-33. doi:10.1016/j.jaridenv.2018.11.012

Midgley, G., Hoffman, T., 1991. Heuweltjies: nutrient factories. Veld Flora September, 72-75.

Midgley, G., Musil, C.F., 1990. Substrate effects of zoogenic soil mounds on vegetation composition in the Worcester-Robertson valley, Cape Province. South African J. Bot. 56 (2), 158-166.

Midgley, J.J., Harris, C., Harington, A., Potts, A.J., 2012. Geochemical perspective on origins and consequences of heuweltjie formation in the southwestern Cape, South Africa. South African J. Geol. 115, 577-588. doi:10.2113/gssajg.115.4.577

Midgley, J.J., Harris, C., Hesse, H., Swift, A., 2002. Heuweltjie age and vegetation change based on δ 13 C and 14 C analyses. S. Afr. J. Sci. 98, 202-204.

Moore, J.M., Picker, M.D., 1991. Heuweltjies (earth-mounds) in the Clanwilliam district, Cape Province, South Africa. Oecologia 87, 424-432.

Picker, M.D., Hoffman, M.T., Leverton, B., 2007. Density of Microhodotermes viator (Hodotermitidae) mounds in southern Africa in relation to rainfall and vegetative productivity gradients. J. Zool. 271, 37-44. doi:10.1111/j.1469-7998.2006.00189.x

Potts, A.J., Midgley, J.J., Harris, C., 2009. Stable isotope and 14C study of biogenic calcrete in a termite mound, Western Cape, South Africa, and its palaeoenvironmental significance. Quat. Res. 72, 258-264. doi:10.1016/j.yqres.2009.04.008

Rohland, J., 2010. Investigating the actinomycete diversity inside the hindgut of an indigenous termite, Microhodotermes viator. PhD Thesis. University of Cape Town. doi:10.3390/su7022189

Schmiedel, U., Röwer, I.U., Luther-Mosebach, J., Dengler, J., Oldeland, J., Gröngröft, A., 2016. Effect of grazing on vegetation and soil of the heuweltjieveld in the Succulent Karoo, South Africa. Acta Oecologica 77, 27-36. doi:10.1016/j.actao.2016.08.012

Soderberg, K., Compton, J.S., 2007. Dust as a nutrient source for fynbos ecosystems, South Africa. Ecosystems 10, 550-561. doi:10.1007/s10021-007-9032-0

van Gend, J., Francis, M.L., Watson, A.P., Palcsu, L., Horváth, A., Macey, P.H., le Roux, P., Clarke, C.E., Miller, J.A., 2021. Saline groundwater in the Buffels River catchment, Namaqualand, South Africa: A new look at an old problem. Sci. Total Environ. 143140. doi:10.1016/j.scitotenv.2020.143140

Vernon, C.J., 1999. Biogeography, endemism and diversity of animals in the Karoo, in: Dean, W.R.J., Milton, S. (Eds.), The Karoo: Ecological Patterns and Processes. Cambridge University Press, Cambridge, pp. 57-86. doi:10.1017/cbo9780511541988.008

Wilcox, B., Le Maitre, D., Jobbágy, E., Wang, L., Breshears, D., 2017. Ecohydrology: Processes and Implications for Rangelands. pp. 85-129. doi:10.1007/978-3-319-46709-2_3

3 ENVIRONMENTAL SETTING

By J. van Gend, A.P. Watson, M.L. Francis, C.E. Clarke and J.A. Miller

The Buffels River catchment is situated in the north west of Namaqualand in the Northern Cape of South Africa, comprising an area of 9250 km^2 (Fig. 3.1). The Buffels River is the largest ephemeral river in Namaqualand, with headwaters located in the Kamies Mountains on the Bushmanland Plateau. The river cuts down through the escarpment before emerging onto the Tertiary coastal plain and enters the Atlantic Ocean at Kleinsee (Benito et al., 2010; Benito et al., 2011a).

3.1 Climate

Namaqualand is classified as a semi-arid to arid region, climatically controlled by the Benguela upwelling system and mid-latitude westerlies (Weldeab et al., 2013). Daily temperatures in summer often exceed 35°C, while the daily maximum temperature during winter averages 17°C, reaching sub-zero at night (Davis et al., 2016). The Buffels River catchment falls within a winter rainfall regime and mean annual precipitation (MAP) is highly variable. Inland mountainous areas in the catchment typically have a higher MAP than the low-lying coastal areas due to orographic effects (Benito et al., 2011b; Pietersen et al., 2009; Titus et al., 2009). The coast itself is hyperarid with a MAP of 50 mm/year while the MAP on the coastal plain towards Komaggas is higher at 110 mm/year (Fig. 3). The MAP for the Kamies Mountains, the highest elevation in the Buffels River catchment, is 400 mm/year (Benito et al., 2011b; Davis et al., 2016; Titus et al., 2009). Heavy dewfalls occur in mid-winter while coastal fog generated by the cold Benguela current is common in summer with up to 75 fog days per year (Davis et al., 2016). However, climate change will cause a poleward shift of the austral mid-latitude westerlies and weakening of the southern Benguela upwelling system allowing increased leakage of warm Agulhas waters (Beal et al., 2011; Biastoch et al., 2009; Weldeab et al., 2013). These authors note that climatic shifts will not only decrease precipitation in the winter rainfall zone but will cause an increase in sea surface temperature along the coast and therefore a likely reduction in coastal fog formation. This contrasts with our understanding of the regional palaeoclimate during the last glacial periods, where the winter rainfall zones were thought to be wetter than present due to northward displacement of the Southern Hemisphere westerlies (Zhao et al., 2016).

3.2 Geomorphology

Three geomorphological zones exist in Namaqualand: (1) a western coastal lowland or plain, characterised by crystalline basement rocks overlain by younger sedimentary rocks and sands; (2) an escarpment zone of exposed granitic domes, interspersed with thick layers of weathered material cut by alluvial palaeochannels; and (3) the gently undulating Bushmanland Plateau consisting of a complex sequence of erosional and aggradational phases (Adams et al., 2004; Titus et al., 2009). The most prominent geomorphological features are the Bornhardts of the escarpment zone and the African and post-African erosion surfaces on the Bushmanland Plateau and the coastal plain, respectively. Bornhardts host extensive orthogonal fracture systems which formed during their emplacement and could be linked to groundwater flow paths. The African Surface (mid-Cretaceous) is characterised by deep kaolinized profiles capped by pedocrete cappings (Partridge and Maud, 1987; Titus et al., 2009). Post-African Surface I (Miocene) and Post-African Surface II (Late Tertiary) occur on the coastal plain and represent periods of crustal uplift followed by erosion and periods of aridification (Partridge, 1998; Partridge and Maud, 1987; Roberts and White, 2010).

Heuweltjies are common surface features throughout the west coast of Southern Africa, with a minimum coverage of approximately 67 000 km^2 (Cramer and Midgley, 2015). They are particularly concentrated throughout the Buffels River catchment, specifically in the Buffels River valley, where the town of Buffelsrivier is situated, and on the coastal plain towards Kleinsee. Towards the coast, they become covered by wind-blown sands and paleodune systems and their distribution is difficult to discern except from satellite imagery. Due to the composition of the heuweltjie soils, they are distinctly lighter in colour and typically have vegetation patterns that are distinct from the surrounding off heuweltjie or inter-heuweltjie areas (Francis et al., 2013; Midgley et al., 2002; Picker et al., 2007).

3.3 Vegetation

The flora in Namaqualand is known to be drought resistant with leaves and roots adapted for the arid climatic conditions (Mucina and Rutherford, 2006). Although the vegetation in this region is sparse, the dominant vegetation throughout western Namaqualand is Succulent Karoo biome, generally consisting of shallow rooted drought resistant leaf-succulents, which are C3 plants. Towards the east of the catchment, the Succulent Karoo biome co-exists with the Nama Karoo biome. Although the Nama Karoo biome is also dominated by C3 species, the presence of C4 grass species increase towards the east where they co-exist with C3 low shrubs of the Nama Karoo biome. (Carrick and Krüger, 2007; Mucina and Rutherford, 2006). Sparse Acacia Karoo shrubs and thicket species, which are mostly C3 species,

only exist in the alluvial plains of the Buffels Rive due to their dependence on groundwater. During periods of severe drought these riparian plant species typically do not survive.

3.4 Land Use

Namaqualand hosted large mining operations, specifically for copper and alluvial diamonds in the previous century. However, the mining operations have been scaled down in recent years and only a few small operations are still in existence. In the last two decades, pastoralism, practiced by both commercial and subsistence farmers, has been the dominant land-use activity in the Buffels River catchment (Cousins et al., 2007; Hoffman and Rohde, 2007). Communal land around the small towns and rural settlements, where most of the population resides, has been allocated by government to the local communities for the purposes of livestock grazing for subsistence farmers. Commercial agriculture mainly consists of livestock farming. In recent years, many farmers have moved away from cattle to focus on small stock such as sheep and goats, specifically for the South African meat market (Benjaminsen et al., 2006).

3.5 Geology

The geology of the Buffels River catchment is dominated by the Bushmanland Sub-Province (BSP) of the Namaqua Sector of the Namaqua-Natal Metamorphic Province (Fig. 3.1). The BSP is made up of a granitic gneiss basement complex (± 2.0-1.8 Ga), meta-sedimentary and meta-volcanic supracrustal sequences (± 1.9 to 1.2 Ga) and syn- to late-tectonic granitic to charnockitic intrusive suites (± 1.2 to 0.95 Ga) (Clifford, 2004; Cornell et al., 2006; Macey et al., 2018; Thomas et al., 2016).

The BSP contains an older Palaeoproterozoic sequence of granitic and migmatitic gneisses belonging to the Gladkop Suite followed by younger supracrustal rocks of meta-sedimentary and meta-volcanic origin, the Bushmanland and Kamiesberg Groups, with both Palaeoproterozoic and Mesoproterozoic ages (Bailie et al., 2019; Macey et al., 2018). The Gladkop Suite is found in the north-western parts of the BSP, while the Bushmanland Group occurs to the north of the Buffels River high strain zone and the Kamiesberg Group crops out in the southern portion of the BSP (Bailie et al., 2019; Macey et al., 2018). The dominant rocks of the BSP though are Mesoproterozoic granitic gneisses of the Little Namaqualand Suite (1.21-1.19 Ga) and the Spektakel Suite (1.09-1.03 Ga) (Fig. 3.1). Both suites are highly radiogenic with modern $^{87}Sr/^{86}Sr$ ratios up to 0.90000 (Clifford et al., 1975; Yuhara et al., 2001). The Little Namaqualand Suite consists of deformed ortho-gneisses including biotite-bearing granitic augen gneisses. Several of the main plutons, including the Mesklip and Modderfontein Granitic Gneiss as well

as the Concordia Granites occur in the study area. In contrast, the Spektakel Suite, although largely similar in composition, does not contain a strong gneissic foliation and is interpreted to be late- to post-tectonic (Macey et al., 2018). Also within the BSP are large expanses of generic "pink gneiss" called the Lekkerdrink Gneiss for which the parental material is uncertain but is likely to be some type of quartzo-felspathic igneous protolith (Macey et al., 2011).

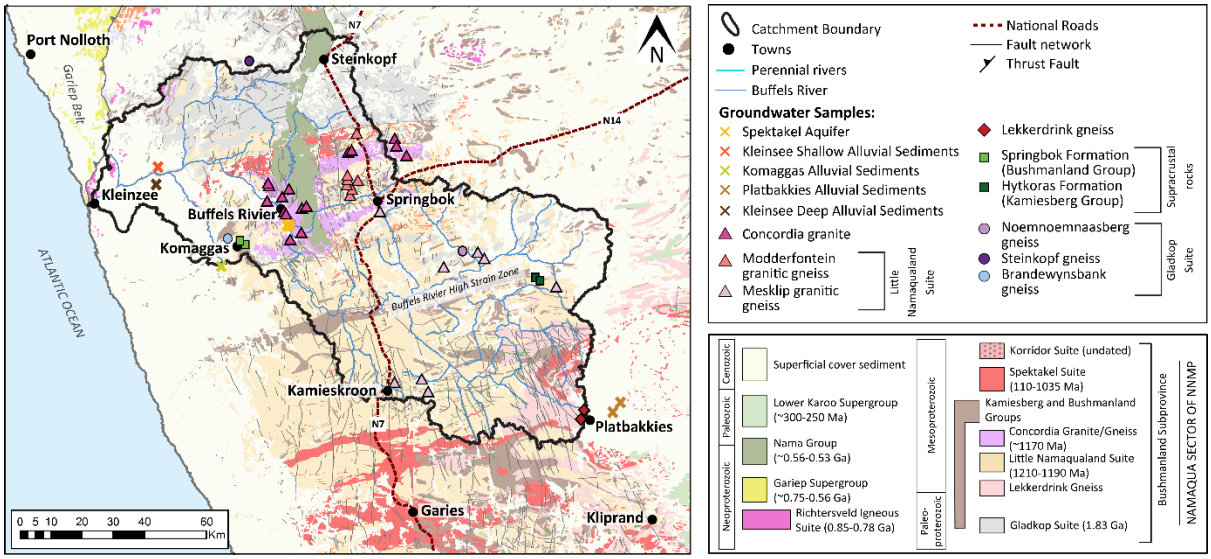

Figure 3.1: Geological map of the study area (based on Macey et al., 2018) with the Buffels River tributaries and groundwater sample locations.

Along the Buffels River valley, the granites and gneisses are capped by the Neoproterozoic to Palaeozoic sedimentary rocks of the Nama and Vanrhynsdorp Groups. These rocks crop out just to the east of the Buffels River valley, where the Buffels River has cut through the escarpment. The Nama and Vanrhynsdorp Groups consist predominantly of quartz-rich sedimentary rocks such as sandstone, siltstones, conglomerates, quartzites and shales with calcareous deposits in some areas (Gresse, 1995). These sediments were originally deposited under fluvial and marine conditions in the southern part of the Nama foreland basin which stretches into southern and central Namibia (Blanco et al., 2011).

Over the last 20-30 million years, the coastal plain along the west coast of southern Africa has experienced multiple phases of transgression and regression followed by various periods of aeolian sediment accumulation, mostly in the last 100 Ka (Roberts et al., 2009, 2006; Roberts, 2006). Kaolinized and deeply weathered quartzo-feldspathic, paleochannel and fluvial sediments forms part of the base of the sediment record and are overlain by Tertiary marine packages of the Buffels Marine Complex

dominated by quartz, feldspar and phosphatic shell fragments, that were deposited during cycles of sea-level regression forming part of the regolith (Roberts, 2006; Roberts et al., 2006). Younger aeolian sediments, including coastal dune fields originating at the mouth of river, cap the marine packages (Roberts et al., 2014, 2009; Roberts, 2006). The oldest of the aeolian sediments are the red sands stretching furthest inland on the coastal plain (Francis et al., 2007). The red sands are covered by yellow sands which forms part of an intermediate zone below the younger grey sands which are of most recent aeolian origin (Francis et al., 2007).

3.6 Hydrogeology

Groundwater in the Buffels River catchment is hosted in alluvial and fractured rock aquifer systems. The shallow alluvial aquifers result from alluvial fill discontinuities in the river valley which are further segmented into smaller aquifers by the irregular surface of the underlying basement gneisses (Benito et al., 2011b). Only two of the alluvial aquifers are thought to be of any significant size and these are the Spektakel aquifer and the Kleinsee aquifer, both of which occur in the low-lying coastal plain (Adams et al., 2004). The alluvial Spektakel aquifer is 4-20 m deep and forms part of an approximately ~15 km long sand-filled basin in the Buffels River valley at the edge of the coastal plain, underlying the town of Buffelsrivier (Benito et al., 2011b; Marais et al., 2001). Groundwater from this alluvial aquifer is the primary source of water to the town of Buffelsrivier (Adams et al., 2004; Benito et al., 2011b). The Kleinsee aquifer is also a sand-filled aquifer of approximately 12 m deep, situated at the mouth of the Buffels River. Here the aquifer feeds into the Buffels Estuary which remains relatively fresh as it is protected from the Atlantic Ocean by a sand berm which is rarely broken by the sea (Massie and Hutchings, 2018). Both of these alluvial aquifers are closely interlinked with deeper fractured bedrock aquifer systems via weathered zones that serve as pathways or conduits for subsurface intergranular flow from the shallow alluvial aquifers to the deeper granitic, gneissic and bedrock aquifers (Benito et al., 2011b; Marais et al., 2001). Although not much is known about the deeper fractured aquifer systems in the Buffels River catchment, granitic and gneissic host rocks are often associated with low primary porosity. Groundwater is therefore likely to be hosted in fractures and joint planes, which are variably interconnected and to some extent dependent on the degree of weathering as previously mentioned. This pattern likely accounts for the highly variable yield on boreholes within the catchment (Titus et al., 2009).

3.7 References

Adams, S., Titus, R., Xu, Y., 2004. Groundwater recharge assessment of the basement aquifers of central Namaqualand, WRC Report No. 1093/1.

Bailie, R., Abrahams, G., Bokana, R., van Bever Donker, J., Frei, D., le Roux, P., 2019. The geochemistry and geochronology of the upper granulite facies Kliprand dome: Comparison of the southern and northern parts of the Bushmanland Domain of the Namaqua Metamorphic Province, southern Africa and clues to its evolution. Precambrian Research 330, 58-100. https://doi.org/10.1016/j.precamres.2019.04.011

Beal, L.M., de Ruijter, W.P.M., Biastoch, A., Zahn, R., Cronin, M., Hermes, J., Lutjeharms, J., Quartly, G., Tozuka, T., Baker-Yeboah, S., Bornman, T., Cipollini, P., Dijkstra, H., Hall, I., Park, W., Peeters, F., Penven, P., Ridderinkhof, H., Zinke, J., 2011. On the role of the Agulhas system in ocean circulation and climate. Nature 472, 429-436. https://doi.org/10.1038/nature09983

Benito, G., Botero, B.A., Thorndycraft, V.R., Rico, M., Sánchez-Moya, Y., Sopeña, A., MacHado, M.J., Dahan, O., 2011a. Rainfall-runoff modelling and palaeoflood hydrology applied to reconstruct centennial scale records of flooding and aquifer recharge in ungauged ephemeral rivers. Hydrology and Earth System Sciences 15, 1185-1196. https://doi.org/10.5194/hess-15-1185-2011

Benito, G., Rohde, R., Seely, M., Külls, C., Dahan, O., Enzel, Y., Todd, S., Botero, B., Morin, E., Grodek, T., Roberts, C., 2010. Management of alluvial aquifers in two Southern African ephemeral rivers: Implications for IWRM. Water Resources Management 24, 641-667. https://doi.org/10.1007/s11269-009-9463-9

Benito, G., Thorndycraft, V.R., Rico, M.T., Sánchez-Moya, Y., Sopeña, A., Botero, B.A., Machado, M.J., Davis, M., Pérez-González, A., 2011b. Hydrological response of a dryland ephemeral river to southern African climatic variability during the last millennium. Quaternary Research 75, 471-482. https://doi.org/10.1016/j.yqres.2011.01.004

Benjaminsen, T.A., Rohde, R., Sjaastad, E., Wisborg, P., Lebert, T., 2006. Land reform, range ecology, and carrying capacities in Namaqualand, South Africa. Annals of the Association of American Geographers 96, 524-540. https://doi.org/10.1111/j.1467-8306.2006.00704.x

Biastoch, A., Böning, C.W., Schwarzkopf, F.U., Lutjeharms, J.R.E., 2009. Increase in Agulhas leakage due to poleward shift of Southern Hemisphere westerlies. Nature 462, 495-498. https://doi.org/10.1038/nature08519

Blanco, G., Germs, G.J.B., Rajesh, H.M., Chemale, F., Dussin, I.A., Justino, D., 2011. Provenance and paleogeography of the Nama Group (Ediacaran to early Palaeozoic, Namibia): Petrography, geochemistry and U-Pb detrital zircon geochronology. Precambrian Research 187, 15-32. https://doi.org/10.1016/j.precamres.2011.02.002

Carrick, P.J., Krüger, R., 2007. Restoring degraded landscapes in lowland Namaqualand: Lessons from the mining experience and from regional ecological dynamics. Journal of Arid Environments 70, 767-781. https://doi.org/10.1016/j.jaridenv.2006.08.006

Clifford, T., 2004. U-Pb Zircon Calendar for Namaquan (Grenville) Crustal Events in the Granulite-facies Terrane of the O'okiep Copper District of South Africa. Journal of Petrology 45, 669-691. https://doi.org/10.1093/petrology/egg097

Clifford, T.N., Gronow, J., Rex, D.C., Burger, A.J., 1975. Geochronological and petrogenetic studies of high-grade metamorphic rocks and intrusives in namaqualand, South Africa. Journal of Petrology 16, 154-188. https://doi.org/10.1093/petrology/16.1.154

Cornell, D.H., Thomas, R.J., Moen, H.F.G., Reid, D.L., Moore, J.M., Gibson, R.L., 2006. The Namaqua-Natal Sector, in: Johnson, M.R., Anhaeusser, C.R., Thomas, R.J. (Eds.), The Geology of South Africa. Geological Society of South Africa, Johannesburg/Council for Geoscience, Pretoria, pp. 325-381.

Cousins, B., Hoffman, M.T., Allsopp, N., Rohde, R.F., 2007. A synthesis of sociological and biological perspectives on sustainable land use in Namaqualand. Journal of Arid Environments 70, 834-846. https://doi.org/10.1016/j.jaridenv.2007.04.002

Cramer, M.D., Midgley, J.J., 2015. The distribution and spatial patterning of mima-like mounds in South Africa suggests genesis through vegetation induced aeolian sediment deposition. Journal of Arid Environments 119, 16-26. https://doi.org/10.1016/j.jaridenv.2015.03.011

Davis, C.L., Hoffman, M.T., Roberts, W., 2016. Recent trends in the climate of Namaqualand, a megadiverse arid region of South Africa. South African Journal of Science 112, 1-9. https://doi.org/10.17159/sajs.2016/20150217

Francis, M.L., 2008. Soil Formation on the Namaqualand Coastal Plain.

Francis, M.L., Ellis, F., Lambrechts, J.J.N., Poch, R.M., 2013. A micromorphological view through a Namaqualand termitaria (Heuweltjie, a Mima-like mound). Catena 100, 57-73. https://doi.org/10.1016/j.catena.2012.08.004

Francis, M.L., Fey, M. V., Prinsloo, H.P., Ellis, F., Mills, A.J., Medinski, T. V., 2007. Soils of Namaqualand: Compensations for aridity. Journal of Arid Environments 70, 588-603. https://doi.org/10.1016/j.jaridenv.2006.12.028

Gresse, P.G., 1995. Transpression and transection in the late Pan-African Vanrhynsdorp foreland thrust-fold belt, South Africa. Journal of African Earth Sciences 21, 91-105. https://doi.org/10.1016/0899-5362(95)00089-C

Hoffman, M.T., Rohde, R.F., 2007. From pastoralism to tourism: The historical impact of changing land use practices in Namaqualand. Journal of Arid Environments 70, 641-658. https://doi.org/10.1016/j.jaridenv.2006.05.014

Macey, P. H., Bailie, R.H., Miller, J.A., Thomas, R.J., de Beer, C., Frei, D., le Roux, P.J., 2018. Implications of the distribution, age and origins of the granites of the Mesoproterozoic Spektakel Suite for the timing of the Namaqua Orogeny in the Bushmanland Subprovince of the Namaqua-Natal Metamorphic Province, South Africa. Precambrian Research 312, 68-98. https://doi.org/10.1016/j.precamres.2018.02.026

Macey, P.H., Siegfried, H.P., Minnaar, H., Almond, J., P.M.W, B., 2011. The geology of the Loeriesfontein area. 1: 250 000 map sheet explanation3018. Council for Geoscience.

Marais, J.A.H., Agenbacht, A.L.D., Prinsloo, M., Basson, W.A., 2001. The Geology of the Springbok Area Explanation: Sheet 2916.

Massie, V., Hutchings, K., 2018. Proposed upgrades to the Diamond Coast Aquaculture facility Kleinzee, Northern Cape – Final basic assessment report. Appendix F: Environmental Impact Assessment. https://doi.org/10.1007/978-3-319-58418-8_13

Midgley, J.J., Harris, C., Hesse, H., Swift, A., 2002. Heuweltjie age and vegetation change based on * 13 C and 14 C analyses. South African Journal of Science 98, 202-204.

Mucina, L., Rutherford, M.C., 2006. The vegetation of South Africa, Lesotho and Swaziland., Strelitzia 19 The vegetation of South Africa, Lesotho and Swaziland. South African National Biodiversity Institute, Pretoria. https://doi.org/10.1007/s

Partridge, T.C., 1998. Of diamonds, dinosaurs and diastrophism: 150 million years of landscape evolution in southern Africa. South African Journal of Geology 101, 167-184.

Partridge, T.C., Maud, R.R., 1987. Geomorphic evolution of southern Africa since the Mesozoic. South African Journal of Geology 90, 179-208.

Picker, M.D., Hoffman, M.T., Leverton, B., 2007. Density of Microhodotermes viator (Hodotermitidae) mounds in southern Africa in relation to rainfall and vegetative productivity gradients. Journal of Zoology 271, 37-44. https://doi.org/10.1111/j.1469-7998.2006.00189.x

Pietersen, K., Titus, R., Cobbing, J., 2009. Effective Groundwater Management in Namaqualand Sustaining Supplies, Effective Groundwater Management in Namaqualand Sustaining Supplies.

Roberts, D., Bateman, M., Murray-Wallace, C., Carr, A., Holmes, P., 2009. West coast dune plumes: Climate driven contrasts in dunefield morphogenesis along the western and southern South African coasts. Palaeogeography, Palaeoclimatology, Palaeoecology 271, 24-38. https://doi.org/10.1016/j.palaeo.2008.09.009

Roberts, D., Cawthra, H., Musekiwa, C., 2014. Dynamics of late cenozoic aeolian deposition along the South African coast: A record of evolving climate and ecosystems. Geological Society Special Publication 388, 353-387. https://doi.org/10.1144/SP388.11

Roberts, D.L., 2006. Lithostratigraphy of the Sandveld Group. S. Afr. Committee Stratigr. Lithostratigraphic Ser 9, 25-26.

Roberts, D.L., Botha, G.A., Maud, R.R., Pether, J., 2006. Coastal Cenozoic deposits. The Geology of South Africa. Geological Society of South Africa, Johannesburg/Council for Geoscience, Pretoria 605-628.

Roberts, G.G., White, N., 2010. Estimating uplift rate histories from river profiles using African examples. Journal of Geophysical Research: Solid Earth 115, 1-24. https://doi.org/10.1029/2009JB006692

Thomas, D.H., Gibson, R.J., Moen, R., Moore, H.F.G.J.M., Reid, D.L., Johnson, N.P., The, R.J., Thomas, B., Cornell, D.H., 2016. Geology of South Africa.

Titus, R., Beekman, H., Adams, S., Strachan, L., 2009. The Basement Aquifers of Southern Africa, WRC Report No. TT428/09. South Africa.

Weldeab, S., Stuut, J.B.W., Schneider, R.R., Siebel, W., 2013. Holocene climate variability in the winter rainfall zone of South Africa. Climate of the Past 9, 2347-2364. https://doi.org/10.5194/cp-9-2347-2013

Yuhara, M., Kagami, H., Tsuchiya, N., 2001. Rb-Sr and Sm-Nd systematics of granitic and metamorphic rocks in the Namaqualand Metamorphic Complex, South Africa:Implications for evolution of marginal part of Kaapvaal craton. Memoirs of National Institute of Polar Research. Special issue 55, 127-144.

Zhao, X., Dupont, L., Schefuß, E., Meadows, M.E., Hahn, A., Wefer, G., 2016. Holocene vegetation and climate variability in the winter and summer rainfall zones of South Africa. Holocene 26, 843-857. https://doi.org/10.1177/0959683615622544

4 GROUNDWATER ANALYTICAL TECHNIQUES

4.1 Water

4.1.1 EC, pH and Alkalinity

In the laboratory, EC of both groundwater and water extracts was measured using a Jenway 4510 conductivity probe. Alkalinity and pH were measured by means of a 702 SM Titrino auto-titrator. For groundwater samples, field EC and pH results were compared to the lab results to ensure that the results were coherent.

4.1.2 Major Cation and Anions

Major cations were initially analysed at the ICER laboratories in Debrecen, Hungary by means of an Agilent 8800 ICP-MS MP-AES and an Agilent 4100. Sr and a duplicate set of basic cation analyses were completed in the Central Analytical Facility (CAF) at Stellenbosch University, South Africa by means of an Agilent 7700 ICP-OES. The basic cation analyses done at the CAF laboratories were used for quality control purposes. Anion analyses were completed at the ICER facilities in Hungary by means of ion chromatography. 75% of the samples had a charge balance better than 10% with the average charge balance across the dataset being -5.65. Nitrate was not collected as part of this study.

4.1.3 $\delta^{18}O$ and $\delta^{2}H$ Ratios

Stable isotopes of oxygen and hydrogen were determined using a Los Gatos LWIA at ICER, Debrecen and reported as $\delta^{18}O$ and $\delta^{2}H$ in standard per mill (‰) notation. Internal institute water standards are calibrated to the V-SMOW, SLAP and GISP standards and reported relative to VSMOW. Analytical uncertainties of the measurements were 0.1‰ and 1.2‰ for $\delta^{18}O$ and $\delta^{2}H$ respectively.

4.1.4 $^{87}Sr/^{86}Sr$ Ratios

Strontium isotope sample preparation and analyses were performed at the University of Cape Town, South Africa. Based on Sr elemental concentration, appropriate volumes of individual groundwater samples were dried down, typically 2-10 ml. A few drops of concentrated HNO_3 was added to the resulting precipitate from each aliquot, followed by a second drying cycle. Finally, 1.5 ml of 2M HNO_3 was added to each Teflon vial and samples loaded onto Sr.Spec columns for standard Sr elemental separation chemistry (after Pin et al., 1994). The collected Sr fractions were dried down, re-dissolved in 0.2% HNO_3 and diluted to Sr concentrations of ±200 ppb. Samples were analysed for $^{87}Sr/^{86}Sr$ ratios using a NuPlasma HR multi-collector-ICP-MS and all data referenced to bracketing analysed of NIST SRM 987 using a $^{87}Sr/^{86}Sr$ reference value of 0.710255. The $^{87}Sr/^{86}Sr$ data are corrected for instrumental mass

fractionation using the measured $^{86}Sr/^{88}Sr$ ratios, a known value for this ratio of 0.1194 and the exponential law. The isobaric interference of ^{87}Rb at 87amu is corrected using the measured signal for ^{85}Rb and the natural $^{85}Rb/^{87}Rb$ ratio.

4.1.5 Tritium

Tritium was analysed at the Isotope Climatology and Environmental Research Centre (ICER), Debrecen, Hungary via the ^{3}He ingrowth method with ^{4}He isotope dilution (Palcsu et al., 2010; Papp et al., 2012). The process can be simplified to four steps; (1) distillation of water samples, (2) removal of all dissolved gasses through vacuum pumping, (3) storage of samples in stainless steel vessels for several months during which tritium decay occurs, producing ^{3}He atoms, and (4) measurement of ^{3}He through admitting the helium fraction that was produced to the dual collector noble gas mass spectrometer (Helix SFT). The tritium concentration is calculated using the abundance of tritogenic helium isotopes. The average analytical uncertainty recorded during analysis of tritium was 0.072 TU.

4.1.6 $\delta^{13}C$ and Radiocarbon

$\delta^{13}C$ values were determined using a Delta^{PLUS} XP isotope ratio mass spectrometer equipped with a Gasbench-II at ICER. During sample preparation, groundwater samples were placed in a separatory funnel with NaOH. $BaCl_2$ was added to form a cloudy solution, which includes a mixture of $BaCO_3$ and $BaSO_4$, and set aside for the precipitate to accumulate at the base of funnel. The wet precipitate was extracted and washed with ultra-pure water until a neutral pH was reached. Contact with atmosphere was kept to a minimum throughout the process. Samples were freeze dried after which 1 mg of the sample was placed in the GasBench II equipment to continue the process in a closed system. Phosphoric acid was added to the dried precipitate and the CO_2 is released in the GasBench II equipment and carried by a helium flow to the mass spectrometer. $\delta^{13}C$ values are reported relative to the V-PBD (Vienna Pee Dee Belemnite) standard and had an analytical uncertainty of 0.1 ‰. Further explanations of the analytical methods used for $\delta^{13}C$ in this study are available in Varsányi et al. (2011).

The remaining precipitate of the sample was used for radiocarbon analysis. The samples were treated with phosphoric acid while in a closed vacuum in order to release carbon as carbon dioxide. Water was injected into the pre-vacuumed digestion reactor vessel through a septum-sealed cap by means of a sterile plastic syringe attached to a 0.45 um pore size membrane filter to filter out the particles from the samples during injection. Samples were heated for one hour at 80°C to allow for most of the carbon-dioxide release. The released CO_2 gas was then transferred into a cleaning vacuum line, where all other gases were removed according to Molnár et al. (2013). In the vacuum line, the water is trapped in a dry ice trap, the CO_2 is trapped in a liquid nitrogen trap and all other gases are pumped away. The obtained pure CO_2 gas was then converted to graphite by sealed tube graphitization method (Rinyu et al., 2013).

The ^{14}C measurements from the graphite targets were performed with a MICADAS accelerator mass spectrometer in the ICER laboratory. Fossil marble, as blank standard material (IAEA-C1, 0.0 pMC) and known age travertine reference material (IAEA-C2, 41.14 pMC) were also treated as control samples for the CO_2 extraction step, to determine if any modern/fossil carbon contamination is introduced during the extraction or graphitisation procedure. The overall measurement uncertainty for modern samples was < 3.0 ‰, including normalization, background subtraction, and counting statistics.

4.1.7 $\delta^{34}S\ SO_4^{2-}$ and $\delta^{18}O\ SO_4^{2-}$

A groundwater sample of 500 ml was placed into a separatory funnel and 1 mg of NaOH was added. The solution was mixed thoroughly before 5-7 ml of BaCl2 was added to form a cloudy solution. It was set aside for the precipitate to accumulate at base of funnel. The wet precipitate was extracted into clean separation funnel and washed with MiliQ water. The washing process was repeated until a pH is of between 6 and 7 was reached. The samples were then frieze dried before the samples were analysed using the same equipment mentioned in section 4.1.3.

4.2 Soils

4.2.1 $\delta^{13}C\ CO_3^{2-}$ and $\delta^{18}O\ CO_3^{2-}$ in Soils

For $\delta^{13}C$ analysis, the sample was placed in the GasBench II equipment extraction device. Phosphoric acid was added to the dried precipitate and the CO_2 was released from where the released CO_2 gas was admitted to the Delta Plus XP isotope ratio mass spectrometer by helium as a carrier gas via an open split interface. Organic samples were converted to CO_2 by an Isolink elemental analyser, and the CO_2 sample gas was admitted to the mass spectrometer via a ConFlow-IV interface. In both cases $\delta^{13}C$ values are reported relative to the V-PBD (Vienna Pee Dee Belemnite) standard and had an analytical uncertainty of 0.15 ‰. Further explanations of the analytical methods used for $\delta^{13}C$ in this study are available in Varsányi et al. (2011).

4.2.2 Radiocarbon in Soils

To analyse the organic carbon fraction, all inorganic carbonate material had to be removed. This was done by reacting a 10g sample with 20 ml of 10% HCl in sterile polypropylene conical tube. The samples were set aside until little to no gas formation was visible, based on visual inspection (fizzing). In cases where samples contained larger concentrations of carbonates and the reaction continued, samples were centrifuged for 3-5 min at 4000 RMP and refilled with 20 ml of 10% acid. This process was repeated until reaction was complete and no gas formation was observed. Once gas formation has stopped, samples were centrifuged before the acid was decanted and the samples were washed with

ultra-pure water until pH was between 5 and 7. Samples were centrifuged for 3-5 min at 4000 RPM between each wash. Samples were oven dried over night at 60°C in same tube. Before analysis, the organic samples were treated once more using the standard acid-base-acid (ABA) method, with a sequence of 1N HCl, distilled water, 1M NaOH, distilled water, and then 1N HCl (Jull, 2006). For bulk samples, only the acid treatment was used. After the final acid wash, bulk samples were washed again with distilled water to neutral pH (4-5) and then dried. Samples were then ready for two-step and MnO_2 combustion.

For combustion and CO_2 purification of all soil samples, an in-line combustion and CO_2 purification system was used (Jull, 2006; Molnar et al., 2013) involving two stages of heating, low temperature heating at 400°C, and high temperature at 800°C. Heating is done in the presence of 5.0 quality oxygen gas for the precise temperature-stabilized gradual fractional oxidation of sediment and bulk samples. The carbon dioxide is cryogenically separated from water at -78°C trap and passed over Cu/Ag column for purification and trapped in a known volume at liquid nitrogen temperature. The gas pressure is measured in a known volume, to calculate the yield, and the purified CO_2 gas sample is transferred to a sealed tube for graphitization.

In the case of the shells a two-finger flask with a special valve was used to react the sample with phosphoric acid. Samples were placed in the standing finger and the phosphoric acid in the other. After closing the flask, the acid (85% H_3PO_4) was be poured onto the sample to produce CO_2. The CO_2 produced from the carbonate in the sample was introduced into the in-line combustion/CO_2 purification system through the valve (Molnar et al., 2013). After purification, CO2 gas captured in a tube before it was sealed and sent for graphitization. All the AMS graphite targets were prepared by a sealed tube graphitization method at HEKAL (Rinyu et al., 2013).

The ^{14}C measurements were performed from the graphite targets with a MICADAS accelerator mass spectrometer in the ICER laboratory. Fossil marble (IAEA-C1, 0.0 pMC) and known age travertine reference material (IAEA-C2, 41.14 pMC) were used a blank standard material and a control sample, respectively. This was done to determine if any modern/fossil carbon contamination is introduced during the extraction or graphitisation procedure. The overall measurement uncertainty for modern samples was < 3.0 ‰, including normalization, background subtraction, and counting statistics.

4.2.3 $\delta^{34}S\ SO_4^{2-}$ and $\delta^{18}O\ SO_4^{2-}$

10 g of sediment was washed with 20 ml of 5% HCl to remove any carbonates. The supernatant was then filtered through a 0.45µm cellulose acetate filter into glass beaker. Milli-Q water was added to the solution in the beaker to make up a solution of 150 ml. $BaCl_2$ was added with a dropper and the solution was swirled and was set aside until a precipitate ($BaSO_4$) has formed and supernatant is clear. The

supernatant was discarded, and the precipitate, containing the sulphate, was washed Milli-Q water until pH was neutral. The precipitate was oven dried at 60°C for approximately 12 hours until it was completely dry. $\delta^{18}O\text{-}SO_4$ and $\delta^{34}S\text{-}SO_4$ were analysed using a DeltaPLUS XP stable isotope ratio mass spectrometer equipped with a Flash Isolink elemental analyser (Thermo Scientific).

4.3 References

Jull, A.J.T., 2006. Radiocarbon dating| AMS method, in: Encyclopedia of Quaternary Science. Elsevier Science Ltd., pp. 2911-2918.

Molnár, M., Rinyu, L., Veres, M., Seiler, M., Wacker, L., Synal, H.-A., 2013. EnvironMICADAS : a mini 14C AMS with enhanced gas ion source. Radiocarbon 55, 338-344. https://doi.org/10.2458/azu_js_rc.55.16331

Palcsu, L., Major, Z., Köllő, Z., Papp, L., 2010. Using an ultrapure 4He spike in tritium measurements of environmental water samples by the 3He-ingrowth method. Rapid Commun. Mass Spectrom. 24, 698-704. https://doi.org/10.1002/rcm

Papp, L., Palcsu, L., Major, Z., Rinyu, L., Tóth, I., 2012. A mass spectrometric line for tritium analysis of water and noble gas measurements from different water amounts in the range of microlitres and millilitres. Isotopes Environ. Health Stud. 48, 494-511. https://doi.org/10.1080/10256016.2012.679935

Rinyu, L., Molnár, M., Major, I., Nagy, T., Veres, M., Kimák, Á., Wacker, L., Synal, H.A., 2013. Optimization of sealed tube graphitization method for environmental C-14 studies using MICADAS. Nucl. Instruments Methods Phys. Res. Sect. B Beam Interact. with Mater. Atoms 294, 270-275. https://doi.org/10.1016/j.nimb.2012.08.042

Varsányi, I., Palcsu, L., Kovács, L.Ó., 2011. Groundwater flow system as an archive of palaeotemperature: Noble gas, radiocarbon, stable isotope and geochemical study in the Pannonian Basin, Hungary. Appl. Geochemistry 26, 91-104. https://doi.org/10.1016/j.apgeochem.2010.11.006

5 CHARACTERISATION OF HEUWELTJIE SOIL PROFILES

By M Vermooten, C.E. Clarke, M.L. Francis, J. van Gend, A. Watson, J.A. Miller

5.1 Introduction

In this part of the report, cross-sections of two heuweltjies, in the Buffels River catchment, were characterised to determine the salt type and concentration profiles to the maximum possible excavation depth. In addition, the relationship between salt accumulations and major termite-related features within the heuweltjie were documented in order to understand the potential reason(s) for the elevated salinity on these mounds.

5.2 Study Location

The study site is located in the Buffels River valley in Namaqualand, 43 km west of Springbok near town of Buffelsrivier (Figure 5.1a). The soils of the region range from shallow leptosols (Classification: IUSS Working Group WRB, 2015) on the closed hills and mountains (1000 amsl) and shallow alluvial and colluvial topsoils underlain by petroduric (dorbank) horizons in the valley bottoms (Francis et al., 2007). The investigation area is located in sandy sediments of the Buffels River floodplain underlain by the Little Namaqualand and Spektakel Suite granites and granite gneisses (Macey et al., 2018).

5.3 Heuweltjie Selection and Sample Collection

Fourteen heuweltjies and adjacent interheuweltjie soils were collected and screened for EC and pH. From these, two heuweltjies were selected for excavation (Figure 5.1b). The final site selection was based on screening results as well as excavator access. Trenches of up to 58 m were excavated through the centre of two heuweltjies (H1 and H4) into the adjacent interheuweltjie soils to a depth of approximately 2-3 m in the heuweltjie centre (figure 5.1c). The trenches were dug in a downslope direction (East-West). Both heuweltjies were situated on a mid to lower footslope position.

Samples were collected from the north wall of both heuweltjie trenches. Approximately 200 g of sample was collected for each soil horizon at 1 m intervals along the trench wall. Detailed sampling was conducted for 10 profiles in H1 (located at 0 m, 2 m, 4 m, 13 m, 16 m, 20 m, 24 m, 25 m, 32 m and 35 m from the west end) and 5 profiles in H4 (located at 19 m, 22 m, 32 m, 38 m and 42 m from the west end) by taking 3 kg bulk samples of each horizon for mineralogy and saturated paste analyses. Termite related features, such as channels and nests were also sampled.

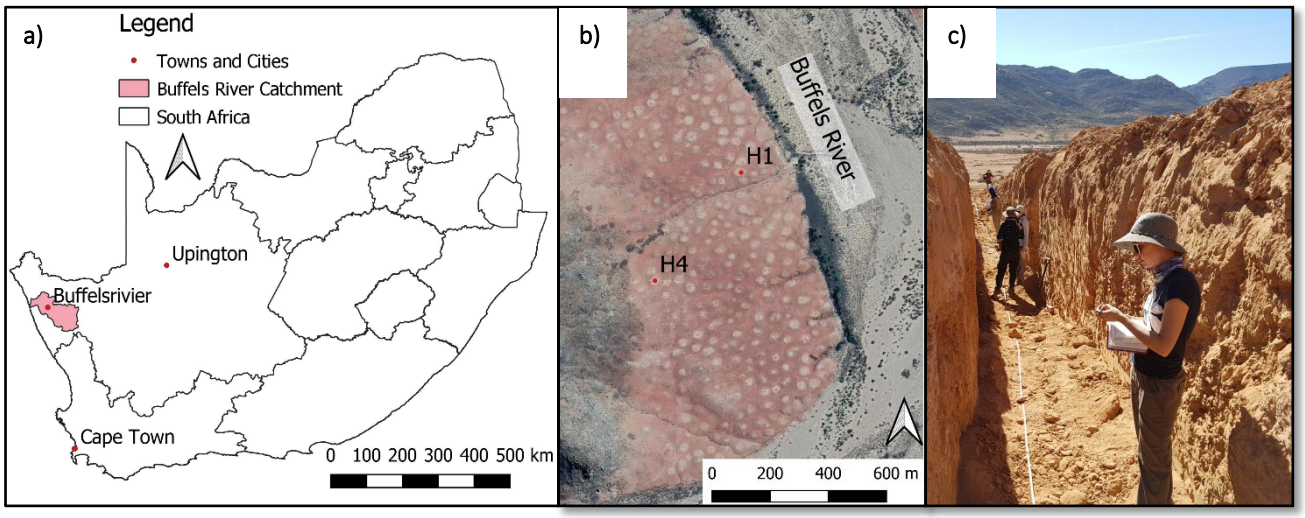

Figure 5.1: The location of Buffels River Catchment within South Africa a), the selected heuweltjies in the sandy sediments of the Buffels River b), and the trench excavated through H1 in an east-west direction c).

5.4 Physical and Chemical Soil Analysis

Samples were air-dried, crushed with a pestle and mortar to ensure no cemented soil fragments remained and sieved through a 2 mm sieve. Soil pH and EC were analysed in a 1:2.5 soil: deionised water (DI) ratio. The EC was converted to a 1:5 soil solution equivalent following the method outlined by Sonmez *et al.* (2008). Soil texture was measured on the representative profiles selected for detailed analysis (33 samples). Texture analysis was conducting using the sedimentation method described by the Soil Classification Working Group (1991) after all organic matter, carbonates and amorphous silica cement had been removed.

The samples prepared for texture analysis were used in the extraction of the clay phase for mineralogical analysis. This was achieved by agitating the samples and syphoning off the suspension above 10 cm from the suspension surface after 8 hours of sedimentation. The extracted volume was replaced by DI water and the procedure repeated until sufficient clay was extracted. The clay suspensions were suction filtered through ceramic discs. Each sample was split in two, and one was washed with 1 M $MgCl_2$ solution and the other with 2 M KCl solution. The samples were washed with deionised water to remove excess salts and left to dry. XRD analysis was conducted on the randomly orientated powders with a step-size of 0.05 degrees and a step-time of 40 seconds using a Bruker D8 Advance Powder Diffractometer with a graphite monochromator, 40 mA and 40kV at iThemba LABS.

A 1:1 soil: DI water extract was prepared from both the grid samples (selecting profiles every second meter) and the 15 representative profiles from both heuweltjies. The samples were shaken for an hour,

as outlined by Rhoades (1996), and extracted through suction filtration with Buchner funnels, collecting the water in plastic containers. The samples were further filtered with 0.45 µm cellulose acetate filters. Major anions (Cl^- and SO_4^{2-}), were analysed via ion chromatography at Integral Laboratories, while cations were analysed using ICP-AES at the Central Analytical Facility at Stellenbosch University. Alkalinity was measured using a 702 SM Titrino automatic titrator with a standard 0.1 M HCl solution. Phosphate analysis was performed colorimetrically following the procedure outlined by Murphy & Riley (1962). Dissolved silica was analysed using the blue silicimolybdous method outlined by Jones and Dreher (1996).

5.5 Soil Solution Modelling and Data Interpolation

Major anion and cation data was modelled using PHREEQC Interactive Version 3.4.0 (Parkhurst and Appelo, 2013) to determine solute speciation and the saturation index (SI) of various mineral phases. PHREEQC uses ion-association and Debye Hückel expressions fitted for the major ions using chloride mean-salt activity-coefficient data to extend the range of applicability of the aqueous model up to ionic strengths of sea water (Parkhurst and Appelo, 1999). According to the PHREEQC calculation for seawater by Nordstrom *et al.* (1979), seawater has an ionic strength of 0.67. Speciation calculations showed that the ionic strength of the soil extracts ranged from 0.002 to 0.620, and hence all fell below that of seawater. The 1:1 extractions correspond to the sodium chloride dominance criteria of PHREEQC. This suggests that the additional Specific Ion Interaction (*sit.dat*) activity coefficient model was satisfactory for performing speciation calculations in these soils.

Major ion data, pH, EC, and SI values from point data were interpolated using kriging and linear variograms in Surfer® to create vertical cross-section heat maps.

5.6 Results

5.6.1 Termite Activity and Features

5.6.1.1 Heuweltjie H1

Active *Microhodotermes viator* were present on the surface and throughout the heuweltjie at cross section distances 2 m, 16 m, 20 m, 24 m, 25 m, and 32 m from the west. Two termite nests or hives and one storage chamber were present in the centre of the heuweltjie (*Figure 5.2*).

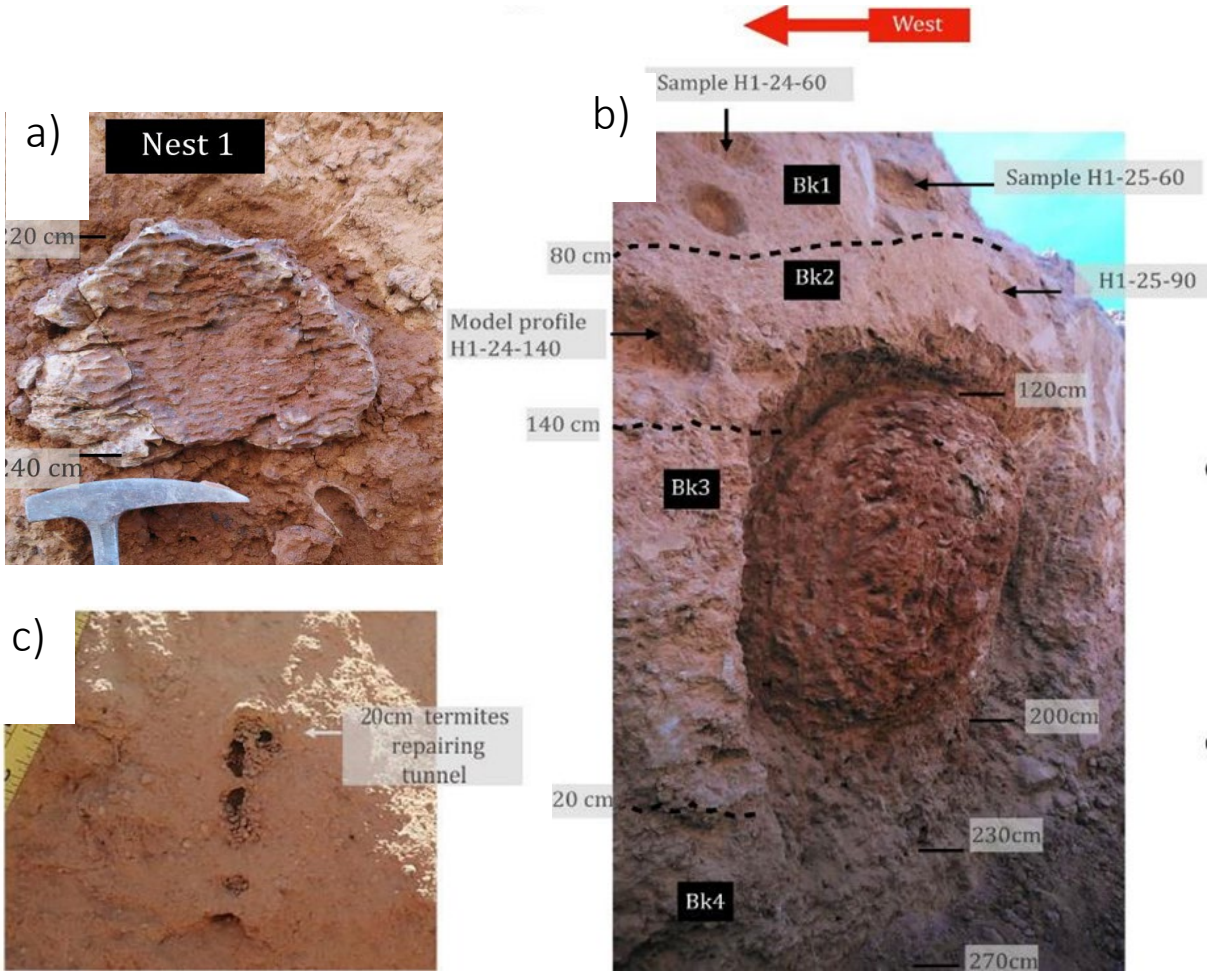

Figure 5.2: Termite features from H1 showing a) H1-24 small nest b) H1-25 large nest and c) H1-32 termite repairing tunnel with 2 mm diameter microaggregates of soil.

The smaller nest (hive) was situated at 220 cm deep at cross-section distance 24 m. The nest was 30 cm wide, 18 cm high, calcareous and very firm throughout (*Figure 5.2*a). The larger nest at cross-section distance 25 m was oval in shape, 110 cm x 80 cm in diameter, tapering downwards, with a 3-5 cm thick very hard calcareous coating (*Figure 5.2*b). Below the nest was a highly bioturbated, much indurated calcareous layer (200-230 cm depth), possibly part of the nest. The material inside the hard carapace of the nest was calcareous, loose, with a strongly developed granular structure (1 mm granules), with fine white gypsum precipitates. Both the shell and filling contained many tunnels 1 cm in diameter. The filling was mottled (1 cm in diameter) and moister than the surrounding soil. The particle size distribution of the nest filling at 160 cm depth was similar to the overlying surrounding horizons and contained more clay than the underlying horizons (*Table 5.1*). At cross-section distance 32 m, there was a 5 x 7 cm food storage chamber at 40 cm depth, and 20 cm above it, tunnels being actively repaired by termites using freshly prepared, moist 1-2 mm diameter aggregated granules of the adjacent soil that dried very quickly (*Figure 5.2*c).

5.6.1.2 Heuweltjie H4

Four nests were spread out throughout the heuweltjie structure. At cross-section distance 19 m, at 110 cm depth, a friable non-calcareous nest 18 cm diameter was set in surrounding indurated, non-calcareous, gypsic petroduric horizons. The nest was slightly moister and contained twice as much silt- as the surrounding soil (*Table 5.1*), with few mottles, a granular structure and many indurated 8 mm diameter burrows. At cross-section distance 32 m, a non-calcareous 30 cm diameter nest was located 60 cm deep between an overlying calcic horizon and underlying non-calcareous petroduric horizon with gypsum. The nest contained more clay than the surrounding horizons, and more silt than the underlying horizon. At cross-section distance 41.5, there were two non-calcareous ca. 25 cm diameter nests 30 cm apart at 80 cm and 95 cm depths. The nests were situated between an upper weakly indurated calcic horizon and a lower weakly indurated duric horizon. The nests were moister and finer textured than the surrounding dry soil. Below the nests (120 cm depth), tunnels 1-2 cm diameter were lined with clay and organic matter in very fine layers orientated parallel to the tunnel wall (*Figure 5.3*). Active *M. viator* were observed around both the nests.

At 42 m on the south wall, between two non-calcareous petroduric horizons there was an oval shaped, non-calcareous nest with a 3-5 cm thick, very hard, non-calcareous carapace on outer edge of nest (*Figure 5.4*) *M. viator* termites were active in the nest along inner edge of lining and there were many 12 mm diameter tunnels inside the nest. Some tunnels were partially filled with 1-2 mm diameter granules of aggregated soil. The nest filling was moist; the surrounding soil outside was dry. The nest contained more silt and clay than the upper and lower horizons (*Table 5.1*).

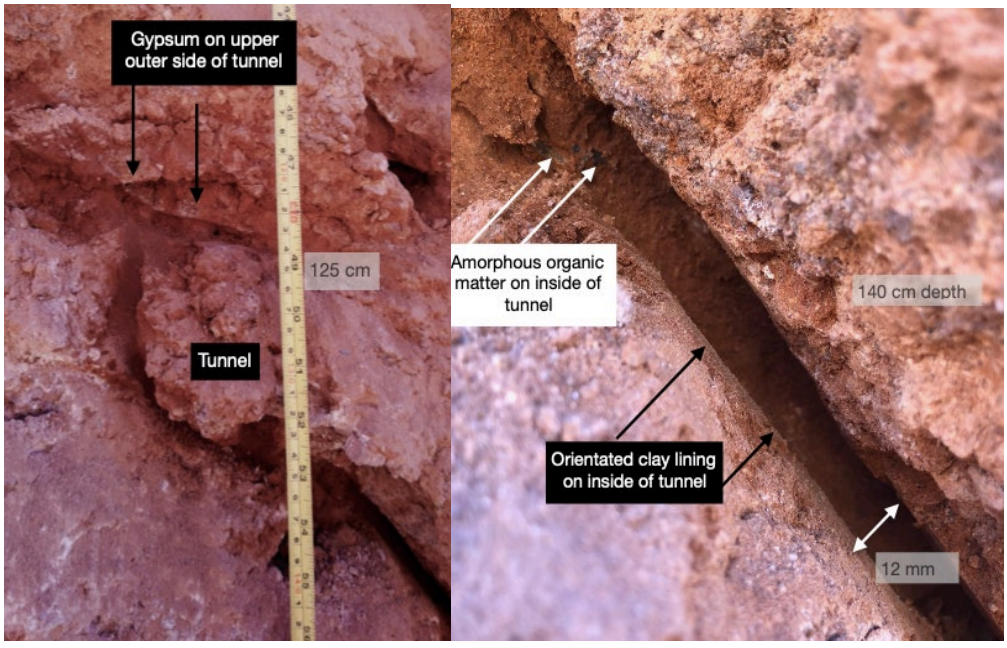

Figure 5.3: Examples of tunnels from H4.

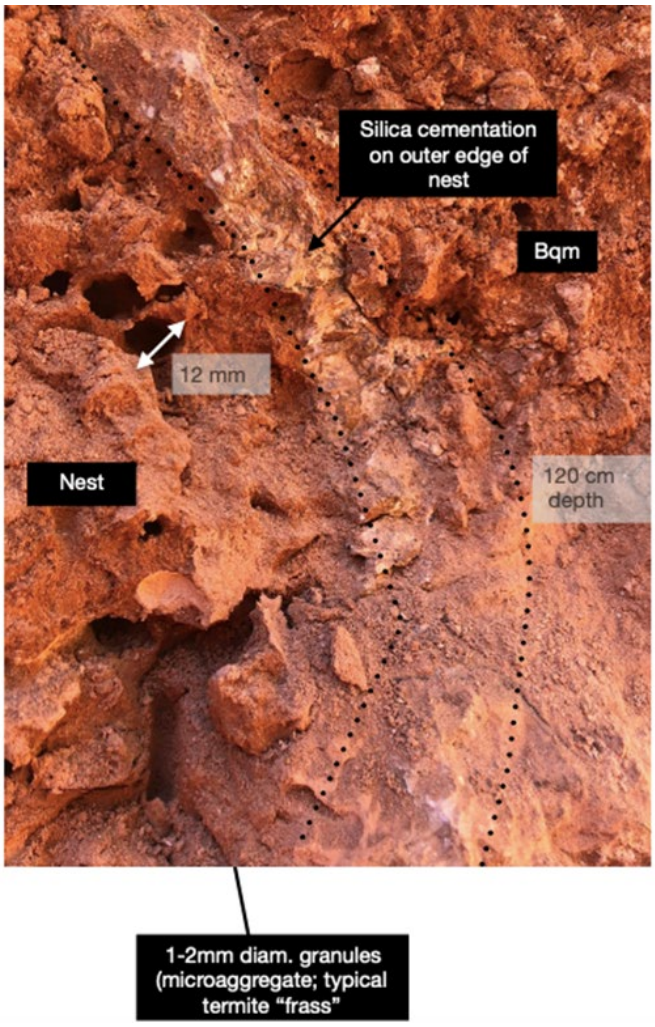

Figure 5.4: Edge of nest structure from H4 showing silica cemented outer edge

5.6.2 Texture

The outer edges of the mound had a soil texture that fined downwards (4 m cross section distance, Table). In contrast, the parts of the heuweltjies associated with nests or other termite activity in the profiles showed a general fining up texture and the nests tended to contain more silt and clay than their underlying horizons (*Table 5.1*). The nests were finer than both their upper and lower surrounding horizons (*Table 5.1*). No textural discontinuities were observed, possibly due to the bioturbation associated with the termite activity.

Table 5.1: Texture data for select profiles from H1 and H4. Cross-section depth from the west.

Heuweltjie	Cross-section distance (m)	Lower depth (cm)	% Sand	% Silt	% Clay	% Silt+Clay
H1	4	10	93	4	3	7
H1	4	38	86	9	6	14
H1	4	50	79	21	0	21
H1	13	40	54	34	12	46
H1	13	50	62	30	8	38
H1	13	110	94	5	1	6
H1	24	5	53	36	12	47
H1	24	30	54	34	13	46
H1	25	160 nest	51	34	15	49
H1	24	220	64	28	9	36
H1	24	270	63	34	3	37
H1	32	76 chamber	63	33	4	37
H1	32	90	75	18	7	25
H1	32	123	65	31	4	35
H1	32	200	95	2	3	5
H4	19	10	67	30	3	33
H4	19	30	68	32	0	32
H4	19	60	80	18	2	20
H4	19	60	49	42	9	51
H4	19	110	86	11	3	14
H4	19	110 nest	74	22	4	26
H4	19	160	92	8	0	8
H4	32	10	70	23	6	30
H4	32	30	65	29	6	35
H4	32	60 nest	70	21	9	30
H4	32	80	80	16	4	20
H4	32	80	88	10	2	12
H4	32	100	80	15	5	20
H4	32	130	61	31	9	39
H4	42	30	64	29	7	36
H4	42	50	85	13	2	15
H4	42	110 nest	63	28	9	37
H4	42	150	89	9	2	11

5.6.3 Soil Horizons

Most of the upper horizons at the center of heuweltjies were loose horizons of calcite accumulation, while the soils at the edges were non-calcareous and showed a weak development of structure and colour. Calcite nodules separated the lower cemented horizons from the top calcic horizons (*Figure 5.5* and *Figure 5.6*). The cemented soils ranged from calcite cemented (petrocalcic) closer to the edges of the heuweltjie to silica cemented (petroduric) horizons closer to the center of the heuweltjie structure. Gypsum was present as loose white powdery accumulations in the horizons immediately below the calcite nodules and was commonly associated with the petroduric lower horizons (*Figure 5.5* and *Figure 5.6*). Below ca 2 m the horizons were much indurated, with rounded and angular cobbles (colluvium, alluvium) up to 15 cm diameter. The interheuweltjie soils were non-calcareous and did not contain gypsum. They consisted of a loose apedal horizon 30 cm to 40 cm thick overlying a petroduric horizon. Manganese oxides (effervescence in 10% H_2O_2) were common on the silica-cemented horizons.

5.6.4 Clay Mineralogy

A summary of the mineralogy of the clay phase extracted from interheuweltjie and heuweltjie soils is presented in *Table 5.2*. The clay fraction of the heuweltjie and interheuweltjie is mostly fine-grained quartz, followed by illite and kaolinite. Calcite and gypsum are common in the heuweltjie soils. In H4, whewellite (Ca-oxalate) was identified in a number of horizons and hydroxyapatite was identified in one silica-cemented horizon (H4-19-60).

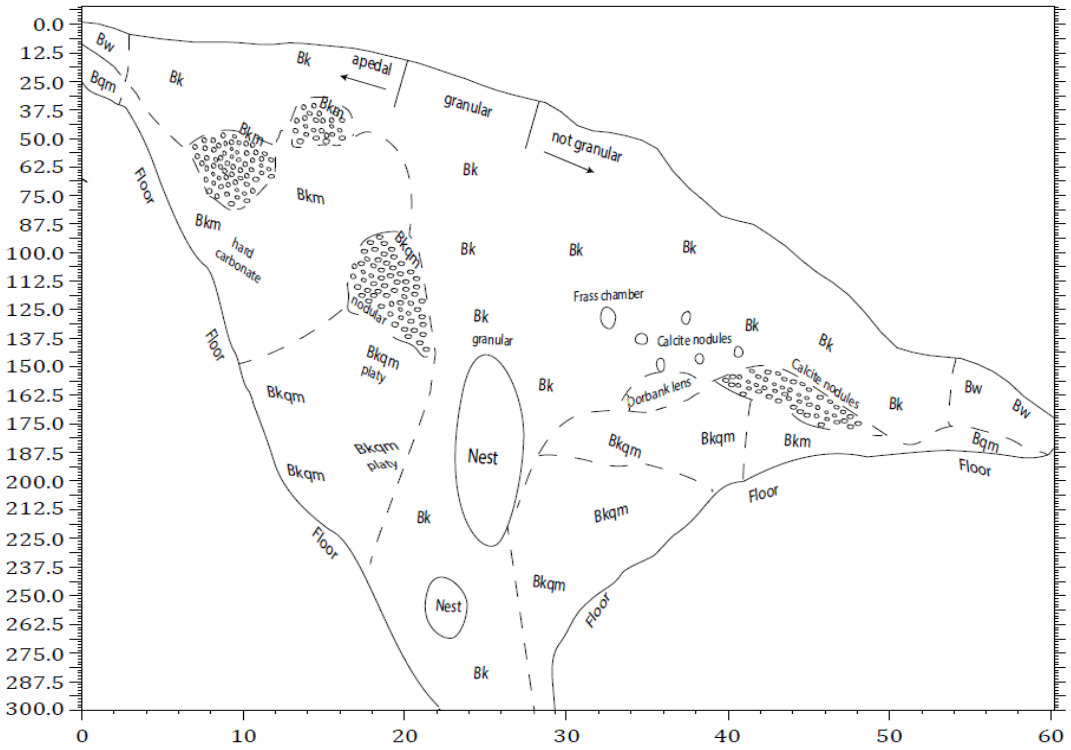

Figure 5.5: Vertically exaggerated cross-sectional sketch of H1 showing termite related features and major soil horizons (Bk= carbonate accumulation; Bkm= carbonate cementation; Bqm = silica cementation; Bkqm= carbonate and silica cementation; Bw= development of colour or structure; By= gypsum accumulation) according to FAO (2006).

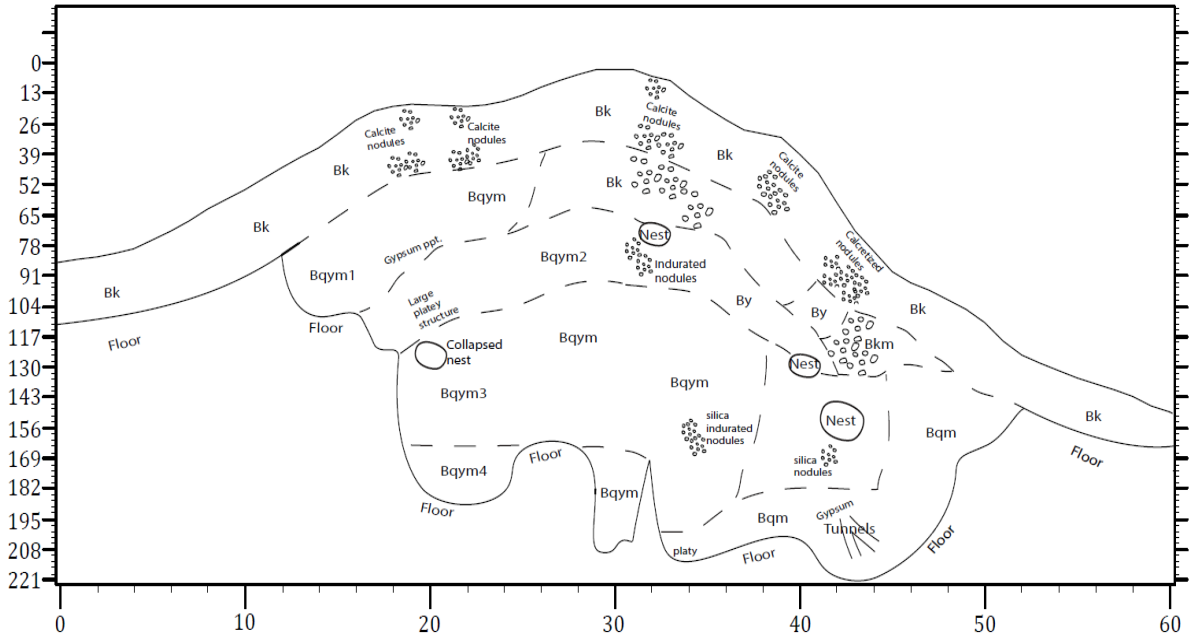

Figure 5.6: Vertically exaggerated cross-sectional sketch of H4 showing termite related features and major soil horizons (Bk= carbonate accumulation; Bkm= carbonate cementation; Bqm = silica cementation; Bkqm= carbonate and silica cementation; Bw= development of colour or structure; By= gypsum accumulation) according to FAO (2006).

Table 5.2: Mineralogy of clay extracts from selected profiles and horizons in the interheuweltjie (IH) and heuweltjie (H) soils, based on patterns presented in Vermooten (2018). Stars represent minerals identified.

Profile**	Depth (cm)	Description	Kaolinite	Illite	Calcite	Whewellite	Hydroxy-apatite	Gypsum	Quartz
H1-4	10	IH	*	*					*
H1-13	38	IH	*	*					*
H1-13	50	IH	*	*					*
H1-24	5	H	*	*	*				*
H1-24	160	H-nest	*	*	*				*
H1-24	76	H	*	*	*	*			*
H1-24	90	H	*	*	*	*		*	*
H4-19	10	H	*		*			*	*
H4-19	60	H			*	*	*	*	

** Number after the dash represent cross-sectional distance from west for H1 and H4.

5.6.5 Saturated Paste Extracts

The highest pH values (up to pH 9.4) are found at the edges of the heuweltjie, decreasing with depth into the heuweltjie structure (down to pH 7.0, *Figure 5.7*a). Electrical conductivity is highest in the centres of both heuweltjies, with the interheuweltjie soils having much lower EC values (*Figure 5.7*b). EC is significantly positively correlated with sample depth (*Table 5.3*). Na and Cl ions are most concentrated in the centre of the heuweltjie and the elevated concentration extends in a vertical direction from the surface to the base of the excavated trench. Both are significantly positively related to sample depth, although the correlation is strongest in H1 (*Table 5.3*). Ca, Na and Cl are strongly associated with the nest and frass chambers. Ca is lowest on the mound surface and interheuweltjie area (*Figure 5.7*d), showing a significant positive correlation with depth (*Table 5.3*). Potassium shows no significant correlation with depth in either heuweltjie (*Table 5.3*). Sulphate has a strong positive correlation with depth being highest towards the base of the excavated trenches (*Table 5.3*; *Figure 5.7*e). Phosphate and alkalinity show a weak but significant negative correlation with depth (*Table 5.3*) with alkalinity being concentrated towards the edges of the heuweltjies. Dissolved silica shows a strong positive correlation with depth and both alkalinity and dissolved silica have a significant negative correlation with pH (*Table 5.3*).

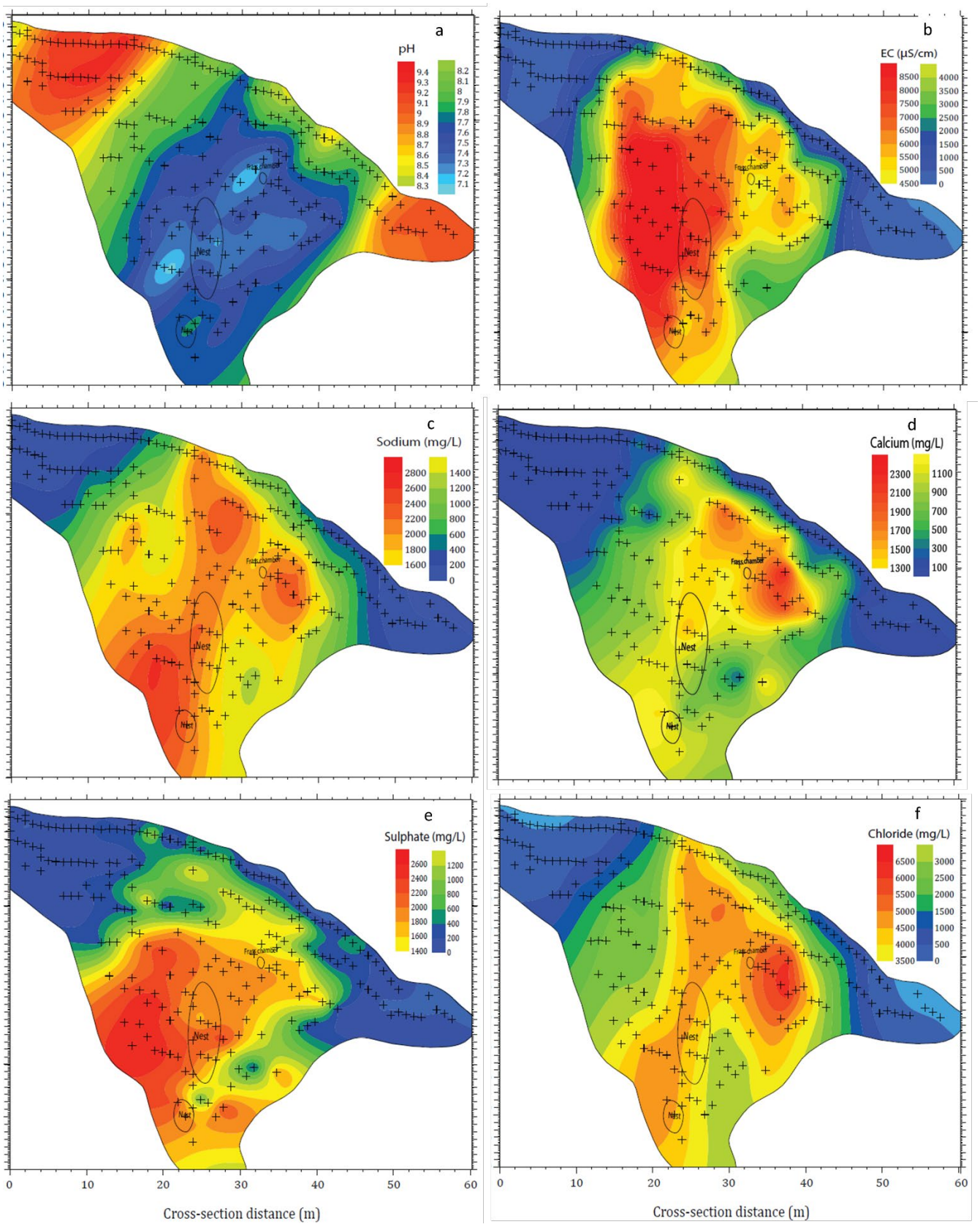

Figure 5.7: Interpolated heat maps for a) pH, b) EC, c) Na^{+}, d) Ca^{2+}, e) SO_4^{2-} and f) Cl^{-} from water extracts of H1 soil samples. Similar trends were shown in H4.

Table 5.3: Correlation matrices for selected chemical properties and sample depth for heuweltjies H1 and H4. Correlations in bold represent significance at p<0.05

H1	pH	EC (uS/cm)	Na	Mg	K	Ca	Cl-	SO42-	PO43-	Alkalinity	Dissolved Si	
EC (uS/cm)	—											
pH		**-0.488**										
Na (mg/L)	**-0.525**	**0.893**	—									
Mg (mg/L)	**-0.588**	**0.803**	**0.905**	—								
K (mg/L)	0.022	**0.314**	**0.243**	0.022	—							
Ca (mg/L)	**-0.634**	**0.817**	**0.9**	**0.976**	0.019	—						
Cl- (mg/L)	**-0.510**	**0.826**	**0.92**	**0.91**	0.082	**0.894**	—					
SO42- (mg/L)	**-0.623**	**0.816**	**0.843**	**0.814**	**0.246**	**0.851**	**0.765**	—				
PO43- (mg/L)	**0.272**	**-0.603**	**-0.676**	**-0.646**	-0.167	**-0.629**	**-0.68**	**-0.596**	—			
Alkalinity (mg/L)	**0.727**	**-0.321**	**-0.343**	**-0.443**	0.045	**-0.469**	**-0.331**	**-0.479**	0.105	—		
Dissolved Si (mg/L)	**-0.257**	**0.366**	**0.339**	**0.304**	-0.13	**0.311**	**0.304**	**0.408**	-0.168	**-0.343**		—
Depth (m)	**-0.445**	**0.562**	**0.632**	**0.576**	0.045	**0.552**	**0.522**	**0.722**	**-0.411**	**-0.358**		**0.554**
H4	pH	EC (uS/cm)	Na	Mg	K	Ca	Cl-	SO42-	PO43-	Alkalinity	Dissolved Si	
pH	—											
EC (uS/cm)	**-0.259**	—										
Na (mg/L)	**-0.266**	**0.788**	—									
Mg (Mg/L)	**-0.370**	**0.81**	**0.836**	—								
K (mg/L)	**0.138**	0.124	0.164	0.089	—							
Ca (mg/L)	**-0.399**	**0.813**	**0.913**	**0.921**	0.023	—						
Cl- (mg/L)	**-0.278**	**0.866**	**0.888**	**0.819**	0.145	**0.845**	—					
SO42- (mg/L)	**-0.486**	**0.408**	**0.442**	**0.506**	-0.21	**0.649**	**0.377**	—				
PO43- (mg/L)	**0.356**	**-0.45**	**-0.474**	**-0.438**	**-0.253**	**-0.472**	**-0.451**	**-0.417**	—			
Alkalinity (mg/L)	**0.618**	**-0.253**	**-0.231**	**-0.332**	0.127	**-0.325**	**-0.233**	**-0.297**	**0.362**	—		
Dissolved Si (mg/L)	**-0.356**	**0.347**	**0.42**	**0.476**	-0.077	**0.5**	**0.336**	**0.644**	**-0.434**	**-0.3**		—
Depth (m)	**-0.445**	**0.269**	**0.281**	**0.366**	-0.15	**0.434**	**0.217**	**0.752**	**-0.333**	**-0.292**		**0.56**

The SI for hydroxyapatite, gypsum, calcite and halite for H 1 are presented in *Figure 5.8*. Gypsum reaches saturation at the middle to base of the heuweltjies (*Figure 5.8*a), while calcite nears saturation towards the surface of the mounds (*Figure 5.8*b). Hydroxyapatite is largely saturated throughout the heuweltjies, but the highest degree of supersaturation is reached in the upper parts of the mound (*Figure 5.8*c). Halite is undersaturated throughout the heuweltjie but it least undersaturated in the centre and towards the base of the heuweltjie (*Figure 5.8*d).

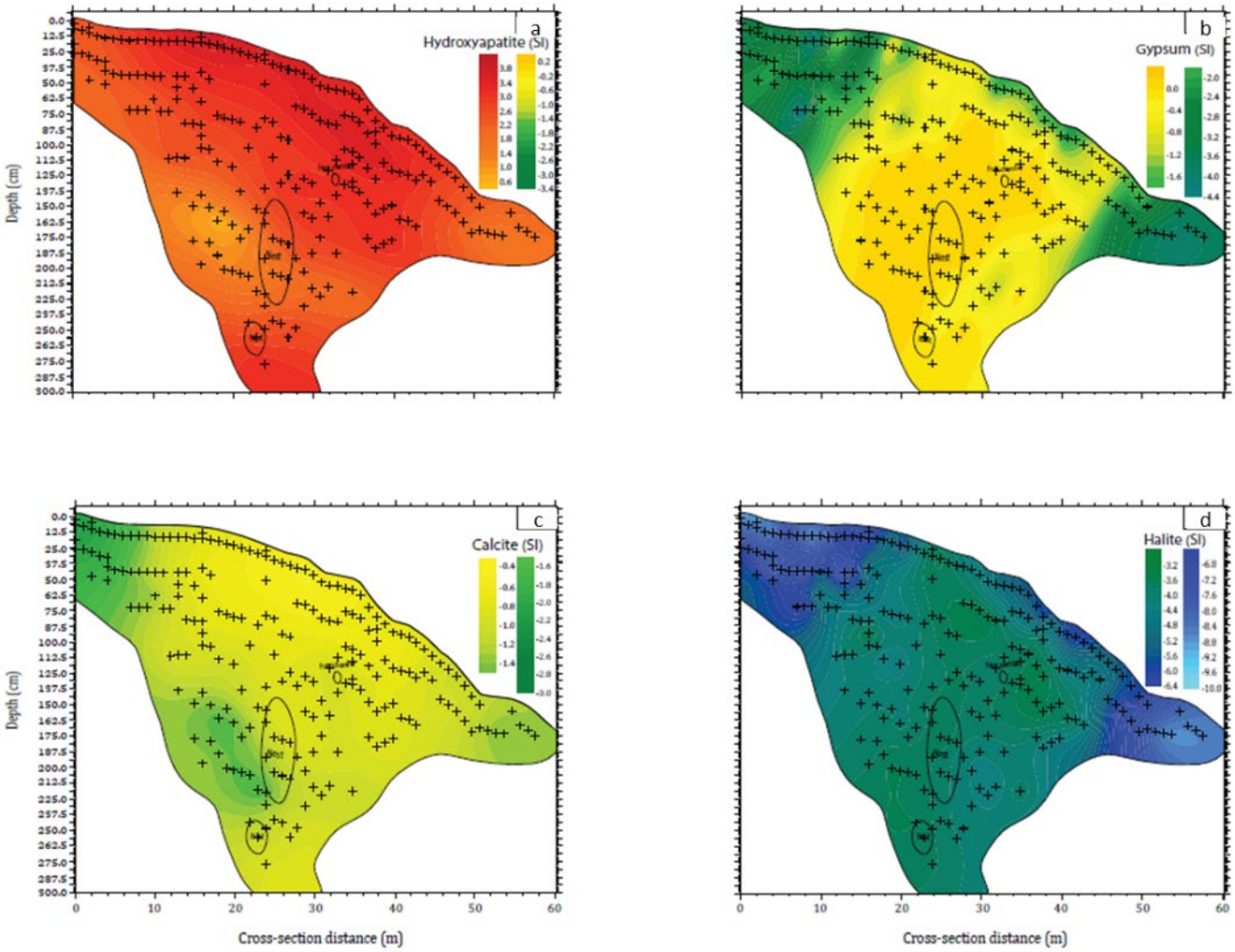

Figure 5.8: Interpolated heatmaps for saturation Indices of a) hydroxyapatite, b) Gypsum, c) Calcite and d) Halite for H1 (similar trends are found in H4).

5.7 Discussion

The faunal pedoturbation within the mounds is evident from the number of channels, nests and inverted texture profiles associated with the nest material (Figures 5.4-5.6; Table 5.1). The difference in soil depth between the heuweltjie and interheuweltjie soils is striking, with a thicker mantel of loose soil material on top the cemented duripans within the heuweltjie. The presence of calcium carbonate in the heuweltjie soils and the lack thereof in the interheuweltjie soils, suggests that the termites are bringing in Ca rich material into the mound (Francis and Poch, 2019). This is supported by the highest Ca concentrations being associated with the nest and frass chambers (*Figure 5.7*d).

The clay phase assemblage of quartz, kaolinite and illite of the interheuweltjie soils is consistent with alluvial and fluvial sediment parent material associated with the Buffels River (Setti et al., 2014). The heuweltjie soils show a similar clay mineral assemblage but are also enriched in calcite, gypsum and occasionally hydroxyapatite and whewellite (*Table 5.2*). The saturation indices for calcite, gypsum and hydroxyapatite show equilibrium with the soil solution chemistry (*Figure 5.8*) suggesting the minerals are in phase with the current pedochemical environment. Unfortunately, whewellite is not included in the databases used and thus equilibrium modelling for this mineral could not be conducted. Ca-oxalate has been identified in other *Microhodotermes* mounds (Mujinya et al., 2011) and the Ca-oxalate -$CaCO_3$ pathway seems to be a plausible mechanism of calcite formation (Francis and Poch, 2019).

The heatmaps and correlation matrices (*Figure 5.7* and 8; *Table 5.3*) show the spatial and statistical relationships between the individual ion species within the heuweltjies and these allow deductions to made about the geochemical interactions taking place as well as the net direction of salt movement. The pH trends within the heuweltjie are noticeable, with the outer zones having the highest pH while the centre remains circumneutral. The negative correlation between pH and Na and Cl concentrations, and the positive correlation between alkalinity and pH, suggests the process of solonisation or alkalinisation (Schaetzl and Anderson, 2007) is taking place on the outer zones of the heuweltjie. This then suggests an inward and downward migration of Cl, allowing the pH to climb in the more leached outer soils, while the pH in the centre of the heuweltjie remains circumneutral due to salinisation (Schaetzl and Anderson, 2007). Dissolved Si is inversely correlated to pH which contradicts the observations of Ellis (2002) and the pH control on silica solubility. The positive correlation between depth and dissolved Si concentration may suggest that Si is being mobilised in the outer, high pH regions of the heuweltjie and is leaching downwards with the salts.

Sulphate and gypsum saturation increase with depth (*Figure 5.7* and 8; *Table 5.3*). Since gypsum is more soluble than calcite, gypsum precipitates at a greater depth than calcite when water movement is downwards (Casby-Horton et al., 2015). This downward separation of increasingly soluble minerals does not support a groundwater source of salinity and suggests a surface source salinity. The source sulphate within the heuweltjies is likely to be marine origin (Chapter 7), however the mechanism for sulphate enrichment in the heuweltjie soils is unclear. One mechanism maybe termite foraging and transport of vegetation exposed to marine aerosols into the heuweltjie, or alternately the raised mound may capture more marine aerosol than the surrounding interheuweltjie soils. The low sulphate concentrations on the surface of the heuweltjie suggest the former mechanism is more likely.

Further evidence for downward movement is the fine precipitation of gypsum in the soil matrix on the above horizontal tunnels (*Figure 5.3*) where percolation through the coarse textured soil matrix of the

overlying horizons is arrested at the textural barrier at the boundary of the finer, more closely packed tunnel lining.

The solubility differential and net downward movement of solutes would also explain the negative correlation of phosphate with depth and the high levels of hydroxyapatite supersaturation towards the top of the mound. Heuweltjies are known to have elevated P levels due to the enrichment of plant materials (Ellis, 2002). Phosphate released from decomposing plant material would quickly precipitate out at the location of its release due to the low solubility of hydroxyapatite. Assuming that the sulphate, and alkalinity are also sourced from the plant material, the progressive downward enrichment of calcite followed by gypsum provides strong evidence for a net downward migration of solutes.

The process of the movement of the heuweltjie salts towards the groundwater could be through high volume rainfall events, and/or could have occurred during a wetter past climate. There is evidence of lateral and vertical water movement in soils of Namaqualand on the regional scale (Francis et al., 2007; Francis and Poch, 2019). Chase & Meadows (2007) showed that climate was wetter in the Namaqualand region of South Africa from 24-18 ka years before present. Along with higher precipitation rates, they also found that evaporation rates were lower during the last glacial maximum. As older heuweltjies can be up to 20,000-35,000 years old (Midgley et al., 2002; Potts et al., 2009), the leaching of solutes in heuweltjie would have been a much faster process than at in the present arid conditions in the Buffelsrivier area. Most of Namaqualand receives less than 150 mm rain per annum (Cowling et al., 1999), and so groundwater recharge is slow (Abiye & Leshomo, 2013). This implies that the salt movement through the heuweltjie structures with infiltrated rainwater would be slow. Evaporation rates of around 2000 mm per year are expected to occur (Francis, 2019) due to high temperatures, and so the rainwater evaporates very soon after it has fallen, limiting the transfer of salts through the heuweltjie structure towards the groundwater even more. On the other hand, rare, high intensity rainfall events are known to take place in Namaqualand periodically (Davis et al., 2016). When these large rainfall events do take place, it would cause the salts present in the heuweltjies to be flushed into the groundwater system quite rapidly via the preferential flow paths present.

5.8 Conclusions

- Salt concentrations are much higher in the heuweltjie soils compared to the interheuweltjie soils.
- The vertical variation with respect to calcite and gypsum indicates that the water movement in the heuweltjie is downwards, transferring the heuweltjie salts to the groundwater, and not vice versa.
- Preferential flow paths, in H1 through the granular textured soil, and H4 through the termite tunnels, aid in the movement of the ions towards the groundwater system.
- The movement of the salts to the groundwater can either be through more recent large rainfall events, or it could have occurred in the past, when the climate was wetter.

5.9 References

Abiye, T.A., Leshomo, J.T., 2013. Groundwater flow and radioactivity in Namaqualand, South Africa. Environ. Earth Sci. 70, 281-293. doi:10.1007/s12665-012-2126-9

Davis, C.L., Hoffman, M.T., Roberts, W., 2016. Recent trends in the climate of Namaqua-land, a megadiverse arid region of South Africa. S. Afr. J. Sci. 112, 1-9.https://doi.org/10.17159/sajs.2016/20150217Casby-Horton, S., Herrero, J., Rolong, N.A., 2015. Gypsum soils – Their morphology, classification, function, and landscapes. Adv. Agron. 130, 231-290. doi:10.1016/BS.AGRON.2014.10.002

Casby-Horton, S., Herrero, J., Rolong, N.A., 2015. Chapter Four – Gypsum Soils – Their Morphology, Classification, Function, and Landscapes. in: Sparks, D.L. (Ed.), Adv. Agron. Academic Press, pp. 231-290.

Chase, B.M., Meadows, M.E., 2007. Late Quaternary dynamics of southern Africa's winter rainfall zone. Earth Sci. Rev., 84, 103-138.

Cowling, R.M., Esler, K.J., Rundel, P.W., 1999. Namaqualand, South Africa – An overview of a unique winter-rainfall desert ecosystem. Plant Ecol. 142, 3-21. doi:10.1023/A:1009831308074

Ellis, F., 2002. Contribution of termites to the formation of hardpans in soils of arid and semi-arid regions of South Africa., Proceedings of the 17th World Congress of Soil Science, Bangkok, Thailand.

FAO, 2006. Guidelines for soil description, fourth. ed. Food and Agriculture Organization of the United Nations, Rome.

Francis, M.L., Fey, M. V, Prinsloo, H.P., Ellis, F., Mills, A.J., Medinski, T. V., 2007. Soils of Namaqualand: Compensations for aridity. J. Arid Environ. 70, 588-603. doi:10.1016/j.jaridenv.2006.12.028

Francis, M.L., 2019. Effect of sepiolite and palygorskite on plant available water in Arenosols of Namaqualand, South Africa. Geoderma Regional.

Francis, M.L., Poch, R.M., 2019. Calcite accumulation in a South African heuweltjie: Role of the termite Microhodotermes viator and oribatid mites. J. Arid Environ. 170. doi:10.1016/j.jaridenv.2019.05.009

IUSS Working Group WRB, 2015. World Reference Base for Soil Resources 2014, update 2015. International soil classification system for naming soils and creating legends for soil maps., World

Soil. ed, World Soil Resources Reports No. 106. FAO, Rome. doi:10.1017/S0014479706394902

Jones, R.L., Dreher, G.B., 1996. Silicon. in: Sparks, D. et al. (Eds.), Methods of Soil Analysis. Soil Science Society of America, Madison. WI, pp. 627-637.

Macey, P.H., Bailie, R.H., Miller, J.A., Thomas, R.J., de Beer, C., Frei, D., le Roux, P.J., 2018. Implications of the distribution, age and origins of the granites of the Mesoproterozoic Spektakel Suite for the timing of the Namaqua Orogeny in the Bushmanland Subprovince of the Namaqua-Natal Metamorphic Province, South Africa. Precambrian Res. 312, 68-98. doi:10.1016/J.PRECAMRES.2018.02.026

McAuliffe, J.R., Hoffman, M.T., Mcfadden, L.D., Bell, W., Jack, S., King, M.P., Nixon, V., 2019. Landscape patterning created by the southern harvester termite, Microhodotermes viator: Spatial dispersion of colonies and alteration of soils. J. Arid Environ. 3, 1-9. doi:10.1016/J.JARIDENV.2018.11.010

Mujinya, B.B. et al., 2011. The origin of carbonates in termite mounds of the Lubumbashi area, D.R. Congo. Geoderma, 165, 95-105.

Murphy, J., Riley, H.P., 1962. A modified single solution method for the determination of phosphate in natural waters. Anal. Chim. Acta 27, 31-36.

Nordstrom, D.K., Plummer, L.N., Wigley, T.M.L., Wolery, T.J., Ball, J.W., Jenne, E.A., Bassett, R.L., Crerar, D.A., Florence, T.M., Fritz, B., Hoffman, M., Holdren, G.R.J., Lafon, G.M., Mattigod, S. V, McDuff, R.E., Morel, F., Reddy, M.M., Sposito, G., Thrailkill, J., 1979. A comparison of computerized chemical models for equilibrium calculations in aqueous systems, in: Jenne, E.A. (Ed.), Chemical Modeling in Aqueous Systems, Speciation, Sorption, Solubility, and Kinetics, Symposium Series 93. American Chemical Society, Washington, D.C., pp. 857-892.

Parkhurst, D.L., Appelo, C.A.J., 2013. Description of input and examples for PHREEQC version 3 – A computer program for speciation, batch-reaction, one-dimensional transport, and inverse geochemical calculations, in: U.S. Geological Survey Techniques and Methods. p. 497.

Parkhurst, D.L., Appelo, C.A.J., 1999. User's guide to PHREEQC (Version 2). A computer program for speciation, batch-reaction, one-dimensional transport, and inverse geochemical calculations: U.S. Geological Survey Water-Resources Investigations Report 99-4259.

Potts, A.J., Midgley, J.J., Harris, C., 2009. Stable isotope and ^{14}C study of biogenic calcrete in a termite mound, Western Cape, South Africa, and its palaeoenvironmental significance. Quat. Res. 72, 258-264. doi:10.1016/j.yqres.2009.04.008

Rhoades, J.D., 1996. Salinity: Electrical conductivity and total dissolved solids, in: Sparks, D. (Ed.), Methods of Soil Analysis. Part 3. Chemical Methods. Madison, WI, USA, pp. 417-437.

Schaetzl, R.J., Anderson, S., 2007. Soils Genesis and Geomorphology. Cambridge, New York.

Setti, M., Galindo, A.L., Padoan, M., Garzanti, E., 2014. Clay mineralogy in southern Africa river muds. Clay Miner. 49, 717-733. doi:10.1180/claymin.2014.049.5.08

Soil Classification Working Group, 1991. Methods of analysis, in: Soil Classification: A Taxonomic System for South Africa. South Africa, pp. 194-197.

Sonmez, S., Buyuktas, D., Okturen, F., Citak, S., 2008. Assessment of different soil to water ratios (1:1, 1:2.5, 1:5) in soil salinity studies. Geoderma 144, 361-369. doi:10.1016/J.GEODERMA.2007.12.005

Vermooten, M., 2019. Investigation of Heuweltjie Structures and Soil Chemistry in the Buffels River Valley and Implications for Transfer of Salts to Groundwater. MSc Thesis, Stellenbosch University.

6 GROUNDWATER RESIDENCE TIME CONSTRAINTS

By J. van Gend, L. Palcsu, M. Molnár, A. Watson, J.D. van Rooyen, M.L. Francis, C.E. Clarke, J.A. Miller

6.1 Introduction

Groundwater sustainability is influenced not just by quality but also by and quantity (van Rooyen et al., 2020; Villholth, 2013). Assessment of groundwater quantity is dependent on a number of factors including the renewal rate of the groundwater system. However, to understand the renewal rate we need also to understand the groundwater residence time in order to evaluate the timescales over which the stored groundwater is being turned over. Groundwater is currently divided into three broad categories based on residence time. Fossil groundwater is regarded as groundwater that has recharged before 12 ka, while modern groundwater has been recharged less than 50 years ago (Bierkens and Wada, 2019; Gleeson et al., 2016; Jasechko et al., 2017). Groundwater that has been recharged between 12 ka and 50 years ago is regarded as young groundwater (Bierkens and Wada, 2019). Methods used to differentiate fossil, young and modern groundwaters include using longer lived radio-isotopes such as radiocarbon (half-life of 5700 years) for fossil and young groundwaters and short lived radio-isotopes such as tritium (half-life of 12.312 years) for modern groundwaters (Cartwright et al., 2020, 2017; Jasechko et al., 2017; Meredith, 2009; Newman et al., 2010). Considering the half-lives of these two isotopes, fossil or young groundwater should not contain any tritium as this would indicate modern recharge. However, detectable levels of tritium are often present in fossil groundwater suggesting that the supposed isolation of fossil groundwater from the modern groundwater system or modern precipitation may not be valid (Jasechko et al., 2017). Not only does this indicate mixing between old and modern groundwater, but it also indicates that fossil or young groundwater is more susceptible to surface water-groundwater interaction than previously thought (Jasechko et al., 2017; Tweed et al., 2018).

Residence times of groundwater in this region have been previously estimated using ^{14}C and the conventional decay equation but a wide range of ^{14}C activities were found, ranging between 1.6 and 120 pMC with associated ages of 32,000 years to modern (Adams et al., 2004). These ages did not show any significant spatial relationships and some of the age data did not agree with the recharge model that was used during this study. However, many of the samples analysed had detectable levels of tritium irrespective of the ^{14}C activity (Adams et al., 2004), indicating interaction between fossil or young waters and modern waters. Given the dependence on the groundwater system in this region, properly

constraining the residence time spectrum is necessary to better understand the potential mixing relationships between fossil and modern groundwater.

In this study, the sustainability of groundwater in the Buffels River catchment in Namaqualand on the west coast of South Africa was evaluated by using ^{14}C, ^{3}H and $\delta^{13}C$ as tracers or groundwater age and flow. Firstly, recharge mechanisms were conceptualised for the different aquifer settings in the different areas within the catchment. Then, conventional radiocarbon age calculations were evaluated and $\delta^{13}C$ values were used to investigate the possibility ^{14}C dilution. Finally, by using a lumped parameter model approach (LPM), total mean ages were calculated and mixing relationships between older and younger waters were identified. The results of this study highlight the complexity of the groundwater system in the region and the challenges the area faces with developing a robust groundwater management strategy. However, understanding these complexities in semi-arid and arid environments, that heavily rely on agriculture, is essential to the development of strategies to address climate change and understand hydrological resilience throughout much of sub-Saharan Africa.

6.2 Sample Collection and Field Methods

A total of 27 groundwater samples were collected between March and September 2018 from boreholes, springs and wells. The infrastructure and the pumping regimes of the boreholes in the Buffels River catchment is highly variable. Therefore, all boreholes were purged until EC values stabilised before sampling radioactive tracers. Purging was done via installed submersible pumps. EC and pH in the field were measured using Extech EC600 portable field probes at the point of discharge. ^{3}H, $\delta^{13}C$ and ^{14}C samples were collected in 500 ml high density PP amber bottles directly from the discharge point. All bottles were rinsed 3 times with the groundwater before the final sample was taken. The final sample was taken by allowing the sample bottles to overfill several times to minimize atmospheric CO_2 contamination before it was closed and sealed by taping the bottle caps to the bottles. All samples were kept refrigerated at 4°C with minimum light exposure until analysis.

6.3 Results

6.3.1 Tritium

Tritium activities in groundwater from the Buffels River catchment range between 0.08 TU and 1.58 TU (Table 6.1). Groundwater with the lowest tritium activities is hosted by the Concordia Granites (n=5). The two samples with the lowest tritium activity of 0.08 and 0.09 TU were both collected from the plateau just east of the Buffels River Valley, while two samples collected within the valley, also hosted in the Concordia Granites, have higher tritium activities of 0.26 and 0.64 TU. Groundwater with the highest tritium activity of 1.58 TU is hosted by the Mesklip Granitic Gneiss (n=6). However, tritium

activities of the remaining five groundwater samples hosted by the Mesklip Granitic Gneisses were all below 1 TU (Fig 6.1). Although the lowest and highest tritium activities were found in groundwater hosted by the Concordia Granites and the Mesklip Granitic Gneisses respectively, groundwater tritium activities from both these host rocks are clearly variable. Groundwater hosted in the Modderfontein Granitic Gneisses of the Little Namaqualand Suite, record tritium activities between 0.21 TU and 0.63 TU, a much narrower range compared to that of the Mesklip Granitic Gneisses, which is also part of the Little Namaqualand Suite.

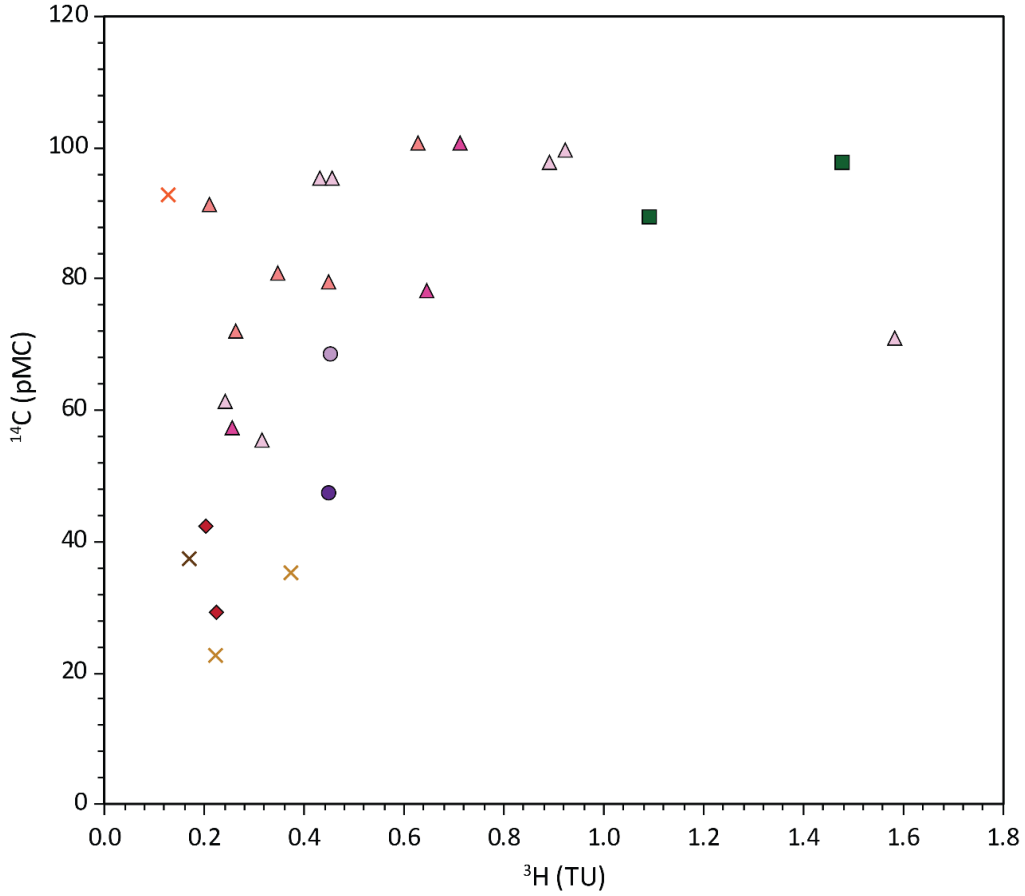

Figure 6.1: ^{14}C activity compared to the tritium activity for groundwater collected in the Buffels River catchment represented according to the host rocks from which the samples were collected. Refer to Figure 3.1 for the explanation of the symbology used.

Groundwater hosted in the alluvial sediments generally have low tritium activities irrespective of the borehole depth with groundwater from the Platbakkies alluvial sediments having slightly higher tritium values than that collected from the Kleinsee sediments (Fig 6.1). Sample KZ01 (shallow Kleinsee alluvial sediments), collected from a well of 3 m deep in the middle of the Buffels River bed close to the town of Kleinsee, has a tritium activity of 0.13 TU which is comparable to the tritium activity of sample KZ02

(deep Kleinsee alluvial sediments) of 0.17 TU that was collected in close proximity but from a borehole with a depth to groundwater of approximately 75 m. Groundwater hosted in the Lekkerdrink gneisses also indicated low tritium activities of 0.20 TU and 0.22 TU, while the two samples collected from the Gladkop Suite had higher tritium activities of 0.45 and 0.46 TU. Although only two samples were collected from the Kamiesberg Group, these samples both have high tritium activities (1.48 and 1.10 TU) compared to the rest of the host rocks in the catchment of which only one sample from the Mesklip granitic gneisses have tritium activity of more than 1 TU.

6.3.2 $\delta^{13}C$ Ratios

Groundwater $\delta^{13}C$ values varied between -17.0 ‰ and -4.95 ‰. Within this range, two samples have low $\delta^{13}C$ values of -17.0 and -16.2 ‰, 18 samples have $\delta^{13}C$ values between -13.8 ‰ and -10.4 ‰ and the remaining five samples have $\delta^{13}C$ values higher than -10.0 ‰. The $\delta^{13}C$ values are not necessarily consistent with the geological host rocks with groundwater hosted by the Mesklip Granitic Gneisses have the most variable $\delta^{13}C$ values, ranging between -16.1 ‰ and -4.95 ‰ (Fig 6.2). $\delta^{13}C$ values for groundwater collected from the Concordia Granite host rocks generally show a narrower range in values between -10.4 ‰ and -11.9 ‰ with the exception of the one sample with the most negative $\delta^{13}C$ value of -17.0 ‰. Groundwater collected from the Modderfontein granitic gneisses also had little variation in $\delta^{13}C$ values, and ranged between -13.7 ‰ and -12.0 ‰ (Fig 6.2). The two samples collected from the Platbakkies alluvial sediments have $\delta^{13}C$ values of -9.12 ‰ and -8.65 ‰. The sample collected from the deep Kleinsee sediments has a $\delta^{13}C$ values -11.8 ‰, while the sample collected from the shallow Kleinsee sediments had a significantly higher $\delta^{13}C$ value of -5.76 ‰. Groundwater from the Lekkerdrink gneisses, Bushmanland Group and Kamiesberg Group, and Gladkop Suite were between -12.4 and -10.6 ‰ (Fig 6.2).

6.3.3 Radiocarbon

Radiocarbon in groundwater in the Buffels River catchment are again variable ranging between 22.6 and 100.8 pmC (Table 6.1). The lowest groundwater radiocarbon activity, 22.6 pmC, was from the Platbakkies alluvial sediments towards the east of the catchment. Similarly, the second sample collected from the same host and the sample collected from the deep Kleinsee Alluvial Sediments towards the west, also have low radiocarbon activities of 35.3 and 37.4 pmC, respectively. Groundwater hosted by the Lekkerdrink gneisses also indicated low radiocarbon activities of 29.3 pMC and 42.3 pmC (Fig. 6.2). Groundwater from the granitic gneisses of the Little Namaqualand Suite have higher radiocarbon activities ranging between 55.6 and 100.7 pmC. The Concordia granites host groundwater with a slightly wider range of radiocarbon activities between 40.3 and 100.8 pmC. The Gladkop Suite and the supracrustal rocks (Bushmanland and Kamiesberg Groups), have radiocarbon activities of 47.2 and 68.4

pmC and 66.5 and 97.4 pmC, respectively. Comparing the radiocarbon data with that of the tritium data, most samples showed higher tritium activities than expected for the radiocarbon activity (Fig. 6.1).

Table 6.2: Tritium activity, radiocarbon activity and $\delta^{13}C$ values in groundwater. HCO_3 data was obtained from van Gend et al. (2021).

Suite/Group	Pluton/Formation	Sample ID	BH depth (m)	^{3}H (TU)	^{3}H Error	HCO_3 (mg/l)	^{14}C (pMC)	^{14}C unc. (1s)	$\delta\ ^{13}C$ sample/VPDB
Little Namaqualand Suite	Shallow Kleinsee Alluvial Sediments	KZ01	3	0.13	0.06	52.80	92.7	0.29	-5.76
	Deep Kleinsee Alluvial Sediments	KZ02	75	0.17	0.06	66.40	37.4	0.21	-11.80
	Platbakkies Alluvial Sediments	KK09	23	0.22	0.08	207.60	22.6	0.10	-9.12
		KK10	45	0.37	0.07	232.20	35.3	0.12	-8.65
	Concordia granite	BR09	-	0.08	0.08	88.70	-	-	-
		BR05	65	0.26	0.05	93.40	57.4	0.29	-11.84
		BR10	30	-	-	60.30	100.0	0.41	-10.40
		BR17	-	-	-	118.90	40.3	0.25	-16.96
		BR19	-	0.09	0.04	78.70	-	-	-
		BR23	-	-	-	164.25	92.94	0.32	-11.35
		BR07	80	0.64	0.15	111.40	78.3	0.30	-11.76
		CD02	-	0.71	0.04	110.00	100.8	0.36	-
		CD03	-	-	-	112.40	77.5	0.34	-10.75
	Modderfontein granite/gneiss	NB01	75	0.26	0.03	44.10	72.2	0.31	-12.31
		NB02	-	0.63	0.04	47.40	100.7	0.38	-11.96
		NB03	-	0.21	0.04	54.60	91.3	0.33	-
		NB04	40	0.35	0.05	78.70	80.9	0.32	-
		SP02	-	0.45	-	164.40	79.6	0.25	-13.66
	Mesklip granite	KK02	30	0.92	0.09	101.30	99.7	0.34	-13.03
		KK05	-	0.43	0.06	62.90	95.5	0.42	-4.95

Suite/Group	Pluton/Formation	Sample ID	BH depth (m)	^{3}H (TU)	^{3}H Error	HCO3 (mg/l)	^{14}C (pMC)	^{14}C unc. (1s)	$\delta\ ^{13}C$ sample/VPDB
		KK07	60	0.89	0.09	218.60	97.8	0.21	-7.44
		KK01	80	1.58	0.11	23.00	71.0	0.28	-13.84
		KK03	50	0.32	0.14	120.70	55.6	0.23	-16.16
		KK04	100	-	-	76.10	95.3	0.35	-
		KK12	86	-	-	128.60	63.8	0.30	-13.02
		SP01	-	0.24	0.05	116.80	61.4	0.23	-
	Lekkerdrink gneiss	KK08	70	0.22	0.07	175.80	29.3	0.12	-12.01
		KK11	150	0.20	0.10	213.70	42.3	0.13	-11.20
Supracrustal Rocks	Bushmanland Group	KG05	80	-	-	26.65	66.5	0.38	-10.58
		KG08	-	-	-	35.00	82.9	0.43	-11.85
	Kamiesberg Group	KK13	27	1.48	0.11	276.10	97.4	0.39	-11.56
		KK14	35	1.10	0.08	235.30	89.1	0.19	-11.67
Gladkop Suite	Noemnoemnaasberg granite	KK06	50	0.46	0.09	176.80	68.4	0.18	-12.39
	Steinkopf gneiss	SK01	100	0.45	0.16	139.90	47.2	0.22	-

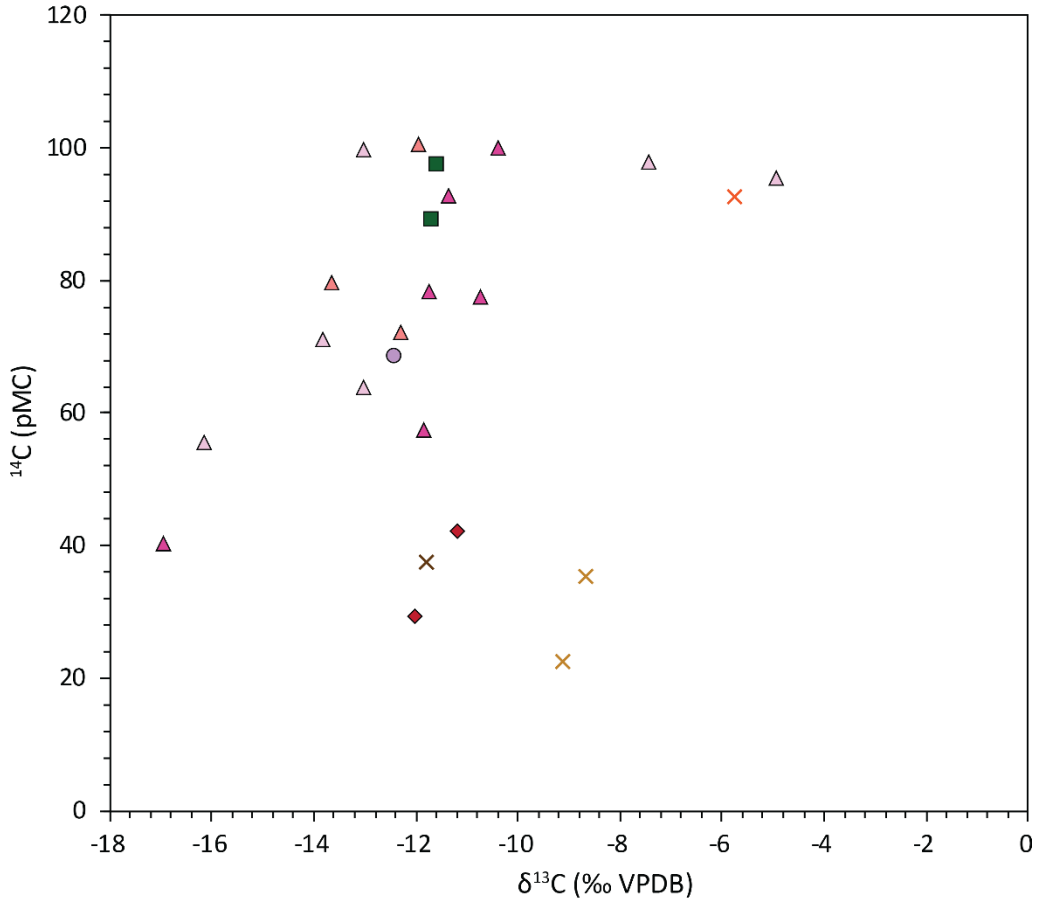

Figure 6.2: ^{14}C vs δ^{13}C values for groundwater collected in the Buffels River catchment represented according to the host rocks from which the samples were collected. Refer to Fig 3.1 for the explanation of the symbology used.

6.4 Discussion

Recharge pathways are not uniform throughout the catchment. Factors such as geology, the thickness of the soil horizons and the presence of heuweltjies, may and are likely to influence these flow paths. The groundwater residence time was calculated using radioactive decay of the ^{14}C isotope and with potential dilution of the radiocarbon addressed via a Pearson's mixing model approach. These results are then compared to that of a lumped parameter model that accounts for the presence of tritium and hence components of modern recharge in an otherwise older groundwater system.

6.4.1 Current Understanding of Recharge in the Buffels River Catchment

The Kamies Mountains, dominated by impermeable granitic gneisses is the main recharge zone and recharge pathways vary depending on the angle of the slopes and the condition of the granite. Groundwater may recharge directly into the crystalline basement, but runoff and ponding in the narrow valleys separating these granitic domes are also recharge sites via percolation through the unsaturated zone (Pietersen et al., 2009). The weathered regolith, consisting of blocks of weathered and fresh

granites, extends deeper allowing for more effective recharge to occur (Titus et al., 2009). Isolated shallow alluvial aquifers may occur where the soils become saturated. As such, groundwater recharge in the Buffels River catchment varies across the catchment. The two main alluvial aquifers in the catchment are recharged by infiltration during flood events that occur once every 5-10 years on average (Benito et al., 2011). The alluvial aquifers are recharged on a more regular basis during precipitation events that do not generate flooding (Benito et al., 2010; Watson et al., 2021).

6.4.2 Residence Time of Groundwater

Given this understanding of recharge in the Buffels River catchment, groundwater ages have previously been calculated using conventional radiocarbon equations and modifications of the equation to account for some environmental factors which may have an effect on the age. These calculations are discussed in the below and validated in light of the new data collected during this study.

6.4.3 Radiocarbon Age Calculations

The conventional calculation for radiocarbon age, *t*, is as follows:

$$t = \frac{5730}{\ln 2} \ln\left(\frac{A_0}{A}\right) \qquad \text{Equation 6.1}$$

where 5730 is the half-life of ^{14}C in years, A_0 is the initial ^{14}C activity, and A is the measured ^{14}C activity. This conventional radiocarbon age equation assumes that the activity of the ^{14}C isotope decreases as a function of radioactive decay only.

In natural systems, a number of processes may act to dilute the activity of ^{14}C which will give an artificially older age if calculated assuming only radioactive decay. To evaluate the dilution of the ^{14}C signal, a number of correction processes have been proposed, with the most common being the Pearson model (Ingerson & Pearson, 1964). In the Pearson model, $\delta^{13}C$ is used to correct for the dilution by assuming that the dilution affect will be the same for ^{14}C as it is for ^{13}C. The model uses a dilution factor q defined as:

$$q = \frac{(\delta^{13}C_{DIC} - \delta^{13}C_{carbonate})}{(\delta^{13}C_{soil} - \delta^{13}C_{carbonate})} \qquad \text{Equation 6.2}$$

where $\delta^{13}C_{DIC}$ is from dissolved inorganic carbon in the groundwater, $\delta^{13}C_{carbonate}$ is the $\delta^{13}C$ value of carbonate rock or solid carbonate in the system, while $\delta^{13}C_{soil}$ is the $\delta^{13}C$ value of the soil which is governed by soil gas CO_2. The q value is incorporated into equation [6.1] as follows:

$$t = \frac{5730}{\ln 2} \ln\left(\frac{q * {}^{14}C_i}{{}^{14}C_m}\right) \qquad \text{Equation 6.3}$$

where $^{14}C_i$ and $^{14}C_m$ are the initial and measured ^{14}C activity in the groundwater, respectively.

Residence times for groundwater in the catchment are thought to range between modern and ~32 850 years (Adams et al., 2004). These ages were calculated using a uniform dilution factor of 0.85 for the samples that were collected from the basement aquifer in accordance with Hendry (1988), who assigned this dilution factor to all hard rock aquifers. The ages for samples from alluvial aquifers were calculated without a dilution factor. For this study, using Equation 6.1, the obtained residence times range between 23 years and 12 294 years. If the groundwater residence times are recalculated using a uniform dilution factor of 0.85 consistent with the Adams et al. (2004) study, the ages range between 209 years and 10 951 years. However, both calculation approaches generate negative values in addition to the ranges specified. In both cases, the calculation of significantly younger ages, as well as the derivation of negative values indicates that the validity of the dilution factor assumptions is questionable and interrogation of $\delta^{13}C_{DIC}$ values is necessary to resolve this issue.

The $\delta^{13}C_{soil}$ for the Buffels River catchment is not known, but in general $\delta^{13}C_{soil}$ is largely controlled by the dominant vegetation type of the area which in the case of the Buffels River catchment is mainly C3 with minor C4 species. $\delta^{13}C_{soil}$ values of -24.0 ‰ and -10.0 ‰ are used to represent the effect of C3 and C4 species, respectively (Appelo & Postma, 2005). The second component of Equation 6.2 is the $\delta^{13}C_{carbonate}$ that is dissolved and incorporated along the flow path. Typically, $\delta^{13}C_{carbonate}$ would result in strong dilution because most carbonate sequences are sufficiently old that they contain no ^{14}C. The geology of the Buffels River catchment is silicate dominated and the current understanding is that there is no carbonate material along the flow path. This value cannot be excluded from the calculation and given that carbonates generally have $\delta^{13}C_{carbonate}$ values of between -2.0 and 2.0 ‰ (Plummer & Sprinkle, 2001; Oehlert & Swart, 2014) a value of 0 ‰ has been assumed. Therefore, if only changes in the $\delta^{13}C_{soil}$ are taken into consideration, 3 different q values can be calculated based on C3 specie dominated environment, a C4 specie dominated environment or an environment where C3 and C4 specie occur together in a ratio of 60% C3 and 40% C4 species (*Table 6.2*). The dilution factors are highly variable and, in some cases, the calculated dilution factors are larger than 1.00 with numerous negative values generated. A new recharge model was therefore conceptualised.

Table 6.2: Calculated groundwater ages using the conventional radiocarbon equation with various dilution factors. All ages given in years. The mixed values have been calculated based on 60% C3 vegetation and 40% C4 vegetation.

Sample ID	No correction	Only Soil $\delta^{13}C$ values						Adams et al. (2004)
	Age	q-value C3	Age C3	q-value mixed	Age mixed	q-value C4	Age C4	Age q = 0.85
KZ01	622	0.24	-11108	0.31	-8911	0.58	-3871	-721
KZ02	8131	0.49	2330	0.64	4526	1.18	9567	6788
KK09	12294	0.38	4365	0.50	6562	0.91	11602	10951
KK10	8616	0.36	251	0.47	2448	0.87	7488	7273
BR05	4594	0.49	-1181	0.64	1016	1.18	6057	3250
BR10	-2	0.43	-6851	0.56	-4654	1.04	387	-1345
BR17	7509	0.71	4709	0.92	6905	1.70	11946	6166
BR23	606	0.47	-5518	0.62	-3322	1.13	1719	-738
BR07	2026	0.49	-3807	0.64	-1610	1.18	3431	682
CD02	-64	-	-	-	-	-	-	-1408
CD03	2109	0.45	-4464	0.58	-2267	1.07	2773	766
NB01	2695	0.51	-2757	0.67	-561	1.23	4480	1352
NB02	-54	0.50	-5743	0.65	-3547	1.20	1494	-1398
NB03	756	-	-	-	-	-	-	-588
NB04	1756	-	-	-	-	-	-	413
SP02	1891	0.57	-2698	0.74	-501	1.37	4540	548
KK02	23	0.54	-4959	0.71	-2762	1.30	2278	-1321
KK05	381	0.21	-12605	0.27	-10409	0.49	-5368	-962
KK07	187	0.31	-9422	0.40	-7226	0.74	-2185	-1156
KK01	2829	0.58	-1653	0.75	544	1.38	5584	1485
KK03	4852	0.67	1650	0.88	3846	1.62	8887	3508
KK04	396	-	-	-	-	-	-	-947
KK12	3715	0.54	-1274	0.71	923	1.30	5964	2371
SP01	4035	-	-	-	-	-	-	2692
KK08	10150	0.50	4497	0.65	6694	1.20	11734	8806
KK11	7113	0.47	878	0.61	3074	1.12	8115	5770
KG05	3372	0.44	-3329	0.58	-1132	1.06	3908	2028
KG08	1553	0.49	-4210	0.64	-2014	1.19	3027	209
KK13	214	0.48	-5757	0.63	-3561	1.16	1480	-1129
KK14	951	0.49	-4945	0.63	-2749	1.17	2292	-393
KK06	3138	0.52	-2261	0.67	-64	1.24	4977	1795
SK01	6205	-	-	-	-	-	-	4861

6.4.4 Conceptualisation of New Model

$\delta^{13}C_{DIC}$ values for the groundwater in the within the Buffels River catchment are heterogeneous. Two explanations could be firstly primary variation in the $\delta^{13}C_{DIC}$ values set by variations in the $\delta^{13}C_{soil}$ value due to different vegetation types (C3 vs C4 or both) in different areas within the catchment. As the water flows through the unsaturated zone, the original $\delta^{13}C_{DIC}$ values of the groundwater reflect the primary $\delta^{13}C$ value of the soils which are heterogeneous because of different proportions of C3 and C4 plants. The second scenario would be that the $\delta^{13}C$ values were originally more homogeneous and that dilution has taken place because of interaction with carbonate material along the flow path. For this heterogeneity to have occurred, some of the groundwater must have experienced different degrees of equilibration at different times causing changes in $\delta^{13}C_{DIC}$ and hence ^{14}C values of the DIC in the groundwater. In order to assess whether the processes outlined in these two scenarios played a role in dilution of ^{14}C signal, the recharge model described above needs to be modified.

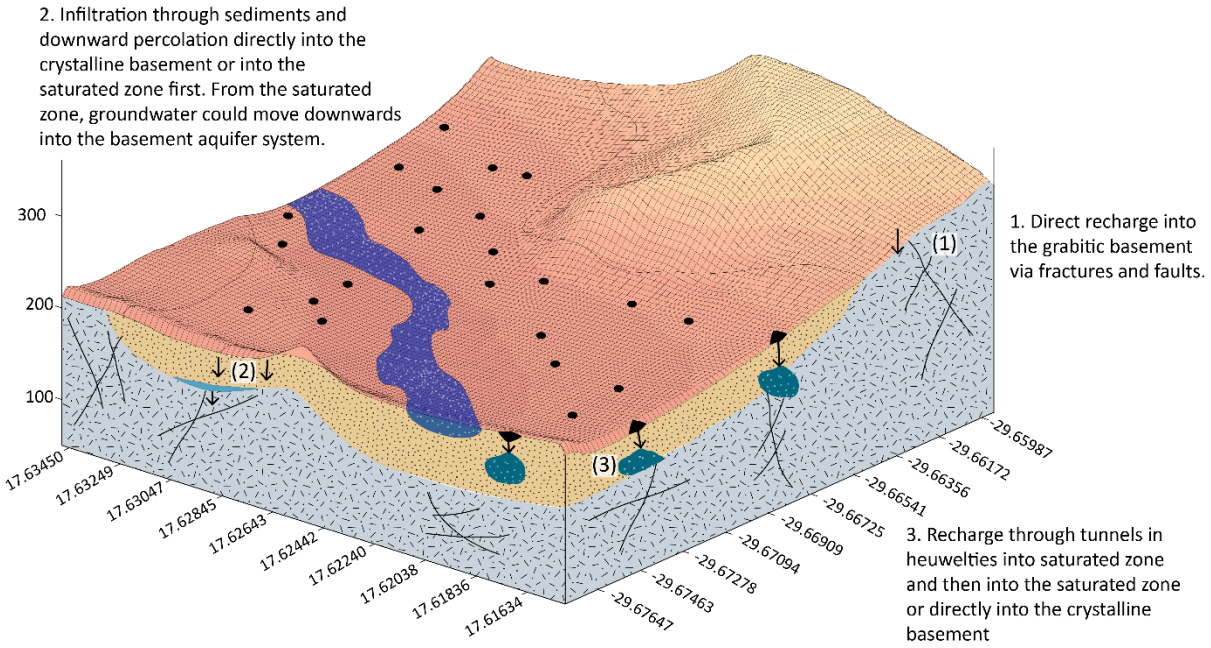

Figure 6.3: Conceptual model showing the three proposed recharge pathways.

The previous recharge model for this area did not account for the presence of heuweltjies, or the possibility of carbonates hosted in their soils. In order to understand the heterogeneity, three conceptual recharge pathways are proposed (Figure 6.3): (1) direct recharge into the basement aquifer through the interconnected fracture network. As precipitation hits the surface of the exposed granites, water infiltrates directly through the fracture network. In this case the $\delta^{13}C_{DIC}$ of the groundwater will remain unchanged; (2) recharge is derived from percolation through soils, into the saturated zone. Here isolated alluvial aquifers may form above the granitic gneisses where groundwater can infiltrate into

the basement aquifer if fracture networks allow for it; (3) recharge into the saturated zone and into the basement aquifer via heuweltjies where the tunnels (bioturbation / "termite" tunnels) act as preferential flow paths. For each of these pathways, potential recharge will be affected by different processes along the flow path that will in turn affect the residence time calculations.

The heterogeneity of the $\delta^{13}C_{DIC}$ values in the Buffels River catchment can be summarised by three trends indicated on Figure 6.4. (1) change in the ^{14}C activity with no or very little change in the $\delta^{13}C_{DIC}$ values; (2) change in $\delta^{13}C_{DIC}$ with no or very little change in the ^{14}C activity; (3) change in both ^{14}C and $\delta^{13}C$ values where ^{14}C decay occurs in combination with dilution in $\delta^{13}C_{DIC}$ values.

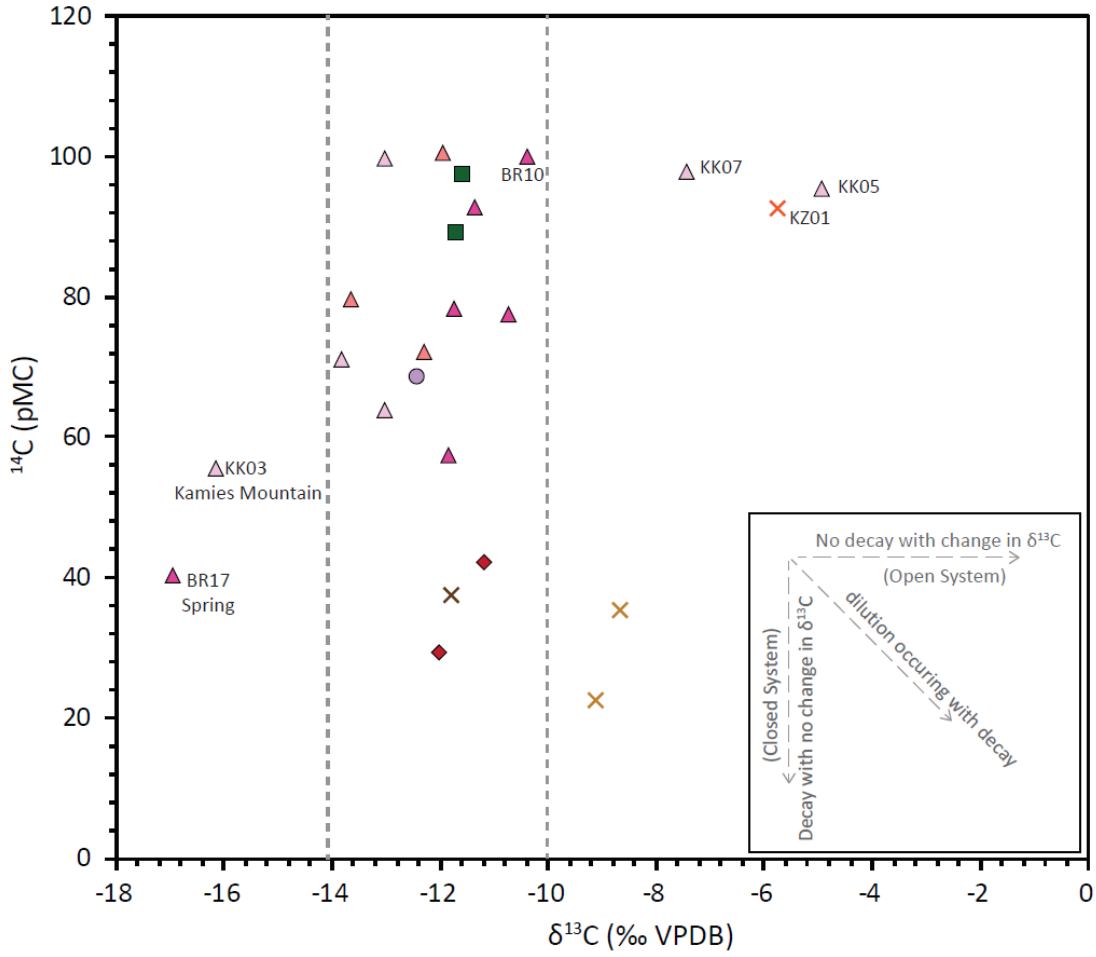

Figure 6.4: ^{14}C vs $\delta^{13}C$ values for groundwater collected represented according to the host rocks from which the samples were collected. The dashed vertical lines group the set of samples that have small variation in the $\delta^{13}C$ values that could have entered the system with these $\delta^{13}C$ values and have not been affected by dilution, but only decay. Refer to Figure 3.1 for the explanation of the symbology used.

The processes that could have contributed to dilution in the Buffels River catchment are interaction with soils in C3 ($\delta^{13}C$=-25‰) or C4 ($\delta^{13}C$=-12‰) dominated environments or inorganic carbonates

during recharge. Although the geology of the area and therefore the aquifer host rocks are dominated by silicates, inorganic carbonates in the form of calcite do occur in the soils of the Buffels River, specifically in the heuweltjie soils (Francis & Poch, 2019; Vermooten, 2019).

Although the $\delta^{13}C$ values of groundwater in the Buffels River catchment may be affected by carbonates in the heuweltjies or the presence of C3 or C4 vegetation, groundwater travelling through the heuweltjies is still within the unsaturated zone. The system behaves as an open system where the radiocarbon activity is kept in equilibrium with atmospheric ^{14}C, but the $\delta^{13}C$ values may be affected by the carbonates or root respiration. Only once the groundwater has passed through the heuweltjies and reached the saturated zone, the system starts behaving as a closed system where the radiocarbon activity will start decreasing. Given that the aquifer matrix in the Buffels River catchment varies from place to place, groundwater chemistry and $\delta^{13}C$ values are affected by different processes in different areas and the groundwater residence times cannot be calculated in the same way for all the samples. To add to this, groundwater in the Buffels River catchment has detectable tritium activity with radiocarbon activities as low as 22.6 pMC implying mixing between younger and older waters via different pathways and in various proportions. For this reason, an alternative approach to calculating the groundwater residence time was used incorporating both tritium and radiocarbon as tracers to evaluate residence times and mixing relationships using a lumped parameter model (LPM) approach. This was done with the USGS TracerLPM program.

6.4.5 Modern Recharge and Theoretical Mixing Relationships

Given the presence of tritium in groundwater with low radiocarbon activities in the Buffels River valley, mixing of modern recharge with older groundwater seems likely. Conventional radiocarbon age calculations do not take this into account and therefore, lumped parameter models (LPMs) were used to calculate total mean ages of the groundwater. LPMs calculate tracer concentrations at the outlet position or the sampling point from historical tracer data at the input location or recharge zone using exit-age distribution functions, decay functions and measured tracer data according to:

$$C_{out}(t) = \int_{-\infty}^{t} c_{in}(t') e^{-\lambda(t-t')} \cdot g(t-t') \cdot dt' \qquad \text{Equation 6.4}$$

Where $C_{out}(t)$ is the concentration of the tracer at the outlet, $C_{in}(t)$ is the concentration at the inlet at time t', the date when the water parcel entered the system while t is the sample date and λ the decay constant (Jurgens et al., 2012).

The mean age of the sample (τ_s) is calculated using the exit-age distribution function that describes the tracer concentrations in the sample as seen in equation 6.4.

$$\tau_s = \sum_{i=1}^{\infty} t_i \, X_i(\Delta t) \qquad \text{Equation 6.5}$$

Where t_i is the age of the water parcel (t-t'), X_i is the fraction of the sample represented by the water parcel at a corresponding age increment while Δt is the age increment.

The mixing model used here is theoretical than fully representative of the actual processes in this system. In order to calculate the ages, a binary mixing model (BMM), incorporating both an exponential mixing model (EMM) and a piston flow model (PFM), was considered as in this theoretical approach, the combination of these models is the most representative of what could be occurring in the Buffels River catchment. Combining the two models allows incorporation of recharge into the fractured basement aquifer as well as the recharge that occurs within the valleys where water percolates through the soils. In the case where heuweltjies are present, the PFM model was still applied as the groundwater recharge will still enter through conduits or fractures, where these are represented by the tunnels and bioturbated soils on the heuweltjies. Historic tritium data from the IAEA's GNIP database for Cape Town and Windhoek was imported into the TracerLPM program and used to plot model tritium curves for the Buffels River catchment. Data from the Buffels River catchment is not available and of the available data, data from these two cities are the most representative of the catchment. For the radiocarbon curves, the preloaded TracerLPM data for the Southern Hemisphere was used as historic radiocarbon data for the west coast of South Africa is not available. Measured tritium and radiocarbon activities were plotted against the model generated using TracerLPM and the BMM-EMM-PFM binary mixing line was used to calculate the total mean age and the mixing fraction of the modern component (Figure 6.5).

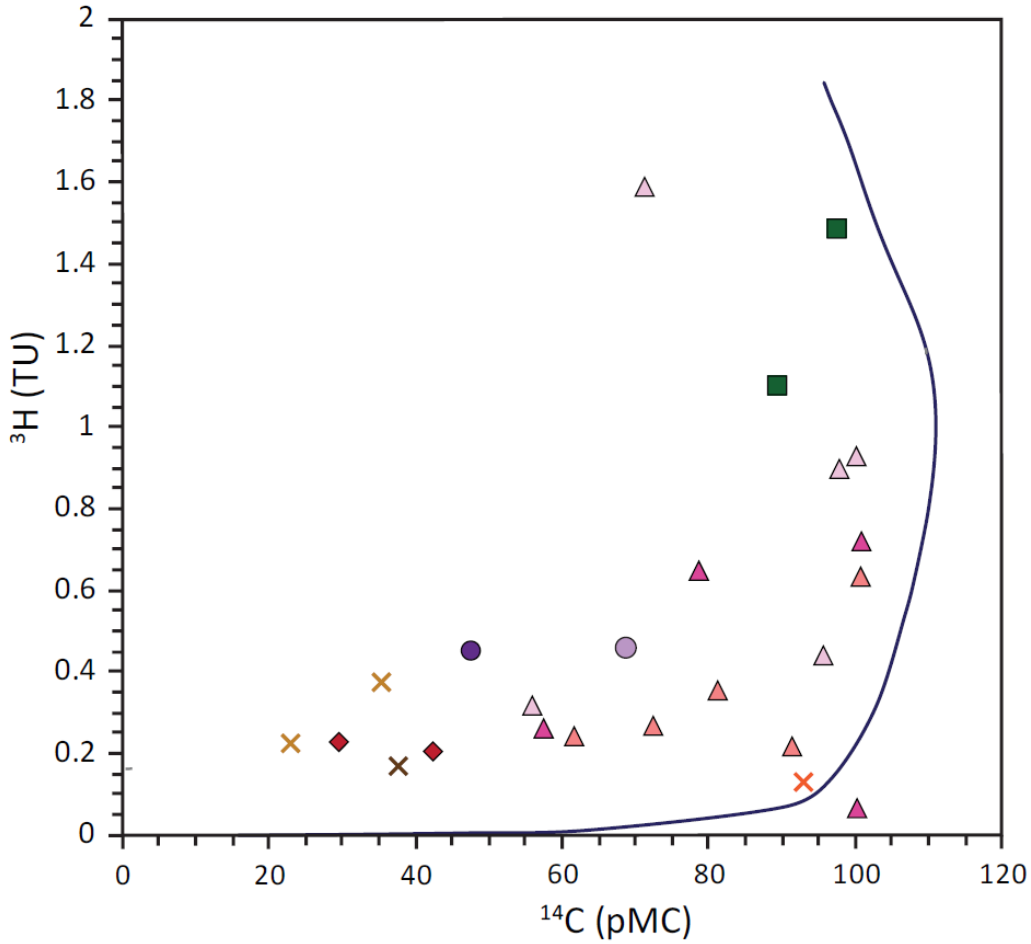

Figure 6.5: Tritium activity vs radiocarbon activity for groundwater in the Buffels River catchment compared to the modelled LPM curve for tritium and radiocarbon activity in the Southern Hemisphere.

The calculated mean residence time of the groundwater in the Buffels River catchment varies significantly with very little geographic correlation. Tritium and radiocarbon values could not be obtained for all 37 samples, but of the 23 samples for which ages could be calculated using the theoretical LPM approach, only 4 samples have total mean ages that can be considered as modern (50 years and younger), while 12 samples have total mean ages that can be classified as young water with residence times between 50 and 12 000 years and 3 samples have total mean ages of older than 12 000 years which can be classified as fossil water (Table 6.3). The total mean age of one sample could not be calculated as the tritium and radiocarbon activity of this sample are outside the modelled range. Groundwater collected from the south east of the catchment generally has the lowest radiocarbon and tritium activity and the longest residence time, irrespective of host lithology. However, groundwater collected from the Kamiesberg Group, have higher radiocarbon and tritium activities with residence times of 21.0 and 621 years in which case the groundwater is classified as modern to young. This is also

the case for groundwater in the known recharge zone of the catchment, as well as in the central and northern parts of the catchment, where groundwater ages range between 38.6 and 5657 years. The two samples collected from far west of the catchment have total mean ages of 553 and 9409 years. This is interesting because both of these samples were collected from sediment host rocks but the younger of the two samples was collected from a large open well with a depth of 3 m in the centre of the dry Buffels River which suggests that the water in this alluvial setting is being recharged by a significant component of older groundwater via lateral flow from the deeper system which in this case is not a pure fractured system but a deeper alluvial system. The second and older sample from this area indicates that the Deep Kleinsee Alluvial sediments hosting older groundwater is present in this region (Table 6.3).

Table 6.3: Groundwater age calculation data obtained by using LPMs

Pluton/Formation	Sample ID	BMM-EMM-PFM				
		Total mean age (years)	Mean age of the modern component (years)	Modern fraction (modern component)	Mean age of the oldest component (years)	Relative error
Shallow Kleinsee Alluvial Sediments	KZ01	552	6.2	8.0%	600	0.79%
Deep Kleinsee Alluvial Sediments	KZ02	9409	2.2	9.5%	10400	0.84%
Platbakkies Alluvial Sediments	KK09	17794	2.0	12.4%	20300	0.01%
	KK10	12638	2.4	21.0%	16000	0.09%
Concordia granite	BR05	5346	2.4	14.5%	6250	0.20%
	BR07	2048	2.2	36.0%	3200	0.42%
Modderfontein granite/gneiss	CD02	50	1.3	19.5%	62	0.53%
	NB01	2778	1.8	14.6%	3250	0.00%
	NB02	49	6.5	23.5%	62	0.01%
	NB03	651	3.0	12.0%	740	0.05%
	NB04	1619	1.7	19.1%	2000	0.00%
	SP02	1908	4.2	26.7%	2600	0.00%
Mesklip granite	KK02	39	1.0	38.4%	62	1.17%
	KK05	301	3.3	25.0%	400	0.01%
	KK07	37	3.6	45.5%	65	0.05%
	KK01	-	-	-	-	-
	KK03	5647	1.1	17.0%	6800	0.00%
	SP01	4743	2.9	13.8%	5500	0.00%
Lekkerdrink gneiss	KK08	13567	2.0	12.5%	15500	0.00%
	KK11	8406	5.6	12.5%	9600	0.00%
Kamiesberg Group	KK13	21	1.2	80.00%	100	1.90%
	KK14	621	1.0	58.64%	1500	0.24%
Noemnoemnaasberg granite	KK06	3517	1.8	25.18%	4700	0.01%
Steinkopf gneiss	SK01	7954	1.0	24.25%	10500	0.99%

6.4.6 Robustness of Groundwater Ages

Previous studies indicated that groundwater in the Buffels River catchment is up to 32 850 years old (Adams et al., 2004). However, these ages were calculated using the conventional decay equation and a dilution factor of 0.85 for all samples, irrespective of host rock geology or variation in $\delta^{13}C_{soil}$ values. In this study, three conventional calculation methods were evaluated. 1) the conventional equation with no correction; 2) the conventional equation with a dilution factor based on the $\delta^{13}C_{soil}$ values of each sample; and 3) the conventional equation with a dilution factor of 0.85 for all samples as was done by Adams et al. (2004). In all cases, some negative age values were obtained, and the ages were generally much younger than what was previously thought. These conventional methods are therefore questionable and an LPM approach was used to obtain total mean groundwater ages. However, there are some flaws in using this approach for this specific study. 1) LPMs are usually used for relatively complex binary mixing models where the recharge pathways are well understood and constrained. In this case, it was used for a simplified conceptual recharge model and there is a possibility that the LPM used here is oversimplified; 2) the historical preloaded database in Tracer LPM for atmospheric radiocarbon for the Southern Hemisphere is small compared to that of the Northern Hemisphere and most of the data is from New Zealand. However, this database is one of the only available for the Southern Hemisphere which could cause some degree of error when used to model groundwater ages in semi-arid to arid southern Africa; 3) it is assumed that tritium activity in groundwater is only from modern recharge but atmospheric contamination is not taken into consideration. If atmospheric contamination has occurred in the sampling process or even along the flow path, the radiocarbon ages will appear much younger than what they actually are, irrespectively of the calculation method. This is therefore also applicable to the conventional methods used to calculate the ages in section 6.4.3.

Although there are some flaws in using LPMs to calculate the total mean age of groundwater in the Buffels River catchment, it does provide valid ages with small apparent error values. In addition to this, the spatial distribution of the percentage modern recharge of samples collected in the same region within the catchment are comparable irrespective of the calculated age, providing an indication that changes in the actual system are consistent with what is seen in the model. In contrast to this, the conventional age calculation methods rely on a dilution factor that could potentially be highly variable across the catchment. The ages calculated using no dilution factor as well as four different possible dilution factors all generate negative ages are regarded as not reliable. In order to get more accurate ages using the conventional approach, the factors that could contribute to radiocarbon dilution will have to be evaluated for each sample individually. This will have to include C3 and C4 plant distribution, soil and soil gas $\delta^{13}C$. In addition to this, the presence of carbonates in the soil will have to be evaluated and the way it interacts with water as it percolates though the soils.

6.4.7 Groundwater salinisation and sustainability

Groundwater plays a significant role in the Buffels River catchment in terms of sustaining the domestic needs of the communities, the local economy, food security and the natural eco-system. Even though this region is classified as an arid environment and most species are adapted to survive in these conditions, climate change predictions suggest this may change. Globally, rainfall events are likely to become more erratic and intense and periods of extreme drought are expected to be more frequent and last for longer periods (Masih et al., 2014; Gizaw & Gan, 2017), which is also expected in the Buffels River catchment. Coastal fog will decrease(Davis et al., 2016; Weldeab et al., 2013) affecting the natural ecosystem which currently relies on fog and the dependence on groundwater to sustain the agricultural sector as well as the natural eco-system will increase. Most of the towns in the catchment are already wholly dependent on groundwater and in some cases, boreholes have dried up which has forced farmers and the local authorities to further tap into the groundwater system or reduce agricultural activity significantly. Given that only 4 of the 23 samples can be classified as modern in terms of the description given by Bierkens & Wada (2019), Gleeson et al. (2016) and Jasechko et al. (2017), together with the current climate predictions and the recent drought resulting in drying up of boreholes, there is a risk of groundwater depletion in the Buffels River catchment.

Apart from the risk of groundwater depletion in the region, further deterioration of the groundwater quality will be detrimental to the social and economic development of the region. However, salinisation of groundwater in the Buffels River catchment is a natural process controlled by various factors, including the saline heuweltjie soils. Although the exact mechanism of groundwater salinisation through heuweltjies have not yet been determined, heuweltjies are such pronounced features, not only in the Buffels River catchment, but along the west coast of southern Africa, that the effect that these saline features may have on the groundwater quality cannot be overlooked. In addition to groundwater salinisation, saline heuweltjie affected soils limit agricultural and hence economic development. These soils cannot be used for agricultural purposes as very few crops will be able to tolerate the extreme soil salinity together with the semi-arid to arid climatic conditions and the lack of sufficient irrigation or the salinity of the groundwater used for irrigation.

6.5 Conclusion

The sustainability of groundwater both in terms of quantity and quality is a major issue in the Buffels River catchment. In order to better understand this issue, the age of the groundwater was determined to gauge recharge times as well as the possible period of salinisation. The absence of inorganic carbon in the geology and the uncertainty about the presence of inorganic carbon along the groundwater flow paths resulted in challenges in using the conventional radiocarbon age calculation methods. A new

conceptual flow model was constructed to include three possible groundwater flow paths 1) direct recharge into the basement aquifer, 2) percolation through sediments, into the saturated zone and depending on the presence of a fracture network, into the granitic basement; 3) through heuweltjies and either directly into the granitic basement or into the saturated zone and then following the same process mentioned in pathway 2. Due to the presence of tritium in samples with lower radiocarbon activities and the uncertainties whether radiocarbon dilution could occur in the system, a simplified and theoretical LPM model was used to calculate total mean groundwater ages. Groundwater in the Buffels River catchment is generally older than 300 years (young groundwater between 50 and 12 000 years) with only 4 of the samples being modern, while groundwater in the east of the catchment is fossil groundwater of older than 12 000 years. Although modern recharge does occur, the percentage of the modern component in most cases are relatively small, indicating that the recharge occurring is not necessarily sustainable and water that is currently being abstracted is not modern water.

6.6 References

Adams, S., Titus, R., Xu, Y., 2004. Groundwater recharge assessment of the basement aquifers of central Namaqualand, WRC Report No. 1093/1.

Appelo, C.A.J., Postma, D., 2005. Geochemistry, groundwater and pollution. 2nd. Ed. Balkema, Rotterdam.

Benito, G., Botero, B.A., Thorndycraft, V.R., Rico, M., Sánchez-Moya, Y., Sopeña, A., MacHado, M.J., Dahan, O., 2011. Rainfall-runoff modelling and palaeoflood hydrology applied to reconstruct centennial scale records of flooding and aquifer recharge in ungauged ephemeral rivers. Hydrol. Earth Syst. Sci. 15, 1185-1196. https://doi.org/10.5194/hess-15-1185-2011

Benito, G., Rohde, R., Seely, M., Külls, C., Dahan, O., Enzel, Y., Todd, S., Botero, B., Morin, E., Grodek, T., Roberts, C., 2010. Management of alluvial aquifers in two Southern African ephemeral rivers: Implications for IWRM. Water Resour. Manag. 24, 641-667. https://doi.org/10.1007/s11269-009-9463-9

Bierkens, M.F.P., Wada, Y., 2019. Non-renewable groundwater use and groundwater depletion: A review. Environ. Res. Lett. 14. https://doi.org/10.1088/1748-9326/ab1a5f

Cartwright, I., Cendón, D., Currell, M., Meredith, K., 2017. A review of radioactive isotopes and other residence time tracers in understanding groundwater recharge: Possibilities, challenges, and limitations. J. Hydrol. 555, 797-811. https://doi.org/10.1016/j.jhydrol.2017.10.053

Cartwright, I., Currell, M.J., Cendón, D.I., Meredith, K.T., 2020. A review of the use of radiocarbon to estimate groundwater residence times in semi-arid and arid areas. J. Hydrol. 580, 124247. https://doi.org/10.1016/j.jhydrol.2019.124247

Davis, C.L., Hoffman, M.T., Roberts, W., 2016. Recent trends in the climate of Namaqualand, a megadiverse arid region of South Africa. S. Afr. J. Sci. 112, 1-9. https://doi.org/10.17159/sajs.2016/20150217

Francis, M.L., Poch, R.M., 2019. Calcite accumulation in a South African heuweltjie: Role of the termite Microhodotermes viator and oribatid mites. J. Arid Environ. 103981. https://doi.org/10.1016/j.jaridenv.2019.05.009

Gleeson, T., Befus, K.M., Jasechko, S., Luijendijk, E., Cardenas, M.B., 2016. The global volume and distribution of modern groundwater. Nat. Geosci. 9, 161-164. https://doi.org/10.1038/ngeo2590

Gizaw, M.S. and Gan, T.Y., 2017. Impact of climate change and El Niño episodes on droughts in sub-Saharan Africa. *Climate Dynamics*, *49*(1), pp.665-682.

Ingerson, E. and Pearson, F.J., 1964. Estimation of age and rate of motion of groundwater by the 14C-method. *Recent researches in the fields of atmosphere, hydrosphere and nuclear geochemistry*, pp.263-283.

Jasechko, S., Perrone, D., Befus, K.M., Bayani Cardenas, M., Ferguson, G., Gleeson, T., Luijendijk, E., McDonnell, J.J., Taylor, R.G., Wada, Y., Kirchner, J.W., 2017. Global aquifers dominated by fossil groundwaters but wells vulnerable to modern contamination. Nat. Geosci. 10, 425-429. https://doi.org/10.1038/ngeo2943

Jurgens, B.C., Bohlke, J.K., Eberts, S.M., 2012. TracerLPM (Version 1): An Excel workbook for interpreting groundwater age distributions from environmental tracer data, U.S. Geological Survey Techniques and Methods Report 4-F3.

Masih, I., Maskey, S., Mussá, F.E.F. and Trambauer, P., 2014. A review of droughts on the African continent: a geospatial and long-term perspective. *Hydrology and Earth System Sciences*, *18*(9), pp.3635-3649.

Meredith, K., 2009. Radiocarbon age dating groundwaters of the West Canning Basin , Western Australia.

Newman, B.D., Osenbrück, K., Aeschbach-Hertig, W., Solomon, D.K., Cook, P., Rózánski, K., Kipfer, R., 2010. Dating of "young" groundwaters using environmental tracers: Advantages, applications, and research needs. Isotopes Environ. Health Stud. 46, 259-278. https://doi.org/10.1080/10256016.2010.514339

Oehlert, A.M. and Swart, P.K., 2014. Interpreting carbonate and organic carbon isotope covariance in the sedimentary record. *Nature Communications*, *5*(1), pp.1-7.

Plummer, N.L. and Sprinkle, C.L., 2001. Radiocarbon dating of dissolved inorganic carbon in groundwater from confined parts of the Upper Floridan aquifer, Florida, USA. *Hydrogeology Journal*, *9*(2), pp.127-150.

Pietersen, K., Titus, R., Cobbing, J., 2009. Effective Groundwater Management in Namaqualand Sustaining Supplies, Effective Groundwater Management in Namaqualand Sustaining Supplies.

Titus, R., Beekman, H., Adams, S., Strachan, L., 2009. The Basement Aquifers of Southern Africa, WRC Report No. TT428/09. South Africa.

Tweed, S., Celle-Jeanton, H., Cabot, L., Huneau, F., De Montety, V., Nicolau, N., Travi, Y., Babic, M., Aquilina, L., Vergnaud-Ayraud, V., Leblanc, M., 2018. Impact of irrigated agriculture on groundwater resources in a temperate humid region. Sci. Total Environ. 613-614, 1302-1316. https://doi.org/10.1016/j.scitotenv.2017.09.156

Van Gend, J. et al., 2021. Saline groundwater in the Buffels River catchment, Namaqualand, South Africa: A new look at an old problem. Science of The Total Environment, 143140.van Rooyen, J.D., Watson, A.P., Miller, J.A., 2020. Combining quantity and quality controls to determine groundwater vulnerability to depletion and deterioration throughout South Africa. Environ. Earth Sci. 79, 1-20. https://doi.org/10.1007/s12665-020-08998-1

Vermooten, M., 2019. Investigation of heuweltjie structure and soil chemistry in the Buffels River valley and implications for transfer of salts to groundwater. Stellenbosch University.

Villholth, K.G., 2013. Groundwater irrigation for smallholders in Sub-Saharan Africa – a synthesis of current knowledge to guide sustainable outcomes. Water Int. 38, 369-391. https://doi.org/10.1080/02508060.2013.821644

Watson, A.P., Kralisch, S., van Rooyen, J.D., and Miller, J.A., 2021. Quantifying and understanding the source of recharge for alluvial systems in arid environments through the development of a seepage model. Journal of Hydrology, 601, 126650.

Weldeab, S., Stuut, J.B.W., Schneider, R.R., Siebel, W., 2013. Holocene climate variability in the winter rainfall zone of South Africa. Clim. Past 9, 2347-2364. https://doi.org/10.5194/cp-9-2347-2013

7 HEUWELTJIES AND GROUNDWATER FLOW

By J. van Gend, M.L., Francis, C.E. Clarke, L Palcsu, and J.A. Miller

7.1 Introduction

The aim of this part of the report is to examine the mechanisms and timing of salt input in the groundwater of the Buffels River catchment. Results presented already have shown that salts present in the groundwater are linked to dry deposition of marine aerosols and ion-exchange reactions between the aquifer host rock and the groundwater (van Gend et al., 2021). This suggests strong leaching of marine-originated salts in order to reach groundwater, which is a paradox given the aridity of the region. The hypothesis is that it is the wetter periods, which were also the most habitable periods in Namaqualand (Dewar and Stewart, 2017; Jones and Stewart, 2016), were responsible for flushing salts from the regolith into the groundwater system, and that this effect is amplified by the presence of preferential flow paths associated with the hotspots of saline, termite-affected soils (heuweltjies) that are so striking in the catchment. By understanding the mechanism and timing of salinisation in this region, groundwater management and climate change strategies for Namaqualand can be adapted to include the possible causes and risks of salinisation.

7.2 Sampling Method

Samples were collected from two different areas within the Buffels River Catchment. Four samples were collected from various locations towards the west coast. These included heuweltjie sediments and carbonate nodules from other soil horizons. Two heuweltjies in the Buffels River valley were identified and a trench was made through the heuweltjies by means of an excavator. The soil profiles were assessed and described before samples were collected. For this study, the focus was to collect representative samples throughout the heuweltjie and interheuweltjie areas as well as in soils along towards the west coast to analyse for radiocarbon and $\delta^{13}C$ and samples included soils as well as carbonate nodules. Samples were dried in a temperature and humidity-controlled room before they were sieved through a 2 mm soil sieve. Carbon nodules were collected were crushed by using a pestle and mortar to ensure that the sample is homogenous. Three subsamples of 10 g each were weighed off and sent for further processing and analysis.

7.3 Results

7.3.1 Variation of Groundwater Chemistry Over Time

Anion concentrations in groundwater vary with groundwater age (Figure 7.1a). There is an increase in the Cl^- concentration from 18 000 to 13 600 ybp. From here the Cl^- concentration decreases until 8 400 ybp where a slight increase is seen before it drops to the lowest concentration seen across the timeline at around 5 600 ybp after which the concentration increases at 5 500 ybp. From there, the overall Cl^- concentration continues to decrease but there are large spikes in the Cl^- concentration at around 2 000 ybp and 600 ybp. Sulphate and HCO_3^- follow a similar trend but their concentrations are much lower. The magnitude of the SO_4^{2-} changes is greater than that of HCO_3^- , which remains slightly more consistent over time. An increase in concentration of specifically sulphate around 8 000 ybp and between 5 600 and 5 500 ybp is also seen.

The stable isotopes in groundwater also vary through time (Figure 7.1b and 7.1c). Although $\delta^{13}C\ CO_3^{2-}$ and $\delta^{18}O\ CO_3^{2-}$ and $\delta^{34}S\ SO_4^{2-}$ and $\delta^{18}O\ SO_4^{2-}$ do not react in the same way, changes are seen at 5 600 to 5 500 ybp, 2 000 ybp and 600 ybp which are consistent with the timing of changes that occurred in the ion concentrations. The $\delta^{18}O\ H_2O$ of groundwater is more stable over time than the $\delta^{2}H\ H_2O$ (Figure 7.1c). The increases seen in both are consistent with the changes in $\delta^{13}C\ CO_3^{2-}$ and $\delta^{18}O\ CO_3^{2-}$ and $\delta^{34}S\ SO_4^{2-}$ and $\delta^{18}O\ SO_4^{2-}$ isotopes (Figure 7.1b) as well as the changes in groundwater chemistry (Figure 7.1a) with time.

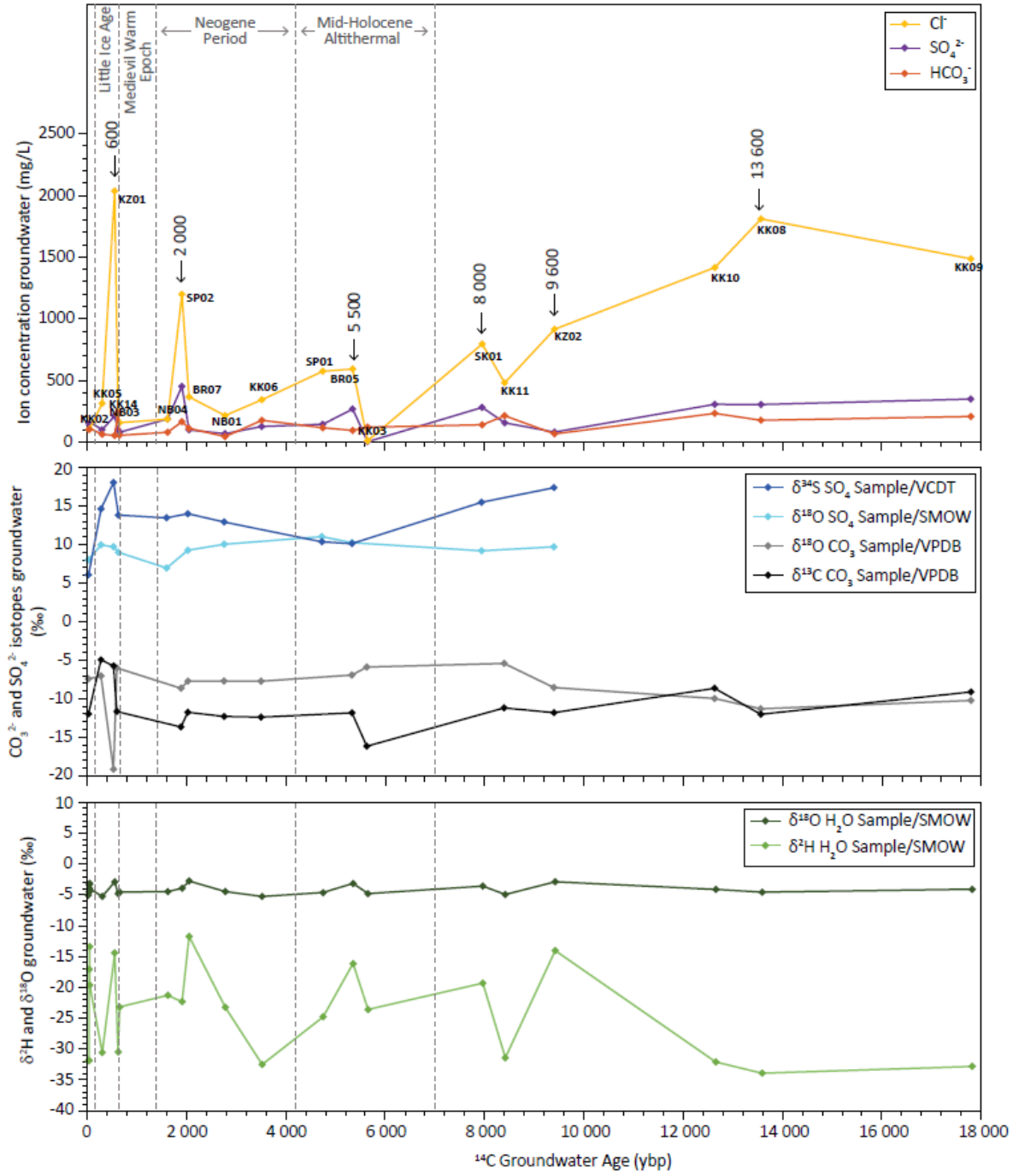

Figure 7.1: Anion concentrations in groundwater and stable isotopes in groundwater and heuweltjies from the Buffels River catchment plotted against age. Groundwater ages as calculated in Chapter 6 (Table 6.3). Previous known climatic periods from (Dewar and Stewart, 2017). a) Anion concentrations over time indicating major salt input events in the past 18 000 years. b) Variation in stable isotopes of CO_3^- and SO_4^{2-} over the past 18 000 years. c) Variation in stable isotopes of H_2O in groundwater for the samples dating up to 18 000 years old.

7.3.2 Soil Carbonate Ages

The deepest carbonates reach a maximum age of 30 500 ± 171 ybp in Heuweltjie 1 at 110 cm depth and 30 500 ± 171 ybp at the same depth in Heuweltjie 4. The youngest carbonates have ages of 2 790 ± 29 ybp and 3 050 ± 41 ybp for Heuweltjie 1 and Heuweltjie 4 respectively and are located at a depth of 10 cm in both heuweltjies. The carbonates in the center of the heuweltjie are situated much deeper than similar-aged carbonates towards the edges, resulting in a U-shaped curve describing the depth to carbonates of similar age in Heuweltjie 1 (Figure 7.2). The ages of the heuweltjie carbonates are consistent with other older pedogenic carbonates from the samples collected towards the west coast.

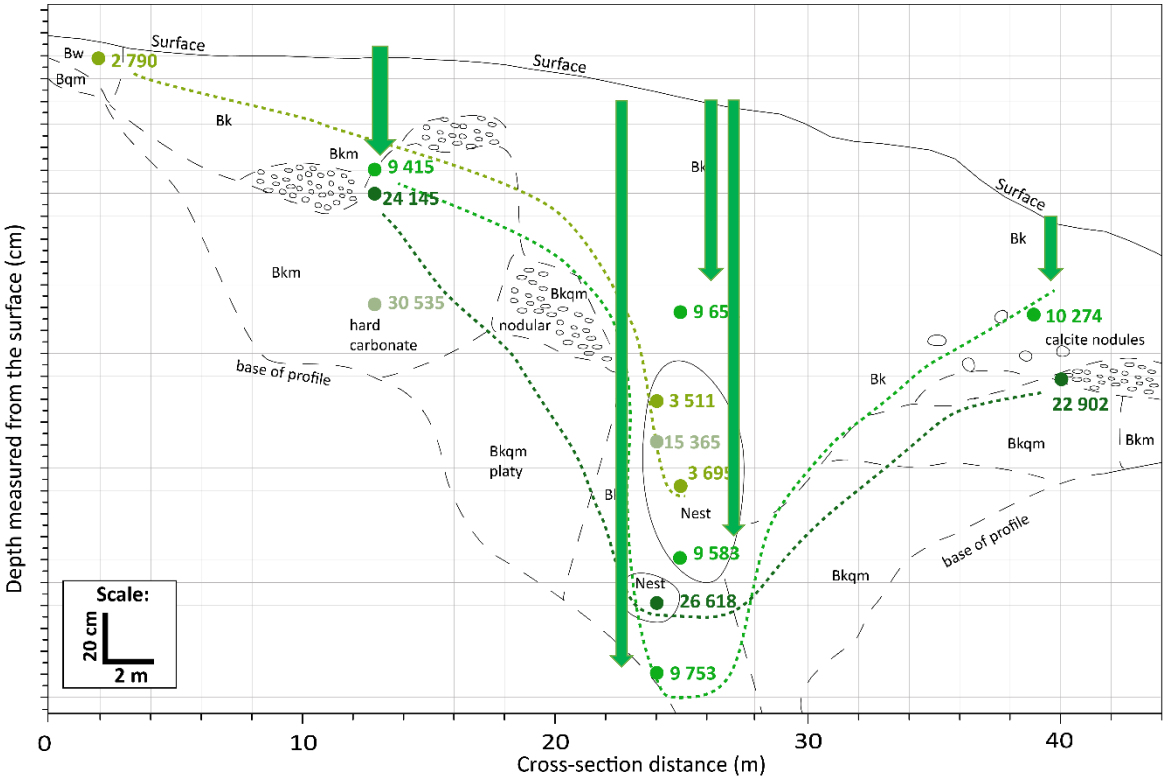

Figure 7.2: Cross-section of heuweltjie 1 showing the distribution of radiocarbon ages for carbonates in the heuweltjie in green. The dotted green lines in different shades of green indicate the depth to calcite of similar ages. Bk = carbonate accumulation; Bw = development of colour and structure; Bkm = carbonate cementation; Bqm = silica cementation; Bkqm = carbonate and silica cementation (Food and Agriculture Organization of the United Nations., 2006).

7.3.3 $\delta^{18}O$ and $\delta^{34}S$ Values from SO_4^{2-} in Heuweltjie Soil and Groundwater

The samples collected from Heuweltjie 1 contained too little sulphate for $\delta^{34}S\ SO_4^{2-}$ and $\delta^{18}O\ SO_4^{2-}$ to be determined. Heuweltjie 4 contained sulphates in the form of gypsum, in some places in sufficient quantity to be classified as a gypsic soil horizon. The $\delta^{18}O\ SO_4^{2-}$ signatures of Heuweltjie 4 (8.3 to 11.4 ‰) are comparable to $\delta^{18}O\ SO_4^{2-}$ of the groundwater (7.0 to 12.0 ‰), showing that the sulphates in the heuweltjie and in the groundwater are likely to be from the same SO_4^{2} source (Figure 7.3).

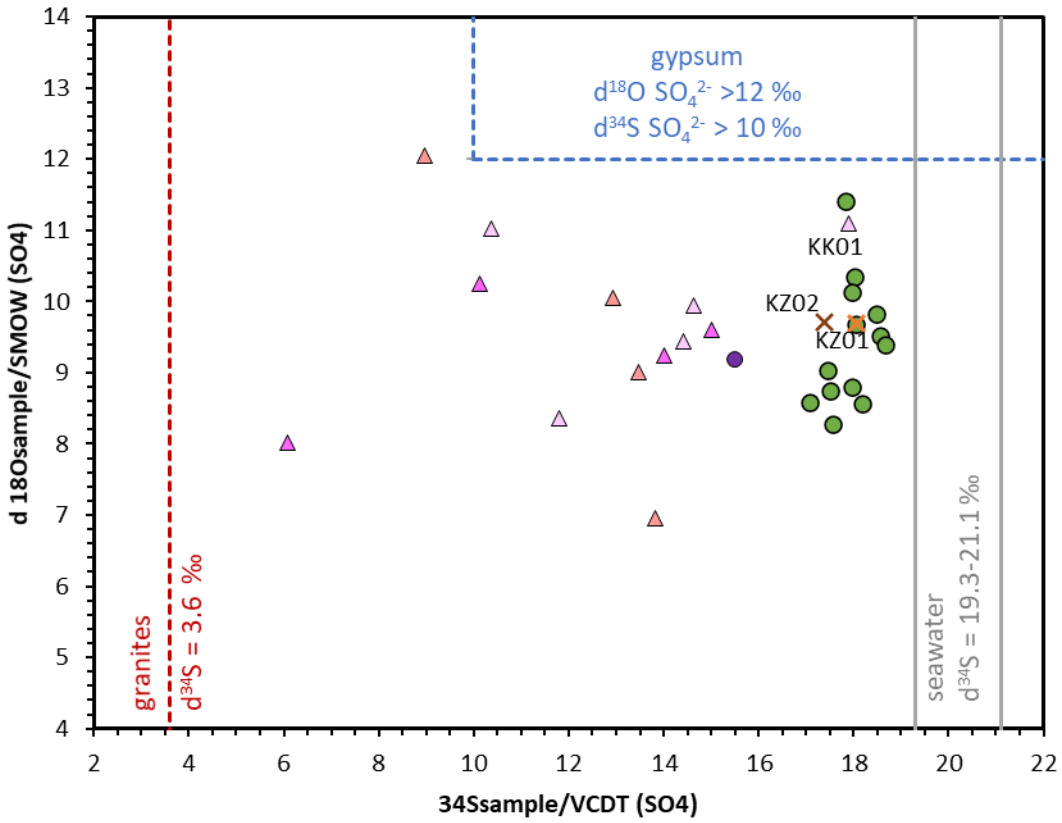

Figure 7.3: $d^{18}O$ and $d^{34}S$ values from SO_4^{2-} in soil samples (Heuweltjie 4) showed in green circles compared to that in groundwater from the Buffels River catchment, marked according to the host rock geology. See the Figure 3.1 for an explanation of the symbology used for the groundwater samples. The reference $d^{34}S\ SO_4^{2-}$ and $d^{18}O\ SO_4^{2-}$ values for gypsum is shown as a field and the reference $d^{34}S$ values for granites and seawater are also shown.

Three of the groundwater samples have $\delta^{34}S\ SO_4^{2-}$ values which are comparable to that of the heuweltjies. Two of these samples (KZ01 and KZ02, see Figure 7.3) were collected from boreholes drilled into sediments where the heuweltjie density is high and show a marine influence. The other groundwater samples from granitic host rocks have lower $\delta^{34}S\ SO_4^{2-}$ values, suggesting that there are processes involved causing a decrease in specifically the $\delta^{34}S\ SO_4^{2-}$ signature of the water by either

enrichment of the light isotope or removal of the heavier isotope in these samples possibly during the process of water-rock interaction in the granitic host rocks (van Gend et al., 2021).

7.4 Discussion

7.4.1 Heuweltjies and Saline Groundwater

Chloride is often used as a tracer in groundwater and soil studies because it does not readily enter oxidation or reduction reactions and does not form soluble complexes with other ions. Moreover, Cl is not commonly adsorbed to surfaces and it remains in solution over the largest concentration range (Bouchaou et al., 2008; Huang et al., 2017). In the Buffels River valley, gypsum and calcite are significant secondary mineral components in the heuweltjie soils (Figure 7.2) where they form gypsic, calcic and petrocalcic horizons (IUSS Working Group WRB, 2015). In the Buffels River valley groundwater, SO_4^{2-} and HCO_3^- are second and third in abundance respectively after Cl- (Figure 1a). During episodes of leaching, while Cl^- (halite log K = 1.59, (Chase, 1998)) is readily flushed into the groundwater system, this would be followed by SO_4^2 during higher intensity leaching events (log K gypsum = -4.61, (Garvin et al., 1987)) and only with the highest leaching volumes is HCO_3^- expected to be flushed into the system as $CaCO_3$ in the profile dissolves (log K calcite = -8.48, (Plummer and Busenberg, 1982)). The variation in the anion concentrations in the groundwater can therefore be related to the intensity of recharge events over time in the Buffels Rivers soil-groundwater system. This is seen in Figure 1a where Cl^- is most concentrated in the groundwater followed by SO_4^{2-} and HCO_3^- for each event age. It is also clear that the magnitude of the Cl^- increase is greater than that of changes in SO_4^{2-} which is in turn greater than that of HCO_3^- (Figure 1a). By looking at these anion concentrations over time, a robust timeline of events is evident. Apart from the major anions in the groundwater, the stable isotope data of the groundwater also shows significant peaks which can be related to these salt flushing events. $\delta^{34}S\ SO_4^{2-}$ and $\delta^{18}O\ SO_4^{2-}$ as well as $\delta^{13}C\ CO_3^{2-}$ and $\delta^{18}O\ CO_3^{2-}$ in groundwater shows distinct changes around 5800 ybp, 1900 ybp and 600 ybp. In the case of $\delta^{18}O\ SO_4^{2-}$, a smaller peak is seen around 1900 ybp while the larger peak is seen around 600 ybp (Figure 1b).

7.4.2 Infiltration Processes through Heuweltjies

The depth to the carbonate horizon in calcareous soils is proportional to the mean annual precipitation (MAP) (Zamanian et al., 2016). The depth to the carbonate-bearing horizons of a similar age in the heuweltjies can therefore be used as an indication of the MAP. Events of increased MAP for a given carbonate age would provide an indication of periods of increased leaching and greater depths to carbonate through the profile. In Heuweltjie 1, there are three U-shaped fronts formed by the ages of

the carbonate nodules (Figure 2): 2700 and 3000 ybp, 9700-9400 ybp, and >24 000 ybp, with the shallowest carbonates generally being younger. These periods correspond to the ages of increased salinity in the groundwater and also to the periods of increases in the $\delta^{18}O$ H_2O and $\delta^{2}H$ H_2O in the groundwater (Figure 1c). The increase in the $\delta^{18}O$ H_2O and $\delta^{2}H$ H_2O signature of the groundwater around 9800 ybp and the sharp increase just before 2000 ybp both indicate an increase in the humidity which suggests an overall wetter period (Hoefs, 2015).

The U-shaped front shows that carbonates situated deeper in the center of the heuweltjie are the same age as those at shallower depths along the edges of the heuweltjie. This shows that the carbonates in the centre of the heuweltjie around the nest have been leached to a greater depths than those at the edges and indicates that water is preferentially transported through the middle of the heuweltjie. The center of the heuweltjie above the nest area is heavily bioturbated, with many tunnels and interconnected macropores. This indicates that heuweltjies and more specifically termite activity plays a role in facilitating infiltration of surface water, and facilitating groundwater recharge especially during specific, episodic, large volume leaching events.

7.5 Conclusions

The ages of the carbonates in the heuweltjies provide valuable information regarding the climate in the past which can in turn be related to the recharge events and salts being flushed into the groundwater system. Furthermore, the distribution of the carbonate ages indicate that the water preferentially flows through the center of the heuweltjie compared to the edges. This would imply that heuweltjies preferentially facilitate recharge. Heuweltjies also contribute to the salinity of the groundwater as heuweltjies act as salt storage zones and the salts in the heuweltjies can be related to the salts in the groundwater through the $\delta^{18}O$ values of sulphate. For the last 18 000 years Cl^- has been flushed into the groundwater system in various concentrations but three major events are worth noting where less soluble salts such as gypsum and even carbonates were flushed into the groundwater system. These are around 14 000 ybp, around 8000 ybp, in the Mid-Holocene Altithermal around 5800 years ago, in the early Neogene Period around 2000 years ago and the last significant event was at the beginning of the Little Ice Age around 550 years ago.

7.6 References

Bouchaou, L., Michelot, J.L., Vengosh, A., Hsissou, Y., Qurtobi, M., Gaye, C.B., Bullen, T.D., Zuppi, G.M., 2008. Application of multiple isotopic and geochemical tracers for investigation of recharge,

salinization, and residence time of water in the Souss-Massa aquifer, southwest of Morocco. Journal of Hydrology 352, 267-287. https://doi.org/10.1016/j.jhydrol.2008.01.022

Chase, M.W., 1998. NIST-JANAF thermochemical tables. J. Phys. Chem. Ref. Data, Monograph 9.

Dewar, G., Stewart, B.A., 2017. Early Maritime Desert Dwellers in Namaqualand, South Africa: A Holocene Perspective on Pleistocene Peopling. Journal of Island and Coastal Archaeology 12, 44-64. https://doi.org/10.1080/15564894.2016.1216476

Food and Agriculture Organization of the United Nations., 2006. Guidelines for soil description. Food and Agriculture Organization of the United Nations.

Garvin, D., Parker, V.B., White Jr, H.J., 1987. CODATA thermodynamic tables.

Hoefs, J., 2015. Stable Isotope Geochemistry, Seventh. ed, Geochemistry. Springer International Publishing, Switzerland. https://doi.org/10.1007/978-3-319-19716-6

Huang, T., Pang, Z., Liu, J., Yin, L., Edmunds, W.M., 2017. Groundwater recharge in an arid grassland as indicated by soil chloride profile and multiple tracers. Hydrological Processes 31, 1047-1057. https://doi.org/10.1002/hyp.11089

IUSS Working Group WRB, 2015. World Reference Base for Soil Resources 2014, update 2015. International soil classification system for naming soils and creating legends for soil maps. World Soil. ed, World Soil Resources Reports No. 106. Rome. https://doi.org/doi:10.1017/S0014479706394902

Jones, S.C., Stewart, B.A., 2016. Africa from MIS 6-2: Population Dynamics and Paleoenvironments. Springer, Dordrecht, 2016. https://doi.org/10.1007/978-94-017-7520-5

Plummer, L.N., Busenberg, E., 1982. The solubilities of calcite, aragonite and vaterite in CO2-H2O solutions between 0 and 90 C, and an evaluation of the aqueous model for the system CaCO3-CO2-H2O. Geochimica et cosmochimica acta 46, 1011-1040.

Van Gend, J., Francis, M.L., Watson, A.P., Palcsu, L., Horváth, A., Macey, P.H., le Roux, P., Clarke, C.E., Miller, J.A., 2021. Saline groundwater in the Buffels River catchment, Namaqualand, South Africa: A new look at an old problem. Science of The Total Environment 762, 143140. https://doi.org/https://doi.org/10.1016/j.scitotenv.2020.143140

Zamanian, K., Pustovoytov, K., Kuzyakov, Y., 2016. Pedogenic carbonates: Forms and formation processes. Earth-Science Reviews 157, 1-17. https://doi.org/10.1016/j.earscirev.2016.03.003

8 MAPPING HEUWELTJIES USING REMOTE SENSING AND MACHINE LEARNING

By M.G. Maponya, Z.E. Mashimbye, M.L. Francis, C.E. Clarke, J.A. Miller

8.1 Introduction

Earth mounds of enigmatic origins occur over vast areas around the world and are prominent features of the south-western landscape in the southern parts of Africa, where they occupy 14-25% of the land surface (Lovegrove & Siegfried, 1989, Midgley, 2010). Earth mounds range between 17 m and 30 m in diameter and 1.45 m to 2.5 m in height (Moore & Picker, 1991). In South Africa, earth mounds popularly known as “heuweltjies” occur largely within the arid and semi-arid Mediterranean-climate, sparsely vegetated Namaqualand, Succulent Karoo and Fynbos biomes across the Western and Northern Cape Provinces (Francis & Poch, 2019; McAuliffe et al., 2019). Generally, heuweltjies are absent from very mountainous areas and are restricted to inland flats and mountain valleys, as well as West Coast lowlands (Lovegrove & Siegfried, 1986; Picker et al., 2007). According to Cramer & Midgley (2015) heuweltjies occur mostly in sparse ($0.1 < NDVI < 0.5$) semi-arid Mediterranean-climate, Succulent Karoo vegetation at modest elevations (<1000 m) with relatively high average annual wind speeds.

These structures have significant consequences for the natural environment, affecting the functionality of ecosystems on which they occur, and the services provided by such ecosystems. Considering the vast areas occupied by earth mounds, their conspicuous nature, and influence on vegetation patterns, soil properties and crop production within South African biomes, it is important to monitor and manage their impacts. To effectively monitor and manage these impacts, there is a need for studying the spatial distribution and density of heuweltjies. This information is essential for land use managers, environmental managers, as well as hydrological and ecological modellers (Bui et al., 2006; Hengl & Reuter, 2009; Vanwalleghem et al., 2011; Zhang et al., 2017).

Generally, heuweltjies form ubiquitous features which contribute considerably to the heterogeneity of the landscapes, both in terms of soil properties and vegetation composition (Midgley & Musil, 1990; Desmet, 2007). Their impacts spread across biotic and abiotic environments. For example, the difference in their physical and chemical soil properties from the surrounding soils results in higher nutrients, water content and higher levels of both macro- and micro-elements (Midgley & Musil, 1990; Petersen et al., 2003; Herpel, 2008). Consequently, the vegetation species composition and cover differ considerably between heuweltjies and their surroundings (Armstrong & Siegfried, 1990; Knight et al.,

1989; Midgley & Musil, 1990; Rahlao et al., 2008). Typically, heuweltjies are visible due to distinct differences in vegetation cover on the domal surface in comparison to the interheuweltjie material (Schmiedel et al., 2015). Heuweltjie vegetation is either denser and higher or sparser than the surrounding vegetation, depending on the climatic conditions and disturbance regime (Turner, 2003). Compared to the surrounding environment, heuweltjie vegetation usually contains more deciduous and opportunistic species, which usually retains their greenness even during dry seasons and this has been ascribed to the better mineral, nutrient, and water supply (Esler and Cowling, 1995; Midgley & Musil, 1990; Rahlao et al., 2008).

Although heuweltjies have a remarkable influence on vegetation patterns, soil properties and general ecosystem functionalities the lack of information regarding their spatial distribution and density presents a significant obstacle to understanding and managing their impact **(**Schmiedel et al., 2015; Francis & Poch, 2019**)**. Satellite-based Earth observations provide a powerful means to this end. Not only does remote sensing (RS) provide the basic data for studying land features (Skidmore et al., 1997), but RS based time series analysis can be used to reveal optimal times for undertaking such studies (Kuenzer et al., 2015; Lasaponara & Lanorte, 2012).

Despite the growing interest in the genesis of heuweltjies, very few studies have been undertaken on the spatial distribution and density of heuweltjies (Cramer & Midgley, 2015; Cramer et al., 2017). Even the few studies conducted on the spatial distribution and density of heuweltjies focused more on the formation of heuweltjies, than the actual distribution. Cramer et al. (2017) investigated the overlap and the degree to which present and past environmental factors explain the distribution of heuweltjies using a combination of geographical information systems (GIS) and modelling techniques, with the intent to establish the role of termites (*Microhodotermes viator*) in the formation of heuweltjies. Although they successfully mapped the extent of heuweltjies in some areas, they found their approach was not transferable as it failed to predict the extent of heuweltjies in other areas.

Remote sensing, which is the acquisition of information about objects or phenomena on the earth's surface without direct contact between the observer and the target (Mather & Koch, 2011) holds great potential for mapping heuweltjies. Remote sensors record electromagnetic radiation (EMR) through one or more regions of the electromagnetic spectrum (ES) emitted and reflected from the earth's surface (Campbell, 2007; Muller, 2017). EMR reflected from the Earth's surface contains information on the chemical, physical and biological properties of objects (Chuvieco & Huete, 2010). Therefore, the practicality of remote sensing depends on the ability of sensors to record energy in any of the wavelength regions of the electromagnetic spectrum where detectable differences in reflected and

emitted radiation for specific objects are large enough to permit individual identification (Barrett, 2013).

Methods involving automated analyses of multi-temporal satellite imagery offer an objective, less tedious and more cost-effective alternative to traditional approaches of mapping land features. The increasing availability of Earth observation satellites that provide imagery with high spatial, spectral and temporal resolution (for example the Sentinel-2 satellite constellation) offers new opportunities for mapping and monitoring land features at regional scales. In addition to freely available satellite images, there are several commercial satellites, examples of which include, very high resolution Geoeye, Rapideye, Quickbird, Kompsat etc. Both single-date and multi-temporal techniques have been employed for land feature mapping with satellite imagery (Zheng et al., 2015; Inglada et al., 2016; Gilbertson & Van Niekerk, 2017; Cai et al., 2018; Maponya et al., 2020). Fast-growing web-based geospatial platforms such as Google earth engine (GEE) are quickly attracting the attention of researchers across academic disciplines, and in recent years it has boosted the emergence of RS-based automated applications at the continental and planetary scale of analysis (Gorelick et al., 2017).

In addition to remote sensing products, geomorphometric processes have been used to study land feature characteristics (Vermeulen, 2018). Geomorphometry involves processes that produces a set of terrain characteristics which are evaluated along with other properties to assign a value to a land unit, expressed either by a numeric value or by a judgement of its worth in qualitative terms (Hengl, Gruber & Shrestha, 2003). An example of this include digital elevation models (DEM), defined as a digital or numerical representation of terrain (Liu et al., 2004). DEMs allow for the extraction of several morphological and hydrological terrain parameters (Vermeulen, 2018). The amount of detail captured with the high spatial resolution remote sensing imagery and terrain variables extracted from DEMs coupled with machine learning is expected to improve the detection of heuweltjies.

The availability of information on the distribution of heuweltjies is critical for many applications, but in most regions this information remains unknown. This study assesses the efficacy of a Random Forest (RF) machine learning classifier when applied to image composites generated from a Sentinel-2 time series to determine the best period for mapping the distribution of heuweltjies. Sentinel-2 derived image composites were used to generate a set of features (predictor variables) – inclusive of spectral bands and indices – which was used as input for the RF classifier. The classifier was trained and validated using sample points. The classifications were undertaken across in three (3) Sites, located in the Northern and Western Provinces of South Africa, to assess the consistency of the results.

8.2 Material and Methods

8.2.1 Study Sites

Three study sites situated in the Northern Cape (Komaggas) and Western Cape Provinces (Piketberg and Klawer) of South Africa were selected for investigation. For this research, the study sites located in Komaggas, Piketberg and Klawer will be referred to as Site A, Site B and Site C respectively. Site A is situated within the Komaggas area, about 70 km west of Springbok in the Northern Cape Province, while Site B is located north of Piketberg; a town situated about 80 km east of Saldanha Bay in the Western Cape Province. Site C is located in Klawer; a town in the Matzikama Municipality in the Western Cape Province. All three sites have a Mediterranean climate and are as such characterised by warm/hot, dry summers and cool, wet winters (Malan, 2016). Although all three sites have a Mediterranean climate, they represent different biomes inclusive of the Fynbos and Succulent Karoo biomes. While the Fynbos biome is a nutrient-poor Mediterranean-climate shrubland, the Succulent Karoo shrubland is comparatively nutrient rich, but like the Desert biome, an arid Mediterranean-climate ecosystem (Cramer & Midgley, 2015). The three sites were chosen to represent heuweltjies within different environmental conditions.

8.2.2 Satellite Imagery Acquisition and Preparation

A selection of cloud-free Sentinel-2 imagery, pre-processed at Level 2A and collected over a period of twelve months was sourced from the Sentinel Hub (https://www.sentinel-hub.com/). A temporal period of 12 months was chosen to capture seasonal variations necessary for identifying the optimal period for mapping heuweltjies (Table 8.1). Sentinel-2 is a European earth polar satellite constellation based on the concurrent operation of two identical satellites orbiting in a single plane (Pahlevan et al., 2017). Each of the twin satellites hosts a multispectral instrument (MSI), covering a spectral range from visible to near- and shortwave infrared. The MSI measures reflected radiance in thirteen (13) spectral bands, including: blue, green, red and near-infrared (measured at 10 m spatial resolution); four (4) 20 m resolution vegetation red-edge bands for vegetation characterisation; two (2) wider shortwave infrared (SWIR) for vegetation moisture stress assessment and 60 m resolution coastal aerosol, shortwave infrared (cirrus) and water vapour bands, mainly for cloud screening and atmospheric corrections (Galoppo et al., 2018). Median values were employed to integrate the different images available to obtain a stable image and minimize the effect of eventual outliers (Orengo et al., 2020).

Table 8.1: Images collected, the different season they represent and the approximate number of images available per month for three sites.

#	Acquisition date	Season	Site A #. Of images available	Site B #. Of images available	Site C #. Of images available
1	June 2019		4	2	3
2	July 2019	Winter	4	4	4
3	Aug 2019		4	3	5
4	Sept 2019		4	4	4
5	Oct 2019	Spring	1	3	4
6	Nov 2019		2	4	5
7	Dec 2019		2	5	5
8	Jan 2020	Summer	5	5	5
9	Feb 2020		4	3	3
10	Mar 2020		6	4	5
11	Apr 2020	Autumn	4	2	3
12	May 2020		6	4	3

8.2.3 Training and Validation Sample Collection

Very high-resolution imagery accessible through Google Earth Engine (GEE) was used in combination with Sentinel-2 imagery to collect samples for both on- and off-heuweltjies. The two classes (mounds and non-mounds) and the number of samples per class for the three study sites are given in *Table 8.2*.

Table 8.2: The number of samples per class in study all three (A, B & C)

Class	Number of sampled fields		
	Study Site A	Study Site B	Study Site C
Mounds	850	850	850
Non-mounds	750	750	750

8.2.4 Feature Set Development

Twenty (20) features (per monthly image composite) were generated from the Sentinel-2 bands (*Table 8.3*). For this study, only the blue (band 2), green (band 3), red (band 4), vegetation red edge (band 5), vegetation red edge (band 6), vegetation red edge (band 7), NIR (band 8), narrow NIR (band 8A), SWIR (band 11) and SWIR (band 12) were used. The coastal aerosol (band 1), water vapour (band 9) and SWIR cirrus (band 10) bands were deliberately excluded, as they were not deemed important for this study. The generated features included indices derived from the equations in *Table 8.4* (Immitzer et al., 2016). Mean values for all spectral features were calculated.

Table 8.3: Features used as input for classifications (refer to Appendix 1 for the full names, formula and bands used to compute each feature).

Variable source	Features
Spectral bands	blue, green, red, vegetation red edge1, vegetation red edge2, vegetation red edge3, NIR, Narrow NIR, SWIR1, SWIR2
Indices	NDVI, SAVI, CI, CBI, CLI, SCI, NDSI, NDWI, BI and BSI

8.2.5 Classification and Accuracy Assessment

Google Earth Engine Cloud Computing (GEE) Geospatial Platform was used to undertake all the classifications. This platform was chosen due to its ability to implement large-scale multitemporal data analysis by granting access to a catalogue of satellite imagery and geospatial datasets, including the Sentinel-2 time-series. GEE further parallelizes and executes codes developed in JavaScript or Python using Google's cloud computing infrastructure, allowing for intensive computational processes at unprecedented scales. For this study JavaScript was implemented. GEE also permits the development of machine-learning processes through the computation of partial machine learning-based classifications which can execute in a minute or a few depending on the size of the training data. In this instance Random Forest (RF) was used to undertake classifications. GEE also incorporates high-resolution imagery (equal to that of Google Earth) that allows the evaluation of the results of the classification and the selection of new training data without needing to export them to GIS software. This made it easy to collet sample points which were used for training the classifier and validating the results. A 3:2 sample split ratio was employed on the collected samples. Thirty percent of the samples were randomly selected and reserved for independent validation of the classifications. The same set of

training and validation samples were maintained for all the classifications in all Sites. GEE provides an automated generation of confusion matrices and calculates overall accuracies (OAs) and Kappa coefficients (Ks) for every classification. OA in this instance is interpreted as the percentage of pixels corresponding to the errors of omission and commission (Campbell & Wynne, 2011), while K assesses the statistical differences between classifications (Foody & Atkinson, 2004).

Table 8.4: Equations used to calculate the vegetation indices considered in the classifications.

Name	Index	Formulation
Brightness Index	BI	*sqrt(((RED*RED)/ (GREEN* GREEN))/2)*
Bare soil Index	BSI	$\frac{SWIR - NIR}{SWIR + NIR}$
Clay Index	CI	$\frac{SWIR}{BLUE}$
Carbonate Index	CBI	$\frac{1}{2}NDVI + 1$
Coloration Index	CLI	$\frac{RED - BLUE}{RED}$
Normalised Difference Salinity Index	NDSI	$\frac{RED - VEG\_RED\_EDGE}{RED + VEG\_RED\_EDGE}$
Normalised difference vegetation index	NDVI	$\frac{NIR - RED}{NIR + RED}$
Normalized Difference Water Index	NDWI	$\frac{NIR - SWIR}{NIR + SWIR}$
Soil-adjusted vegetation index	SAVI	$(1 + L) = \frac{NIR - RED}{NIR + RED + L}$
Soil Composition Index	SCI	$\frac{RED - GREEN}{RED + GREEN}$

8.3 Results

The results of the twelve classifications for each of the three Sites are summarised in Table 8.5. Although all images across all Sites produced high overall accuracies (OA > 85%) images collected during some months obtained better results than others. For example, in Site A, monthly Median composites generated from images collected throughout the twelve months obtaining OAs higher than 90% with

the exception of image composites generated from images collected in October 2019 and January 2020. Contrary to Site A, in Site B image composites generated from images collected in June, August & Sept 2019 obtained OAs lower than 90% while all the other image composites obtained OAs higher than 90%. In Site C all image composites from June 2019 to April 2020 obtained OAs higher than 90% with the last image of the series obtaining an OA less than 90%.

Table 8.5: Overall accuracies (OA), and Kappa coefficients (K) for Site A, Site B and Site C respectively.

Classifications	Site A		Site B		Site C	
	OA	K	OA	K	OA	K
1 (June 2019)	92.6	0.85	89.1	0.78	90.5	0.81
2 (July 2019)	91.1	0.82	91.2	0.82	90.5	0.80
3 (Aug 2019)	91.8	0.83	89.4	0.78	91.2	0.82
4 (Sept 2019)	91.8	0.83	89.4	0.78	90.8	0.82
5 (Oct 2019)	89.6	0.79	90.3	0.80	91.7	0.83
6 (Nov 2019)	91.1	0.82	90.3	0.80	92.6	0.85
7 (Dec 2019)	92.4	0.84	90.1	0.79	90.8	0.81
8 (Jan 2020)	88.7	0.77	90.3	0.80	91.2	0.82
9 (Feb 2020)	90.5	0.81	91.1	0.83	90.5	0.81
10 (Mar 2020)	93.1	0.86	91.0	0.81	91.7	0.83
11 (Apr 2020)	92.6	0.85	91.7	0.83	92.6	0.85
12 (May 2020)	93.3	0.86	91.0	0.81	89.8	0.79

Even though heuweltjies were identifiable with comparable OAs across all Sites, it is clear from the results that the RF classifier picked them more efficiently in Site A (Komaggas) than in the other two Sites (Piketberg & Klawer). While the highest OA (93.3%) in Site A was obtained with an image composite generated from images collected in May 2020, and the lowest OA (88.7%) from images collected in Jan 2020; in Site B the highest OA (91.7%) was obtained form an image composite generated from images collected in April 2020 and the lowest (89.1%) from images collected in June 2019. In Site C the highest OA (92.6%) was obtained from a composite generated from images collected Nov 2019, while the lowest (89.8%) was achieved with a composite generated from images collected

in May 2020. Contrary to what was observed from a statistical analysis of the results, a visual inspection of the results indicate that the approach did not sufficiently outline heuweltjies (For example see Figure 8.1)

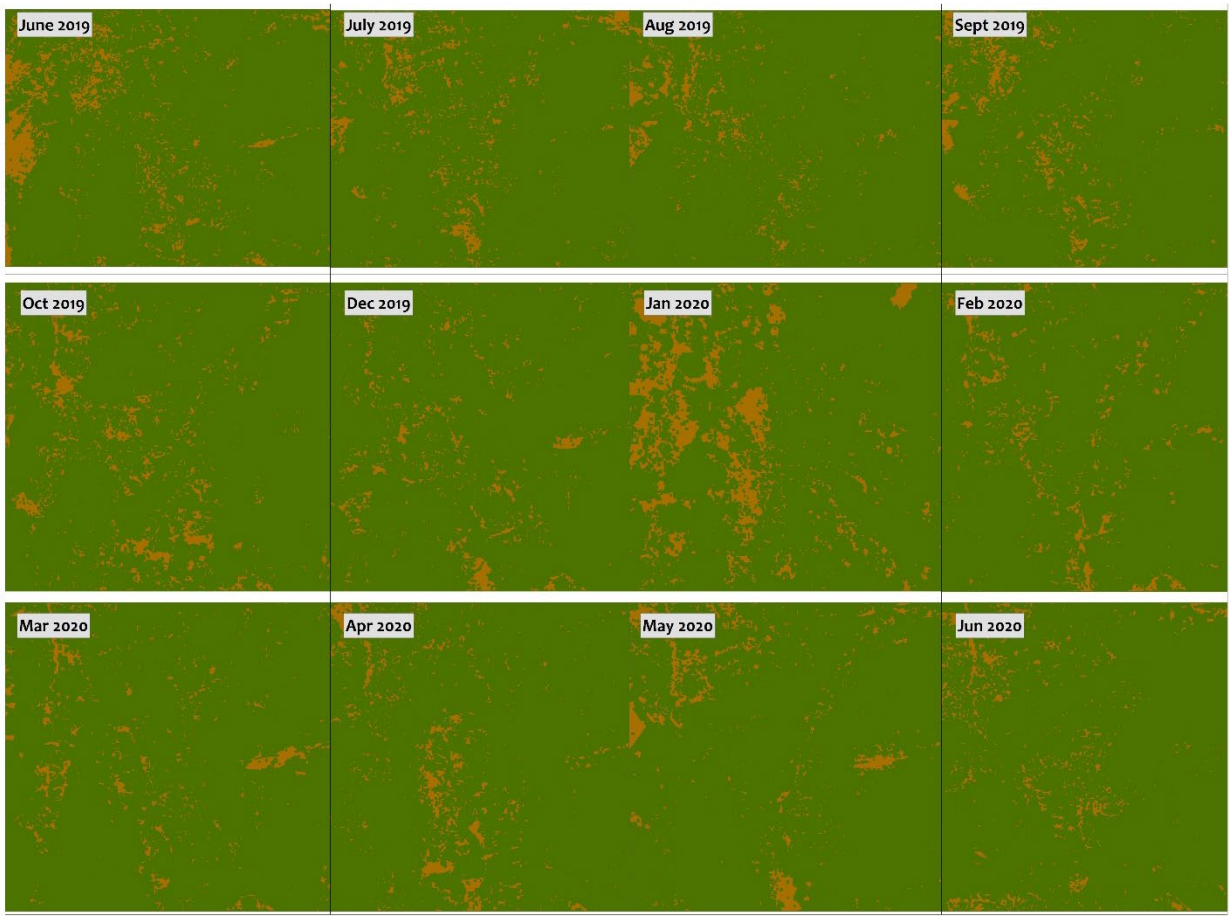

Figure 8.1: An example of the classification results for twelve image composites collected between June 2019 and May 2020 in the Site A (Komaggas) area.

8.4 Discussion

Based on classifications resulting from the monthly image composites generated from a Sentinel-2 time-series collected between June 2019 and May 2020, with machine learning (random forest) and GEE; remote sensing approaches hold great potential for mapping the distribution of heuweltjies in both the Northern and Western Cape provinces of South Africa. Generally, RF appeared to pick up heuweltjies better during dryer periods than wet periods. We suspect this to be due to the explicit differences in vegetation cover on- and off heuweltjies, as off-heuweltjies surfaces would have withered while on-heuweltjie vegetation in most instances remains green even during dry seasons. Although Sentinel-2 image composites demonstrated potential for separating heuweltjies from non-heuweltjies, the approach was not successful in delineating individual heuweltjies. Amongst other reasons the low

spatial resolution at which Sentinel-2 imagery is collected is believed to have been a limiting factor in the performance of this classifier for identifying individual heuweltjies.

To remedy the limitations of the current approach, very high resolution Geoeye imagery has been purchased and will be used to generate more features which will be used as input into the classifiers. Geoeye-2 sensors collect imagery at a very high spatial resolution of 50 cm, measuring reflected radiance in five (5) spectral bands including one (1) panchromatic band and four (4) multispectral bands (blue, green, red and near-infrared). Additionally, more datasets inclusive of digital elevation models (DEM) will be used to generate elevation variables which will also be inputted into machine learning classifiers on GEE. Furthermore, additional classifiers which has been reported successful in mapping lad features such as Support Vector Machines (SVM) will be evaluated to determine their efficacy for mapping the distribution of heuweltjies.

8.5 Conclusions

- This study investigated the use of a Random Forest machine learning classifier with a time-series Sentinel-2 imagery to determine the best period for mapping heuweltjies across three Study Sites. Although the approach tested was not entirely effective in mapping individual heuweltjies; it was clear that heuweltjies are easier to map during drier seasons.
- Even though the spatial resolution of 10 m provided by Sentinel-2 is considered high, it was not sufficient to pick out the details necessary for separating heuweltjies from non-heuweltjies. Therefore, very high spatial resolution is necessary to efficiently map heuweltjies.
- Furthermore, using spectral information derived from Sentinel-2 imagery and indices only did not provide enough information for the classifier to effectively classify heuweltjies, therefore more datasets inclusive of DEMs (terrain variables) will be considered for further analysis.

8.6 References

Armstrong A.J. & Siegfried W.R. 1990. Selective use of heuweltjie earth mounds by sheep in the Karoo. *South African Journal of Ecology* 1: 77-80.

Barrett E.C. 2013. *Introduction to environmental remote sensing*. Routledge.

Bui E., Henderson B. & Viergever K. 2009. Using knowledge discovery with data mining from the Australian Soil Resource Information System database to inform soil carbon mapping in Australia. *Global biogeochemical cycles* 23(4).

Cai Y., Guan K., Peng J., Wang S., Seifert C., Wardlow B. & Li Z. 2018. A high-performance and in-season classification system of field-level crop types using time-series Landsat data and a machine learning approach. *Remote Sensing of Environment* 210: 35-47.

Campbell J. 2007. *Introduction to remote sensing*. 4th ed. London: Taylor & Francis.

Campbell J.B. & Wynne R.H. 2011. *Introduction to remote sensing*. Guilford Press.

Chuvieco E. & Huete A. 2010. *Fundamentals of satellite remote sensing*. Boca Raton: Taylor & Francis Group.

Cramer M.D. & Midgley J.J. 2015. The distribution and spatial patterning of mima-like mounds in South Africa suggests genesis through vegetation induced aeolian sediment deposition. *Journal of Arid Environments* 119: 16-26.

Cramer M.D., von Holdt J.R., Uys V.M. & Midgley J.J. 2017. The present and likely past climatic distribution of the termite Microhodotermes viator in relation to the distribution of heuweltjies. *Journal of Arid Environments* 146: 35-43.

Esler K.J. & Cowling R.M. 1995. The comparison of selected life-history characteristics of Mesembryanthema species occurring on and off Mima-like mounds (heuweltjies) in semi-arid southern Africa. *Vegetatio* 116(1): 41-50.

Foody G.M. & Mathur A. 2004. A relative evaluation of multiclass image classification by support vector machines. *IEEE Transactions on Geoscience and Remote Sensing* 42(6): 1335-1343.

Francis M.L. & Poch R.M. 2019. Calcite accumulation in a South African heuweltjie: Role of the termite Microhodotermes viator and oribatid mites. *Journal of Arid Environments* 170: 103981.

Galoppo A, Castellani C & Carriero F. 2018. *Sentinel-2 products specification document*. Proceedings of the international conference on AI, Simulation, and Planning in High Autonomy Systems held March 2018, Berlin, Heidelberg: Springer.

Gilbertson J.K. & Van Niekerk A. 2017. Value of dimensionality reduction for crop differentiation with multi-temporal imagery and machine learning. *Computers and Electronics in Agriculture* 142: 50-58.

Gorelick N., Hancher M., Dixon M., Ilyushchenko S., Thau D. & Moore R. 2017. Google Earth Engine: Planetary-scale geospatial analysis for everyone. *Remote sensing of Environment*. *202*: 18-27.

Hengl T., Gruber S. & Shrestha D.P. 2003. Digital terrain analysis in ILWIS. *International Institute for Geo-Information Science and Earth Observation Enschede, The Netherlands*. *62*.

Hengl T. & Reuter H.I. 2009. Geomorphometry: Concepts. *Software, Applications, Newnes*.

Herpel N. 2008. The scale-dependent variability of topsoil properties reflecting ecosystem patchiness in drylands of southern Africa. Hamburger Bodenkundliche Arbeiten 62: 1299.

Immitzer M., Vuolo F. & Atzberger C. 2016. First experience with Sentinel-2 data for crop and tree species classifications in central Europe. *Remote Sensing* 8(3): 166.

Inglada J., Vincent A., Arias M. & Marais-Sicre C. 2016. Improved early crop type identification by joint use of high temporal resolution SAR and optical image time series. *Remote Sensing* 8(5): 362.

Knight R.S., Rebelo A.G. & Siegfried W.R. 1989. Plant Assemblages on Mima-like earth mounds in the Clanwillian district, South Africa. *South African Journal of Botany* 55(5): 465-472.

Kuenzer C., Dech S. & Wagner W. 2015. Remote sensing time series revealing land surface dynamics: Status quo and the pathway ahead. In *Remote Sensing Time Series.* Springer, Cham. 1-24.

Lasaponara R. & Lanorte A. 2012. Satellite time-series analysis.

Liu M.W., Ozdogan M. & Zhu 2013. Crop type classification by simultaneous use of satellite images of different resolutions. *IEEE Transactions on Geoscience and Remote Sensing* 52(6): 3637-3649.

Lovegrove B.G. & Siegfried W.R. 1989. Spacing and origin (s) of Mima-like earth mounds in the Cape Province of South Africa. *S. AFR. J. SCI./S.-AFR. TYDSKR. WET* 85(2): 108-112.

Malan G.J. 2016. Investigating the suitability of land type information for hydrological modelling in the mountain regions of Hessequa, South Africa. Masters thesis. Stellenbosch: Stellenbosch University, Department of Soil Sciences.

Maponya M.G., Van Niekerk A. & Mashimbye Z.E. 2020. Pre-harvest classification of crop types using a Sentinel-2 time-series and machine learning. *Computers and Electronics in Agriculture* 169: 105164.

Mather P. & Koch M. 2011. *Computer Processing of Remotely-Sensed Images*. 4th ed. Chichester: John Wiley & Sons, Ltd.

McAuliffe JR, Hoffman MT, McFadden LD, Bell W, Jack S, King MP & Nixon V 2019. Landscape patterning created by the southern harvester termite, Microhodotermes viator: Spatial dispersion of colonies and alteration of soils. *Journal of Arid Environments* 162: 26-34.

Midgley G.F. & Musil C.F. 1990. Substrate effects of zoogenic soil mounds on vegetation composition in the Worcester-Robertson valley, Cape Province. *South African Journal of Botany* 56(2): 158-166.

Midgley J.J. 2010. More mysterious mounds: origins of the Brazilian campos de murundus. *Plant and soil* 336 (1-2): 1-2.

Moore J.M. & Picker M.D. 1991. Heuweltjies (earth mounds) in the Clanwilliam district, Cape Province, South Africa: 4000-year-old termite nests. *Oecologia* 86(3): 424-432.

Muller S.J. 2017. Indirect soil salinity detection in irrigated areas using earth observation methods. Masters thesis. Stellenbosch: Stellenbosch University, Department of Geography and Environmental Studies.

Orengo H.A., Conesa F.C., Garcia-Molsosa A., Lobo A., Green A.S., Madella M. & Petrie C.A. 2020. Automated detection of archaeological mounds using machine-learning classification of multisensor and multitemporal satellite data. *Proceedings of the National Academy of Sciences*, *117*(31): 18240-18250.

Pahlevan N., Sarkar S., Franz B.A., Balasubramanian S.V. & He J. 2017. Sentinel-2 MultiSpectral Instrument (MSI) data processing for aquatic science applications: Demonstrations and validations. *Remote Sensing of Environment* 201: 47-56.

Petersen A., Gröngröft A. & Miehlich G. 2003. Einfluss der Termiten auf die Pedodiversität südafrikanischer Trockengebiete. *Mitteilungen der Deutschen Bodenkundlichen Gesellschaft*, *102*, 313-314.

Picker M.D., Hoffman M.T. & Leverton B. 2007. Density of Microhodotermes viator (Hodotermitidae) mounds in southern Africa in relation to rainfall and vegetative productivity gradients. *Journal of Zoology*, *271*(1), 37-44.

Rahlao S.J., Hoffman M.T., Todd S.W. & McGrath K. 2008. Long-term vegetation change in the Succulent Karoo, South Africa following 67 years of rest from grazing. *Journal of arid environments*, 72(5): 808-819.

Schmiedel U., Röwer I.U., Luther-Mosebach J., Dengler J., Oldeland J. & Gröngröft A. 2016. Effect of grazing on vegetation and soil of the heuweltjieveld in the Succulent Karoo, South Africa. *Acta Oecologica*, 77: 27-36.

Skidmore A.K., Turner B.J., Brinkhof W. & Knowles, E., 1997. Performance of a neural network: mapping forests using GIS and remotely sensed data. *Photogrammetric engineering and remote sensing*, *63*(5): 501-514.

Turner W., Spector S., Gardiner N., Fladeland M., Sterling E. & Steininger M. 2003. Remote sensing for biodiversity science and conservation. *Trends in Ecology & Evolution* 18(6): 306-314.

Vanwalleghem T., Amate J.I., de Molina M.G., Fernández D.S. & Gómez J.A. 2011. Quantifying the effect of historical soil management on soil erosion rates in Mediterranean olive orchards. *Agriculture, ecosystems & environment* 142(3-4): 341-351.

Vermeulen D. 2018. *Efficacy of machine learning, earth observation and geomorphometry for mapping salt-affected soils in irrigation fields* (Masters dissertation, Stellenbosch: Stellenbosch University).

Zhang H., Li Q., Liu J., Shang J., Du X., Zhao L., Wang N. & Dong T. 2017. Crop classification and acreage estimation in North Korea using phenology features. *GIScience & Remote Sensing* 54(3): 381-406.

Zheng B, Myint S.W., Thenkabail P.S. & Aggarwal R.M. 2015. A support vector machine to identify irrigated crop types using time-series Landsat NDVI data. *International Journal of Applied Earth Observation and Geoinformation* 34: 103-112.

9 CONCLUSIONS

9.1 General Conclusions

Natural salinisation of soils and groundwater occurs across various climatic regions, but in semi-arid to arid environments this phenomenon is generally ascribed to the high evaporation rates coupled with low mean annual rainfall. However, this is not always the case. Given that the population in sub-Saharan Africa is expected to increase by 45% in the next 20-30 years and that surface water resources in this region won't be able to sustain the population, many communities will rely on groundwater as their only source of potable water, if they aren't already doing so (UNDESA – United Nations, Department of Economic and Social Affairs, 2017; Gerten et al., 2011; Ojeda Olivares et al., 2020). With much of sub-Saharan Africa experiencing semi-arid to arid climatic conditions and being one of the region's most vulnerable to climate change, it is important to understand the factors that play a role in the sustainability of the groundwater resources, both in terms of quality and quantity. In this study, it was shown that biophysical features, heuweltjies, play a large role in groundwater salinisation in a semi-arid to arid environment and have been doing so for thousands of years. Although there is some controversy exists regarding the formation of heuweltjies, but most authors agree that heuweltjies are the result of termite activity, more specifically *Microhodotermes viator* (Moore & Picker, 1991b; Potts et al., 2009; Picker et al., 2007; McAuliffe et al., 2019b). Given that termites, though not the same species, occur all over Africa and in many other parts of the world, it is likely that other groundwater sources may also be affected by termite related salinisation.

9.1.1 Groundwater in the Buffels River catchment

The Buffels River catchment experiences semi-arid to arid climatic conditions and many communities are wholly reliant on groundwater as their only source of potable water. In addition to this, much of the local economy is also reliant on groundwater but the groundwater is variably saline which poses a risk to both human health and the economy. In order to better constrain the extent and cause of salinisation in the region a combination of various isotopes and basic hydrochemistry was used. Saline groundwater in the Buffels River catchment is hosted in in both alluvial and fractured rock aquifers. Low $^{87}Sr/^{86}Sr$ ratios together with patterns and trends in the groundwater chemistry suggest that several isolated alluvial aquifer systems exist. One large known alluvial aquifer, the Spektakel Aquifer situated in the Buffels River valley, is the least saline of the alluvial aquifers, while the smaller more isolated alluvial aquifers to the east and the west of the Spektakel aquifer host more saline groundwater. The chemistry of groundwater hosted in fractured aquifer systems were related to the specific host rock by using the variation in $^{87}Sr/^{86}Sr$ ratios in combination with major cations and anions. Elevated $^{87}Sr/^{86}Sr$ ratios

confirmed that the host rocks are different granitic gneisses as these rocks are highly radiogenic in this region.

In terms of the groundwater chemistry, most of the major cation and anion concentrations in the groundwater from the Buffels River catchment are elevated, but the main concerns are elevated Na^+, Cl^- and SO_4^{2-} concentrations. These concentrations are in most cases above the limits of the World Health Organisation standards for drinking water, but yet the water is still utilised as potable water. Local water management authorities should be advised on this and assisted in finding a solution to treat the water to drinking water standards. Given the elevated Na and Cl concentrations, it was previously thought that evaporative concentration of salts followed by flushing events is the leading cause of salinisation in this region. However, $\delta^{18}O$ and $\delta^{2}H$ isotope plots showed no distinct evaporation trend and it was established that this process could play a minor role in salinisation but does not appear to be the leading cause of salinisation in the Buffels River catchment. Instead, the dry deposition of marine aerosols containing salts and water-rock interaction also plays a role in controlling the groundwater chemistry. Once in the aquifer, ion exchange and mineral weathering reactions may alter the groundwater chemistry. Although, salts are not produced in heuweltjies, they act as salt storage zones. Geophysics data indicated that ECa values (a proxy for salinity) are the highest in the centre of heuweltjies and that these values increase with depth in heuweltjies. This was one of the first indications that heuweltjies could potentially contribute to groundwater salinisation.

9.1.2 Groundwater sustainability in the Buffels River catchment

Groundwater sustainability in this region, in terms of quantity and quality is questionable. Although salinisation processes are directly related to the quality of groundwater, groundwater ages and temporal relationships are also related to the sustainability of the resource. The use of conventional radiocarbon age calculations with a dilution factor was evaluated and in doing so, the variability of $d^{13}C_{DIC}$ values was assessed together with the effect that factors such as geology and vegetation (C3 and C4 species) may have on $d^{13}C_{DIC}$ values. The heterogeneity in $d^{13}C_{DIC}$ values resulted in testing of multiple scenarios with different dilution factors but none of these preliminary scenarios provided sensible ages from the calculations. The challenges encountered using conventional radiocarbon calculations in a semi-arid to arid silicate dominated environment, showed that alternative models should be used, especially if there is very little pre-existing data for the area. A new groundwater recharge model was conceptualised to include factors that may have an impact on the groundwater chemistry and hence the radiocarbon ages. Heuweltjies or the variability of the aquifer type or host rock have not been included in the previous understanding of groundwater flow and recharge paths and the new conceptual model for groundwater recharge in the Buffels River catchment was

constructed to include all these variables. The simplified conceptual model for groundwater hosted in the Buffels River catchment suggests that recharge occurs in three potential ways. 1) Direct recharge into the fractured system through the fracture network; 2) in areas where thin soil horizons exist, groundwater will move through the soil horizon and into saturated zone, from where it may flow into the fractured system if the fracture network allows it; 3) where thicker soils exist, heuweltjies may be present. Here, the water will preferentially flow through the tunnels and bioturbated soils where it will either end up in the saturated zone or flow onto the granitic basement. If water enters the saturated zone, small localised aquifers could form above the granitic basement from where the water will move into the granitic basement system through fracture networks where they exist.

Given that the geology of the catchment is dominated by granitic gneisses and the only inorganic carbon present in the system is found in heuweltjies, together with the fact that heuweltjies behave as open-systems when groundwater passes through them, the radiocarbon signature in groundwater is likely to be dominated by decay rather than dilution. However, the presence of tritium together with low radiocarbon activities suggested that modern recharge to older groundwaters may be occurring and a simplified and theoretical lumped parameter model approach was used to calculate total mean ages. For the most part, groundwater in the Buffels River catchment can be classified as young groundwater (recharge received between 12 000 and 50 years ago). Groundwater towards the east of the catchment has a fossil component, while only samples from five locations can be classified as modern groundwater with ages younger than 50 years. These five samples were all situated towards the middle of the catchment. Although the average percentage modern recharge in the catchment is 24.75%, the recharge is not spatially uniform and has implications for the local communities in terms of the future groundwater availability and quality. In areas where groundwater resources are already under pressure, some measures will have to be put in place to manage the use of groundwater as many of the boreholes have dried up or are starting to do so. The fact that modern recharge in some areas are as little as 8.0%, alternative resources should be investigated as there is a risk of exploiting older or fossil groundwater resources that are not regularly recharged, which is likely to leave the region without a reliable water resource. Although the conceptual model is simplified, it should be used as a base to start educating the local authorities about the groundwater system and the risks involved in tapping into the fossil groundwater. These resources may not be renewable and will not necessarily be able to sustain the local water requirements in the long term.

9.1.3 Heuweltjies and salinisation

Salinisation has not been a continuous process in the Buffels River catchment but it has rather occurred as specific events over time. Specific increases in the EC and anion concentrations of groundwater have

been recognised. In order to validate the salinisation events, the ages and distribution of carbonates in heuweltjies were determined and used as a proxy for salinisation periods. Radiocarbon age dating on heuweltjie carbonates revealed that heuweltjie soils date back to between ~35 400 years and ~2 700 years before present. Along the edges of the heuweltjies, soil ages increase with depth while a similar pattern was observed in the centre of the heuweltjies, but soils with the same ages as that found along the edges, are situated much deeper. The depth to the carbonate horizons in calcareous heuweltjie soils was used as a proxy to assess the flow paths of water through the heuweltjie and a clear U-shaped wetting front is recognised. This suggests that heuweltjies facilitate downward movement of groundwater with termite nests facilitating the water movement. The ages of these wetting events are comparable to the groundwater ages and to periods of major increases in dissolved salts in the groundwater over the past 18 000 years. This suggests that although the groundwater ages were calculated as theoretical ages, they can be correlated to the ages of the wetting fronts and hence recharge periods. During wetter and more humid periods in the past 18 000 years (Neogene period and the Little Ice Age), recharge occurred during which salts were flushed into the groundwater system.

The salts stored in heuweltjies were related to saline groundwater by using $\delta^{34}S\ SO_4^{2-}$ and $\delta^{18}O\ SO_4^{2-}$. In areas of higher heuweltjies densities, the $\delta^{34}S\ SO_4^{2-}$ and $\delta^{18}O\ SO_4^{2-}$ isotope signatures of heuweltjies soils and groundwater are comparable. This suggests that groundwater is vulnerable to salinisation caused by heuweltjie and hence termite affected soils. Saline groundwater in regions of lower heuweltjie density was related to the influence of water-rock interaction together with salinisation because of dry deposition of marine aerosols. Although the salinisation process in the Buffels River catchment is a natural process that cannot be prevented, the previous idea of salinisation occurring because of the evaporative concentration in the arid climate has now been proved incorrect. Salinisation in the Buffels River catchment is a more complex process where aerosols containing marine and non-marine-salts are either stored in the heuweltjies before being flushed into the alluvial aquifers or directly transported into the fractured aquifers where the heuweltjie density is low. Once in the fractured aquifer, water-rock interaction controls the chemistry. The flushing events mostly occurred in the wet and humid periods in the past 18 000 years proving that salinisation of groundwater in the Buffels River catchment is related to periods of increased rainfall and humidity. Future climate predictions for Namaqualand and the west coast of southern Africa include periods of prolonged drought, but erratic and intense rainfall events are also expected. During the periods of drought, groundwater will be necessary to sustain the social and economic needs of the region but when intense rainfall events occur there is a risk salts stored in heuweltjies being flushed into the system, resulting in increasingly saline groundwater. Given that groundwater sustains much of the communities' needs as

well as a large part of the economic sector, plans should be made to find alternative water resources or treating the groundwater that is available to meet the requirements of what it will be used for.

This study has shown that heuweltjies can be used as a proxy for saline groundwater. If it is assumed that heuweltjies are related to termite activity as many authors have confirmed, the mounds of other species of termites in other parts of the world can also possibly be used as a proxy for saline soils and groundwater. In the Buffels river catchment, groundwater hosted in the fractured aquifer is relatively unaffected by the heuweltjie salts which can be related to the extremely thin if any soils above the bedrock and hence low heuweltjie density. However, the alluvial aquifers or aquifers present where thick sediments exist are affected by the heuweltjie salts. Many communities in sub-Saharan Africa are becoming increasingly dependent on groundwater, mainly tapped from alluvial aquifers which are more easily accessible that deeper fractured systems, biophysical features such as termite mounds could be used as indicators of groundwater quality.

Although it is uncertain whether the mounds of all termites are associated with salt accumulation, termite activity facilitate downward movement of groundwater through the tunnels and bioturbated soils. This has implications for contamination of groundwater sources. Heuweltjies are present in large parts of the Western Cape of South Africa (Midgley et al., 2012; Picker et al., 2007; Cramer et al., 2017), which is also one of the large crop producing agricultural regions in southern Africa and also heavily dependent on groundwater. A small fraction of the fresh produce from this region is for local use while the rest is for international markets. Apart from groundwater and soil salinisation, heuweltjies facilitate rapid groundwater recharge and given that intensive agriculture requires fertilization and the application of pesticides and herbicides, heuweltjies increase the risk of contaminating the groundwater resources. Moreover, there is a risk that this contaminated water is reused as groundwater in this region is often used for irrigation purposes.

9.2 Recommendations

This study has shown that there is a relationship between saline groundwater and heuweltjies in the Buffels River catchment in the Northern Cape of South Africa. It was also found that salinisation of groundwater in this region is not a continuous process but occurs during wetter and more humid periods during which the dependence on groundwater will decrease as enough surface water will be available. A few recommendations can be made with regards to the managing the impact of heuweltjies and saline groundwater and future research that should be conducted:

- The conceptual model should be refined and incorporated a large-scale hydrological model for the Buffels River catchment to better the understanding regarding of the large-scale impact that heuweltjies may have on groundwater chemistry and recharge.
- To educate authorities, local communities, and farmers in regions where heuweltjies occur in high densities (including other parts of South Africa) about the relationship between heuweltjies, saline soils and saline groundwater for the purposes of future developments and investments.
- To further understand the dynamics salt accumulation in heuweltjies and to compare that to termite mounds in other regions.
- To evaluate the relationship between termite activity and saline soils and groundwater in other parts of the world.
- To assess the relationship between heuweltjies and agricultural contaminants in groundwater along the west coast of Southern Africa where agriculture is the dominant land use.
- To investigate the relationship between past climatic periods, heuweltjie ages and groundwater salinisation periods in other regions with similar climatic conditions to refine the understanding of the impact that climate change had and may have on groundwater quality.
- To use heuweltjie carbonate isotope data for paleoclimate reconstruction to aid in the future climate predictions.

9.3 References

Cramer, M.D., von Holdt, J.R.C., Uys, V.M. & Midgley, J.J. (2017). The present and likely past climatic distribution of the termite Microhodotermes viator in relation to the distribution of heuweltjies. *Journal of Arid Environments*. [Online]. 146. p.pp. 35-43. Available from: http://dx.doi.org/10.1016/j.jaridenv.2017.07.010.

Gerten, D., Heinke, J., Hoff, H., Biemans, H., Fader, M. & Waha, K. (2011). Global water availability and requirements for future food production. *Journal of Hydrometeorology*. 12 (5). p.pp. 885-899.

McAuliffe, J.R., Hoffman, M.T., McFadden, L.D., Jack, S., Bell, W. & King, M.P. (2019). Whether or not heuweltjies: Context-dependent ecosystem engineering by the southern harvester termite, Microhodotermes viator. *Journal of Arid Environments*. [Online]. 163 (January). p.pp. 26-33. Available from: https://doi.org/10.1016/j.jaridenv.2018.11.012.

Midgley, J.J., Harris, C., Harington, A. & Potts, A.J. (2012). Geochemical perspective on origins and consequences of heuweltjie formation in the southwestern cape, South Africa. *South African Journal of Geology*. 115 (4). p.pp. 577-588.

Moore, J.M. & Picker, M.D. (1991). Heuweltjies (earth mounds) in the Clanwilliam district, Cape Province, South Africa: 4000-year-old termite nests. *Oecologia*. 86 (3). p.pp. 424-432.

Ojeda Olivares, E.A., Belmonte Jiménez, S.I., Sandoval Torres, S., Campos Enríquez, J.O., Tiefenbacher, J.P. & Takaro, T.K. (2020). A simple method to evaluate groundwater vulnerability in urbanizing agricultural regions. *Journal of Environmental Management*. 261 (January).

Picker, M.D., Hoffman, M.T. & Leverton, B. (2007). Density of Microhodotermes viator (Hodotermitidae) mounds in southern Africa in relation to rainfall and vegetative productivity gradients. *Journal of Zoology*. 271 (1). p.pp. 37-44.

Potts, A.J., Midgley, J.J. & Harris, C. (2009). Stable isotope and 14C study of biogenic calcrete in a termite mound, Western Cape, South Africa, and its palaeoenvironmental significance. *Quaternary Research*. [Online]. 72 (2). p.pp. 258-264. Available from: http://dx.doi.org/10.1016/j.yqres.2009.04.008.

UNDESA – United Nations, Department of Economic and Social Affairs, P.D. (2017). *World Population Prospects 2017: Data Booklet. ST/ESA/SER.A/401*.